RSC Pharmaceutics

ROYAL SOCIETY OF CHEMISTRY

REVIEW

View Article Online
View Journal | View Issue

Cite this: *RSC Pharm.*, 2025, **2**, 1227

Recent advances in biomedical applications of smart nanomaterials: a comprehensive review

Manoj Kumar Goshisht, *[a,b] Ashu Goshisht,*[c] Animesh Bajpai[d] and Abhishek Bajpai[e]

Smart nanomaterials (NMs) have emerged as a transformative tool in the biomedical field owing to their distinct physicochemical properties and multifunctional abilities. In this comprehensive review, we have featured the current advancements in utilization of smart NMs in four critical domains of biomedical science: (i) wound healing, (ii) cancer theranostics, (iii) tissue engineering and regeneration, and (iv) nanotoxicity assessment. In section 3, we have discussed the wound healing applications of metallic and non-metallic smart NMs in controlled drug delivery, rapid tissue repair/regeneration, and antimicrobial properties in synergism with photodynamic and photothermal therapy. Section 4 encompasses recent breakthroughs in cancer theranostics that leverage the dual functionality of smart NMs for simultaneous diagnosis and therapy. Nanocarriers designed with imaging agents and therapeutic payloads enable targeted drug delivery along with a reduction in side effects and improvement in treatment efficacy. The integration of stimulus-responsive mechanisms, such as pH and temperature sensitivity, further enhances their theranostic potential. Section 5 underscores NM-based efficient scaffolds and 3-dimensional (3D) bioprinting strategies to boost tissue engineering and regeneration by delivering growth factors, genetic materials, and bioactive chemicals. Section 6 encompasses recent breakthroughs in nanotoxicity assessment through *in vitro*, *in vivo*, and *in silico* approaches. The section also includes key toxicity mechanisms and challenges of smart nanomaterials in clinical translation.

Received 24th May 2025,
Accepted 16th August 2025

DOI: 10.1039/d5pm00137d

rsc.li/RSCPharma

1. Introduction

Nanoscale materials with unique features allowing them to respond dynamically to different extraneous stimuli like pH/light/temperature, chemical signals, and magnetic or electric fields are called smart nanomaterials.[1] Stimulus-responsive quantum dots, polymers, metal–organic frameworks (MOFs), metal oxide nanoparticles (NPs) (*e.g.*, iron/zinc/copper/titanium oxide), Au/Ag NPs, carbon NPs (*e.g.*, fullerenes and carbon nanotubes), and nanocomposites are generally used as smart nanomaterials.[2] Their dynamic responsiveness makes them supreme candidates in wound healing treatments, cancer theranostics, drug release, environmental monitoring, sensing, and various other fields requiring materials with "intelligent" behaviour.

The skin, as the body's largest organ, is essential for overall health, functioning both as a protective barrier and an active participant in physiological processes. It helps maintain homeostasis by detecting environmental changes, regulating the temperature of the body, and preserving the humoral balance.[3,4] Wounds occur when the skin's structure as well as integrity are disrupted by various interior and exterior factors. Common causes include burns, trauma, and/or diabetes.[5] Once the skin is compromised, the body becomes more vulnerable to microbial infections. Although the natural wound healing process is initiated to restore skin wholeness,[6] certain conditions, including infections and uncontrolled inflammation, can hinder recovery, leading to chronic wounds.[7,8] In the United States, approximately 6.5 million patients suffer from chronic wounds each year.[9]

Nanotechnology has made significant strides in the field of wound repair over the past few decades.[10] The distinct properties of NMs, like their quantum size effects and surface chemistry, have led to innovative strategies in wound healing. These properties of NMs play a crucial role in regulating the wound microenvironment, controlling infections, promoting angiogenesis, and enhancing reepithelialization.[11] Moreover,

[a]*Department of Chemistry, Shaheed Mahendra Karma Vishwavidyalaya, Jagdalpur, Bastar, Chhattisgarh 494001, India*
[b]*Department of Chemistry, Government Naveen College Tokapal, Bastar, Chhattisgarh 494442, India. E-mail: mkgh07@gmail.com*
[c]*Department of History, Indira Gandhi National Open University, Maidan Garhi, New Delhi, 110068, India*
[d]*Department of Chemistry, Hindu College, University of Delhi, Delhi 110007, India*
[e]*Department of Physics, Government Kaktiya Post Graduate College, Jagdalpur 494001, India*

the high surface area of NMs makes them an outstanding candidate for target-specific drug release owing to their capability to encapsulate therapeutic drugs, thereby regulating wound healing processes. Moreover, NM-based composite scaffolds, hybrid bioinks, and 3D bioprinting strategies have advanced the tissue engineering and regeneration (TER) field.[12]

Cancer represents a serious public health challenge, with mortality rates rising rapidly worldwide,[13] resulting in approximately 10 million deaths each year.[14] Chemotherapy remains the most prevalent anticancer drug approach owing to its high effectiveness.[15] However, chemotherapy's effectiveness is often hindered by its poor selectivity toward tumour cells as well as difficulties in releasing medicines to the site of tumour efficiently.[16] In addition, the emergence of multi-drug resistance (MDR) further poses obstacles in the successful outcome of chemotherapy. The intricate nature of the microenvironment of tumours[16] as well as variation in nature of all patients also add to the challenges of development of worthwhile therapeutic agent options.

Smart NMs represent remarkable progress in cancer therapy, offering a promising alternative to conventional therapeutics. These NMs are designed to respond to different biomolecules, pH, and stimuli, leading to their aggregation at tumour sites and subsequent release of therapeutic payloads.[17,18] This targeted and triggered drug delivery mechanism establishes a smart treatment mode, allowing for enhanced efficacy and reduced off-target effects.[18–21] Moreover, smart NMs have the capability to co-deliver therapeutics and diagnostic reagents simultaneously. This aspect has greatly contributed to the development of theranostics, which combines therapy and diagnostics in a single platform. By integrating therapeutic and diagnostic functionalities, smart NMs hold immense potential for personalized cancer treatment strategies.[22]

Different types of smart nanomaterial with distinct morphologies and properties used in biomedical applications are presented in Fig. 1.[23]

Although smart NMs offer significant benefits in healthcare and other fields, their potential menace to the environment and health cannot be ignored.[24–26] In the last decade, worthy attention has been given to nanotoxicity assessment. Nanotoxicity is influenced by various factors related to both the NMs themselves (*e.g.*, their chemical composition, shape, size, and coating) and the biological systems they interact with.[27] Exposure of cells/tissues to NMs can affect them through multiple mechanisms, each contributing to potential health risks. NMs can reduce the ability of cells to survive and proliferate, hinder tissue growth and repair processes, and lead to the generation of reactive oxygen species (ROS)/cytokines, damage to cell membranes/DNA/mitochondria, apoptosis, lipid peroxidation, cell cycle dysregulation, genotoxicity, necrosis, and metabolic/cell morphology changes.[27–32]

In this review, applications of smart NMs based on wound healing, cancer theranostics, and tissue engineering and regeneration have been discussed comprehensively. Different types of nanocarrier, such as metallic, non-metallic, and polymeric or biomimetic, used for the delivery of drugs, bioactive chemicals, and genetic materials in wound healing, cancer therapy and tissue engineering and regeneration have been highlighted

Manoj Kumar Goshisht

Dr Manoj Kumar Goshisht is an Assistant Professor of Chemistry at Govt Naveen College Tokapal, Bastar, Chhattisgarh, India. He obtained his master's degree from the Guru Jambheshwar University of Science & Technology, Hisar, Haryana, and PhD degree from the Dr B. R. Ambedkar National Institute of Technology, Jalandhar, Punjab, India. He has cleared the National Eligibility Test (CSIR-UGC NET) for Assistant Professorship in the subject of Chemical Sciences. He is a winner of the Editors Pick Award of the '9th DST & ACS Workshop'. Dr Goshisht completed his post-doctoral assignments at the University of Wisconsin, Green Bay, Wisconsin, USA. His research interests include materials chemistry, water purification, sensing, artificial intelligence, supramolecular chemistry, and nanomaterials. He has published various research papers in reputed international peer-reviewed journals of The American Chemical Society, The Royal Society of Chemistry, Springer Nature, Wiley, and Elsevier. He also has an international book to his credit published by CRC Press (an imprint of the Taylor & Francis group).

Ashu Goshisht

Ashu Goshisht completed her schooling in science, where she studied Physics, Chemistry, and Mathematics. She then earned her graduation degree from the Autonomous Heritage Institution, Kanya Maha Vidyalaya (KMV), Jalandhar, Punjab, India. Afterward, she pursued her master's degree at Indira Gandhi National Open University, New Delhi, India. Her research interests include inclusive research, environmental history, palaeography, and the history of science and technology.

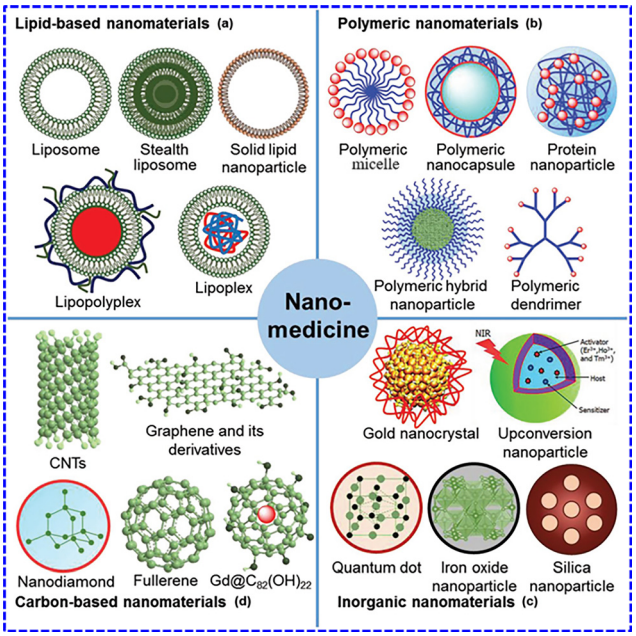

Fig. 1 Schematic representation of different smart nanomaterials employed in wound healing, tissue engineering/regeneration, and cancer therapy. Reprinted with permission from ref. 23. Copyright 2019, WILEY-VCH Verlag GmbH & Co. KGaA, Weinheim.

throughout the article. However, the applications of smart NMs are not without concern. That is why in the last section, we have discussed the *in vivo*, *in silico*, and *in vitro* toxicities of NMs and summarized them in table format (Tables 6 and 7).

2. General description of smart NMs

NMs' possess notable properties and characteristics owing to nanoscale facets, which usually range between 1 and 100 nm. This size range gives nanomaterials a high surface area and results in quantum effects which significantly alter their physical/chemical/biological effects compared with their bulk analogues.[33] Smart/responsive/intelligent nanomaterials are fabricated to respond to various environmental and biological stimuli in a controlled manner. Thermo-responsive NMs change their properties in response to temperature. For instance, poly(*N*-isopropylacrylamide) exhibits a phase transition near human body temperature, making it useful in drug delivery and tissue engineering.[34] pH-responsive NMs respond to changes in pH and are useful for delivering drugs to specific parts of the body (such as infection/tumour sites that have a typically lower pH).[35] Photoresponsive NMs change their chemical or physical properties in response to light.[36] These NMs are employed in targeted drug delivery, optical devices, and sensors. Smart magnetic NMs can be manipulated by external magnetic fields, allowing precise control for applications like hyperthermia and targeted drug delivery therapy. Conductive NMs can respond to electrical stimuli, making them useful in electronics and wearable devices.[37]

In biomedical applications, smart NMs are usually engineered to be biocompatible as well as biodegradable, reducing the menace of adverse reactions. For instance, smart NMs in medicine delivery systems are fabricated to degrade harmlessly after releasing their cargo.[38] Some smart NMs, such as silver and zinc oxide NPs, exhibit inherent antibacterial properties.[39,40] They are commonly employed in medical coatings, textiles, and food packaging. Hydrogels, especially those integrated with NPs, can swell as well as contract because of pH, temperature, or even magnetic field changes. They are promising for tissue engineering and drug-release vehicles that release drugs following specific body conditions.[41] Smart textiles and wearable electronics utilize NMs to add flexibility, durability, and responsiveness to devices. These effects can be tuned by altering the material composition, proportion, size, and functional groups attached to the NPs. Nowadays, smart NMs are constantly utilized to improve performance, reduce costs, and enhance compatibility with existing systems.

2.1. Surface chemistry and conjugation of nanomaterials

Surface chemistry and conjugation strategies play a vital role in designing smart or stimulus-responsive nanomaterials. The surface chemistry governs the interaction of nanomaterials with their surrounding environment, affecting key characteristics such as stability, solubility, and biocompatibility.[42,43]

Covalent bonding provides a strong and stable connection between different functional groups and nanomaterial surfaces, helping to maintain the integrity and activity of the pairing in aqueous and biological conditions. Covalent strategies like amide bond formation, thioether and disulfide linkages, gold–thiol (Au–S) interactions, Schiff base chemistry, and click reactions are frequently utilized in the development of durable nanomedicine systems.[44]

Noncovalent attachment of different functional groups/biomolecules to nanomaterials is driven by fundamental molecular interactions, including electrostatic forces, hydrogen bonds, π–π stacking, and hydrophobic effects.[45] The inherent sequence tunability and structural adaptability of biomolecules like nucleic acids, lipids, and proteins facilitate these interactions. This approach is economical and maintains the native functionality of the attached biomolecules without the need for chemical alterations. However, compared with covalent strategies, noncovalent methods offer lower stability and are more susceptible to variations in environmental conditions such as pH and ionic strength. Conjugation techniques like covalent and non-covalent, which involve attaching functional molecules to the nanomaterial surface, impart responsiveness to endogenous (pH, enzymes, hypoxia, glutathione, *etc.*) and exogenous (temperature, light, magnetism, *etc.*) stimuli.[46] This enables a controlled and adaptive behaviour of the nanomaterials under varying conditions (Fig. 2).

2.2. Stability and degradation kinetics of smart nanomaterials

Stability governs the circulation time, shelf-life, and targeting precision of smart nanomaterials. Degradation kinetics

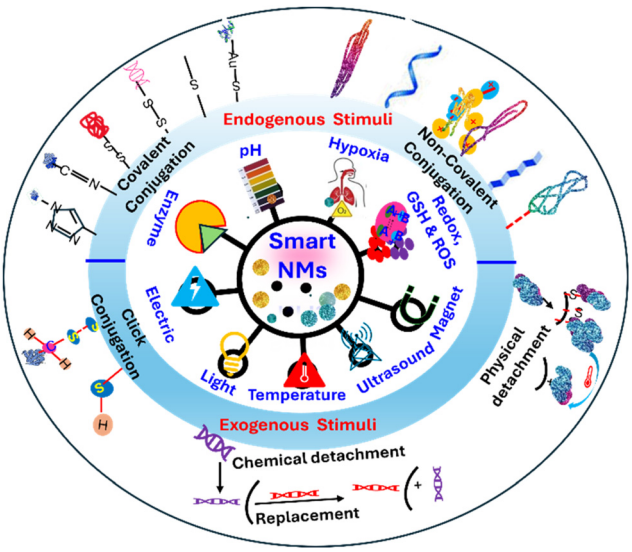

Fig. 2 Schematic representation of conjugation and detachment strategies along with endogenous and exogenous stimuli. Responsible for targeted and controlled therapeutic action of smart nanomaterials.

involves the timing and location of therapeutic release and clearance from the body. Guo *et al.*[47] synthesized triblock polymer functionalized superparamagnetic Fe_3O_4 nanomaterials with pH-responsive properties. In addition, the synergistic effect between ionic bonding and hydrophobic interactions increased the loading efficiency of the drug at 7.4 pH. However, at endosomal or lysosomal acidic pH (<5.5) ionic bonding breaks and the drug is released, showing target-specific release of the drug. In another study, Fuoco *et al.*[48] prepared redox-responsive PEG-SS-PLA-based nanomaterials where PEG stands for poly(ethylene glycol) and PLA stands for poly(lactide). The nanomaterials were stable extracellularly but degrade in high glutathione (GSH) environments due to disulphide bond cleavage, showing the tumour-specific targeting ability of nanomaterials.

2.3. Drug loading and release efficiency

The drug loading and release efficiency of smart nanomaterials depends on the encapsulation technique, material matrix, and intermolecular interactions (hydrophobic, electrostatic, H-bonding, *etc.*).[49] The drug loading and release efficiency of different types of smart nanomaterial has been discussed in Table 1.

3. Wound healing applications of smart nanomaterials

Wounds are injuries to the skin and underlying tissues that disrupt normal anatomical structure and function.[50] The wound healing process involves four coordinated stages: hemostasis, inflammation, proliferation, and remodeling.[51] Smart nanomaterials can sense and respond to biochemical or biophysical cues at the wound site. Smart nanomaterials enhance each phase by delivering bioactive agents or modulating cellular responses in a stimulus-responsive manner (Table 2). These materials exhibit adaptive, targeted, and controlled therapeutic functionalities, enabling them to address the dynamic and complex nature of acute and chronic wounds.[52]

The mechanism of smart nanomaterials is inherently adaptive, targeted, and intelligent, tailored to wound microenvironment dynamics.[53] They surpass conventional nanomaterials, which offer static and non-selective functions. By combining real-time sensing with precise therapeutic delivery, smart nanomaterials represent a next-generation platform in advanced wound healing technologies. Mechanistic advancement of smart nanomaterials over conventional nanomaterials for wound healing and cancer therapy applications is presented in Tables 3 and 5, respectively.

Despite the promising applications, clinical translation faces obstacles of (i) the toxicity and biocompatibility of

Table 1 Summary of drug-loading efficiency of smart nanomaterials

S. no.	Smart nanomaterial type	Drug loading (%)	Method	Ref.
1	Liposomes	5–15%	Passive loading, remote loading	49
2	Polymeric micelles	10–20%	Self-assembly of amphiphilic polymers	55
3	Dendrimers	>20%	Covalent or electrostatic conjugation	56
4	Mesoporous silica NPs	>30%	Pore loading, pH-labile caps	57
5	Nanogels	~10–30%	Swelling in drug solution and trapping	58

Table 2 Stimulus-responsive behaviour of smart nanomaterials in wound healing

S. no.	Stimulus	Typical wound condition	Smart nanomaterial response
1	pH	Acidic pH in chronic/infected wounds	Trigger drug/gene release
2	Enzymes like matrix metalloproteinase (MMPs)	Overexpressed in chronic wounds	Enzyme-triggered therapeutic release
3	Temperature	Elevated in inflamed/infected tissue	Thermosensitive drug release
4	ROS	Excess ROS during chronic inflammation	Scavenge ROS, release antioxidants
5	Bacterial toxins	Infection	Smart antimicrobial release or membrane disruption

Table 3 Comparative mechanistic insights of smart nanomaterials over conventional nanomaterials in wound healing applications

S. no.	Aspect	Conventional nanomaterials	Smart nanomaterials
1	Design	Passive delivery systems with fixed properties	Engineered to respond to specific stimuli (*e.g.*, ROS, pH, temperature, enzymes, *etc.*) in the wound microenvironment
2	Stimulus response	None/minimal	Responsive to internal (*e.g.*, infection, ROS, pH, *etc.*) or external (*e.g.*, light, magnetic field, *etc.*) cues
3	Drug release	Continuous/burst release, often non-specific	Controlled and on-demand release of therapeutics in response to wound-specific stimuli
4	Targeting capability	Non-targeted accumulation at wound site	Localized and targeted delivery based on microenvironmental characteristics
5	Healing modulation	May offer antimicrobial/antioxidant support	Multifunctional: antibacterial, anti-inflammatory, haemostatic, pro-angiogenic, and even immune-modulatory
6	Biocompatibility and safety	Biocompatible but potential risk of overdose/toxicity owing to uncontrolled release	Reduced/minimal side effects through spatial and temporal control of therapeutic action

certain nanomaterials; (ii) scale-up and reproducibility in manufacturing; (iii) long-term safety and regulatory approval; and (iv) cost-effectiveness in healthcare settings.[54] Advancements in biodegradable smart polymers, personalized wound care, and real-time biosensing will guide the next generation of smart nanomaterial-based wound treatments.

3.1. Wound healing applications of metal-based smart NMs

Metal-based NMs, such as metal NPs (MNPs), metal oxide NPs (MONPs), and metal nanoclusters (MNCs), exhibit significant antimicrobial properties against a wide range of bacteria.[59,60] The antibacterial mechanistic actions of these NMs usually involve destruction of the bacterial cell membrane, interference with cytoplasmic enzyme activities, and oxidative stress-induced damage to DNA and plasmids.[61] Among these, MNPs and MONPs are particularly noteworthy for their potent antibacterial activity, in the context of wound healing.

Silver NPs are extensively employed in wound dressings and coatings due to their broad-spectrum antibacterial effects and ability to advance wound healing.[62] They are often incorporated into ointments, hydrogels, and bandages. The antibacterial action of AgNPs involves multiple pathways, including silver ion release, which can derange the bacterial cell wall and membrane, leading to cell lysis. Silver ions also interact with thiol groups in proteins, disrupting bacterial enzymes and metabolic processes.[63] Additionally, AgNPs engender oxidative stress by creating ROS, causing damage to bacterial DNA and other cellular components.

Gold nanoparticles (AuNPs) are employed in wound healing primarily for their anti-inflammatory properties and ability to enhance the healing process.[64] They are often combined with other therapeutic agents to improve their efficacy.[65,66] While AuNPs are less toxic to bacteria compared with silver and zinc oxide nanoparticles (ZnO-NPs), they can still exert antibacterial effects. These mechanisms include disrupting bacterial cell membranes, binding to bacterial DNA and proteins, and inducing oxidative stress.[67,68] Moreover, AuNPs can enhance the efficacy of antibiotics by facilitating their entry into bacteria.[69] Recently, Singh *et al.*[70] developed a smart drug delivery system (DDS) employing core–shell nanofibers fabricated *via* coaxial electrospinning. The system was engineered to achieve sequential drug release, which is vital for treating complex wounds that require stage-specific therapeutic interventions. The shell is composed of poly-L-lactic acid loaded with lidocaine drug, enabling immediate release at room temperature. The core contains poly(*N*-isopropylacrylamide) polymer infused with gold nanorods (GNRs) and levofloxacin. GNRs enable near-infrared (NIR) light-triggered heating which induces swelling and shrinking of the core polymer to enable on-demand, sustained release of levofloxacin. In the absence of smart nanomaterials, it is not possible to deliver on-demand and sustained release of drugs effectively.

ZnO-NPs are commonly employed in wound dressings and topical applications owing to their antimicrobial benefits, biocompatibility, and capability to promote wound healing.[71,72] These NPs provide UV protection, which is beneficial for skin applications. ZnO-NPs also cause antibacterial activity by releasing zinc ions (Zn^{2+}), ultimately disrupting bacterial cell membranes and interfering with enzyme activities.[73] Additionally, ZnO-NPs generate ROS, resulting in oxidative destruction of bacterial proteins, lipids, and DNA. The targeted antimicrobial treatments contribute to better clinical outcomes and improved patient care. The photocatalytic potential of ZnO-NPs in the presence of UV light further intensifies their antibacterial effects.[74]

Smart metal-based nanomaterials outperform conventional ones by offering controlled, targeted, and multifunctional wound healing support *i.e.*, antibacterial, antioxidant, angiogenic, and pro-regenerative actions tailored to wound microenvironments.[75] While they reduce toxicity risks through precision delivery, the long-term safety of the nanocarriers (polymers, ligands, composites, *etc.*) and metal ion release profiles still require extensive *in vivo* and clinical validation. The clinical and translational studies of metal nanomaterials have been presented in Table 4.

Moreover, scale-up production with reproducibility, regulatory hurdles for complex nanostructures, and comprehensive toxicity and pharmacokinetic profiles are some of the challenges that need to be addressed.

3.2. Wound healing applications of non-metallic NMs

The integration of non-metallic NMs in biomedical applications, particularly in wound healing, has shown promising

Table 4 Clinical and translational studies on metal-based nanomaterials in wound healing

Material/product	Nanomaterial and formulation	Study type	Model/ population	Key findings	Ref.
Silver colloid dressing	Ionic silver colloid	Randomized controlled trials (RCT) (n = 25 silver *vs.* n = 25 standard)	Diabetic foot ulcers (Wagner grade I–II)	85.7% healed in silver group *versus* 41.7% in controls at 12 weeks; mean wound reduction 85.6% *versus* 68.6%, $p < 0.05$	76
Silver-based dressing materials		Observational study included 50 diabetic foot ulcer cases	Diabetic foot ulcers	3 cases (6%) showed purulent discharge from the wound, absence of granulation tissue, presence of microorganisms and hence poor healing rate. The remaining 47 cases (94%) showed minimal/serous discharge, presence of healthy granulation tissue, no microorganisms on culture report and thus a good healing rate	77
Silver colloid dressing	Ionic silver colloid	Double-blind experiment included 50 patients	Non-ischemic DFUs	67.77 ± 17.82% reduction in ulcer area in the silver group compared with 21.70 ± 23.52% in the conventional saline group Silver group (23.15 ± 8.15 days) required fewer days to reach the endpoint compared with saline group (48.35 ± 18.07 days)	78
Silver colloid nanoparticle dressing	Nanoparticulate silver hydrogel	Prospective observational (n = 800)	Acute diabetic foot ulcers	Complete healing at 4 weeks in ≤10 cm^2 ulcers: 100% silver *vs.* 68.4% control; faster rate overall	79
Copper dressing	Copper oxide microparticles	*In vitro* study	—	The dressing showed microbial titer reductions (4-logs) within 3 h of exposure at 37 °C ($p < 0.001$)	80
Copper dressing	Copper oxide impregnated dressings	Randomized controlled trials (n = 23)	Diabetic foot wounds	47.83% (11/23) and 34.78% (8/23) of wounds closed in the copper dressings and NPWT (negative pressure wound therapy) arms, respectively ($p > 0.05$)	81

results due to their broad-spectrum antimicrobial properties. Their ability to be functionalized and incorporated into various forms such as dressings, hydrogels, and coatings makes them versatile tools in the fight against bacterial infections and in enhancing wound healing processes.[82]

3.2.1. Wound healing applications of graphene together with its derivatives. Graphene, GO (graphene oxide), and rGO (reduced graphene oxide) hold significant promise in antimicrobial applications and wound healing. Their ability to damage the membrane of microbes (by their sharp edges) and induce oxidative stress, combined with their potential for functionalization and photothermal therapy, makes them versatile and powerful tools in the fight against bacterial infections.[83] These properties facilitate the development of advanced wound dressings and Xie *et al.*[84] developed an edge-selectively passivated black phosphorus (BP) nanosheet (BPNS) hybrid by covalently fixing fullerene C_{70} at the edges, resulting in BPNSs-C_{70}, aiming to create a novel hybrid antibacterial agent with outstanding antibacterial potency (Fig. 3). The synthesis of BPNSs-C_{70} was obtained *via* a sustainable and straightforward one-step mechanochemical process. The BPNSs-C_{70} hybrid demonstrated superior hydroxyl radical ($^{\bullet}OH$) and singlet oxygen ($^1O_2$) production capabilities compared with pristine BPNSs and BP-C_{70}, under light irradiation. This resulted in improved antibacterial performance (99.97%) against MRSA (methicillin-resistant *Staphylococcus aureus*) after irradiation for just 5 minutes. *In vivo* examination confirmed the superior antibacterial capability of the synthesized hybrid, showcasing faster disinfection and recovery of

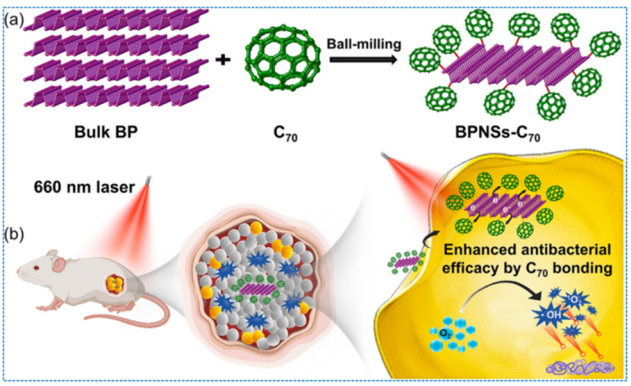

Fig. 3 (a) Schematic representation of synthesis of the BPNSs-C_{70} hybrid; (b) antibacterial efficacy of the hybrid (BPNSs-C_{70}) under 660 nm irradiation. Reprinted with permission from ref. 84. Copyright 2023, Elsevier.

abscesses. The escalated antibacterial efficacy of BPNSs-C_{70} was ascribed to the synergistically revamped $^{\bullet}OH$ and singlet oxygen production owing to intramolecular transfer from BPNSs to C_{70}. This innovative approach opens new routes for antibacterial applications of BPNSs, leveraging the improved stability and ROS generation capabilities imparted by the fullerene modification.

3.2.2. Wound healing applications of black phosphorus. BP, first synthesized in 1914, has achieved remarkable recognition owing to its distinctive properties and potential biomedical applications.[85] High-energy mechanical milling is a favoured tech-

nique to fabricate BPNPs because it produces NPs with excellent biocompatibility and biodegradability, making them promising wound healers.[86] For instance, Huang *et al.*[87] reported a wound dressing loaded with silk fibroin-functionalized BPNSs, demonstrating excellent photothermal effects that accelerated wound healing by eliminating bacterial infections.

Recently, Huang *et al.*[88] presented BP quantum dots lodged nanohydrogel (BPQDs@NH) for photodynamic and photothermal elimination of MDR bacterial infections of diabetic wounds (Fig. 4). *In vitro* investigations showed around 90% MRSA destruction due to the BPQDs and increased temperature of the hydrogel due to NIR irradiation (808 nm), suggesting potential improvements in diabetic wound healing. The strong bactericidal potential of BPQDs was preferentially ascribed to several mechanisms: (i) the destruction of cell integrity, (ii) ROS production, (iii) the induction of lipid peroxidation, and (iv) the disruption of bacterial metabolism. Additionally, *in vivo* animal model experiments revealed that treatment with the BPQDs lodged nanohydrogel under NIR irradiation attained the highest rates of healing of MRSA-infected diabetic wounds. This treatment also resulted in the highest expression of vascular endothelial growth factor (VEGF), indicating enhanced wound healing.

3.2.3. Wound healing applications of MXenes. MXenes are innovative 2D NMs characterized by the formula $M_{n+1}X_nT_x$, where M, X, *n*, and T represent an early transition element (V, Cr, Zn, Ti, *etc.*), carbon and/or nitrogen, 1–3, and surface terminating groups (*e.g.*, –F, –O, –OH),[66] respectively. Here, M is an early transition metal (*e.g.*, V, Ti, Cr, Zr, and Nb), X can be either carbon (C) or nitrogen (N), *n* ranges from 1 to 3, and T denotes surface-terminating functional groups (*e.g.*, –F, –O, –OH).[89] To date, approximately 70 different MXenes have been discovered, with $Ti_3C_2T_x$ being the first and most extensively studied member of this family.[90] $Ti_3C_2T_x$ MXene nanosheets have demonstrated sturdy antibacterial efficacy, particularly toward *B. subtilis* and *E. coli.* bacteria. Studies have shown that $Ti_3C_2T_x$ exhibits significantly stronger antibacterial activity compared with graphene oxide (GO) nanosheets at equivalent concentrations.[91] The mechanism of antibacterial activity of MXene nanosheets is primarily attributed to the combination of mechanical damage to the cell membranes of the microbes by the nanosheet's sharp edges together with oxidative stress induced by electron transfer.[92] Furthermore, photothermally active MXenes possess strong antibacterial efficacy. Gao *et al.*[93] indicated that the antibacterial efficacy of $Ti_3C_2T_x$ MXenes correlates inversely with the size of the nanosheet in the presence of light. Due to their notable antibacterial properties and photothermal conversion efficiency, MXene nanosheets can be combined with other compounds to create composite antibacterial NMs. For instance, Yu *et al.*[94] fabricated indocyanine green (ICG)-laden $Ti_3C_2T_x$ nanosheets to establish a dual effect of PDT and PTT for treating bacterial infections. The biocompatibility as well as cytotoxicity of MXenes are influenced by several factors, including dosage, lateral size, and surface modifications.[95] It is important to note that MXenes are prone to oxidation, which can compromise the integrity and functionality of the nanosheets. Therefore, chemical modifications are necessary to prevent oxidation and preserve their properties.[96]

Park *et al.*[97] developed ciprofloxacin and MXene-based hydrogel (CIPMX@Gel) groups for *in vivo* treatment of skin wounds of mice (Fig. 5). The CIPMX@Gel with NIR group exhibited outstanding wound healing ability at all time points (Fig. 5A and B). It showed 61.03% (±5.60%) and 90.14% (±2.31%) wound closure on day 7 and 14, respectively. This was notably faster than the other groups, where the sham set attained 77.41% and the 0 μg mL^{-1} set attained 75.15%. The groups with 100 μg mL^{-1} and 100 μg mL^{-1} with NIR had even slower healing rates of 53.07% (±7.80%) and 50.93% (±10.73%), respectively. In the absence of light, the CIP-MX@Gel set showed 85.74% (±5.71%) closure of the wound by day 14. Hematoxylin–eosin staining on the seventh and fourteenth days revealed that the CIP-MX@Gel with NIR group had only a small panniculus gap and the highest granulation threshold, indicating superior tissue regeneration (Fig. 5C–G). These trends were consistent over time, with the CIP-MX@Gel with light group showing the best results. Masson's trichrome staining showed that the CIP-MX@Gel with NIR group had the highest collagen fibre abundance on days seven and fourteen, indicating that the regenerated tissue in this group was most similar to normal, uninjured skin.

3.2.4. Wound healing applications of molybdenum disulphide. MoS_2, as a member of the TMDs (transition metal dichalcogenides) family, offers a range of beneficial properties that make it worthy of various advanced applications, distinctly in the biomedical field.[98,99] MoS_2-based NMs (*e.g.*, MoS_2 nanosheets, MoS_2 quantum dots, and MoS_2 nanoflowers) offer promising solutions for antibacterial applications, particularly in treating infected wounds. Their ability to generate ROS, induce physical damage to bacterial membranes, and convert NIR light into heat makes them effective

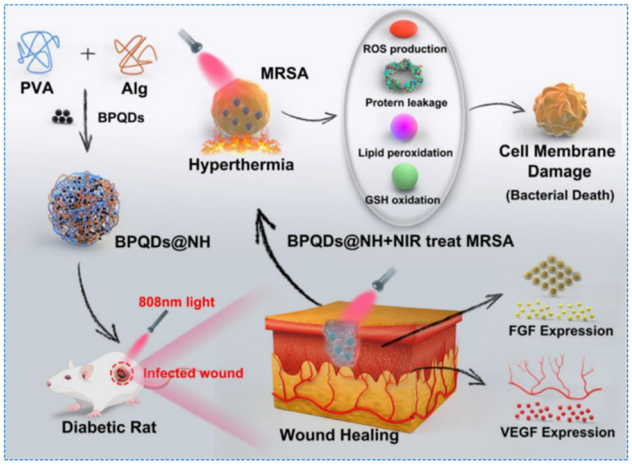

Fig. 4 Schematic illustration of the preparation of black phosphorus quantum dots lodged nanohydrogel (BPQDs@NH) and its synergistic antibacterial efficacy in the presence of NIR irradiation for MRSA-infected wound treatment. Reprinted with permission from ref. 88. Copyright 2022, Elsevier.

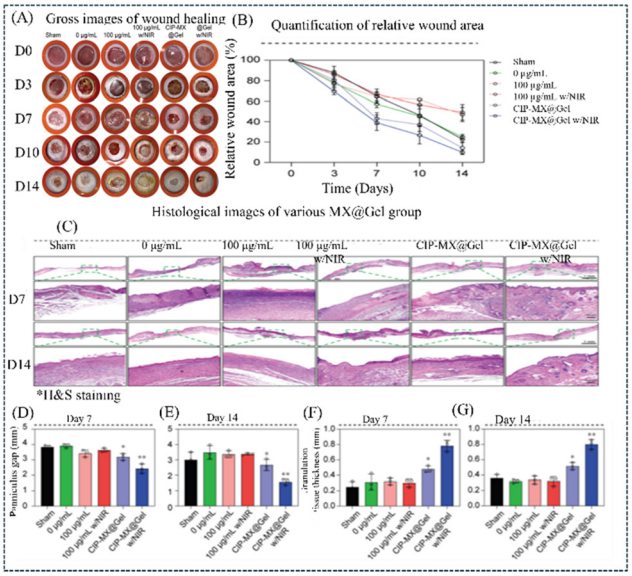

Fig. 5 Evaluation of *in vivo* healing of wounds by CIP-MX@Gel. (A) Wound images during the treatment period of 14 days. (B) Quantification of wound area. (C) H&E staining pictures of treated wound tissues on day 7th and 14th. (D, E) panniculus gap quantification of the treated wound tissues on the 7th and 14th days. (F and G) Granulation tissue thickness quantification of the treated wound tissues on the seventh and fourteenth days. Reproduced with permission from ref. 97. Copyright 2023, Elsevier.

in combating resistant bacterial infections.[100] The high biocompatibility and low cytotoxicity of MoS_2 further enhance its potential for clinical applications. Yin *et al.*[101] demonstrated an enhancement of healing of wounds by PEG-modified MoS_2 nanoflowers (NFs). They converted H_2O_2 into hydroxyl radicals ($^{\bullet}OH$) and utilized NIR irradiation for synergistic antibacterial action toward *Bacillus subtilis* and ampicillin-resistant *E. coli in vitro* and acceleration of infected wound healing *in vivo*. In another study, Cao *et al.*[102] loaded Ag^+ ions into MoS_2 nanosheets for enhancing infected wound healing. This nanocomposite combined the antibacterial properties of both MoS_2 and silver ions. When applied to MRSA-infected wounds, the nanocomposite promoted faster wound healing.

3.3. NM-based drug delivery systems for the treatment of wounds

NMs have shown great promise not only as direct therapeutic agents for promoting wound alleviation but also as effective DDSs (drug delivery systems).[103] NMs enhance the wound healing process by ensuring the sustained release of drugs at the affected site. This approach ensures a consistent therapeutic effect and minimizes the need for frequent application. Vascular dysfunction at the wound site can impair the delivery and effectiveness of therapeutic agents. Strategies need to be developed to enhance drug penetration and retention in such environments. The wound environment contains various detrimental factors which can degrade and dismantle the delivered drugs. Protective and stabilizing mechanisms should be incorporated into the DDSs. Therapeutic agents must be delivered in a controlled manner to avoid various off targets due to excessive dosages. This includes the precise timing and localization of drug release to match the wound healing stages.[104,105]

Recently, Mao *et al.*[106] developed antibiotic-free remarkable nanocomposite hydrogels possessing impressive antioxidant and antimicrobial virtues, utilizing gelatine (Gel), bacterial cellulose (BC) as well as selenium NPs for wound-alleviating applications (Fig. 6). The BC@Gel@SeNPs hydrogel displayed notable mechanical strength, swelling capability, biodegradability, and flexibility, together with a controlled release of selenium NPs. The SeNP decoration endowed the hydrogels with outstanding antioxidant and anti-inflammatory capacities. The BC/Gel/SeNP hydrogel demonstrated remarkable wound healing capabilities owing to the collaborative effect of the Gel and SeNPs. It accelerated the *in vivo* wound healing process by lessening inflammatory responses, increasing wound closure, promoting granulation tissue formation, encouraging collagen deposition, stimulating angiogenesis, and activating and differentiating fibroblasts into myofibroblasts (Fig. 6).

Wang *et al.*[107] developed a novel approach to wound healing by incorporating antimicrobial peptides (AMPs) and collagen III (Col III) into microneedle (MN) patches. These patches were designed to release AMPs and Col III slowly and in a controlled manner, targeting deep wound tissues. By encapsulating AMPs in a chitosan (CS) and gum arabic (GA) based nanogel and embedding them within microneedle patches, the researchers improved the stability and biocompatibility of the AMPs. Once the MN patches penetrated the biofilm formed by *Staphylococcus aureus*, they dissolved and released CGA-NPs. These nanoparticles then responded to the infected sites, efficiently killing the bacteria. Simultaneously, Col III facilitated wound healing, making this dual-action delivery

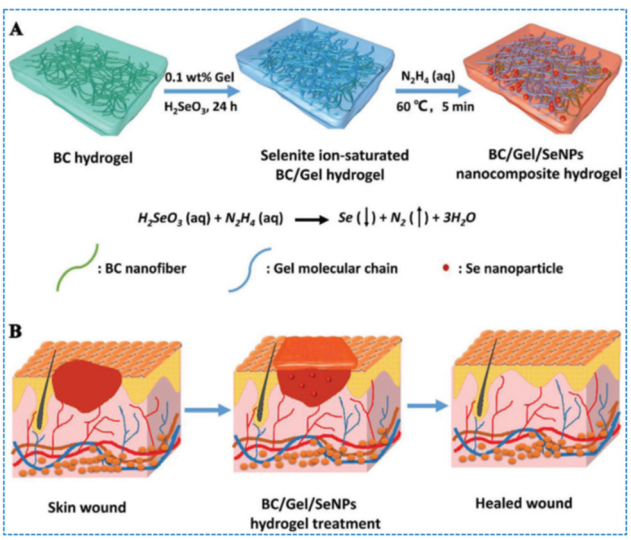

Fig. 6 Schematic representation (A) of BC/Gel/SeNPs nanocomposite hydrogel synthesis; (B) applicability of the synthesized hydrogel in healing a wound. Reprinted with permission from ref. 106. Copyright 2021, Wiley-VCH GmbH.

system a promising solution for treating infected wounds. The study observed wound healing in mice over a period of 10 days following six different treatments (see Fig. 7A and B). The treatments worked efficiently against *S. aureus*. The other treatments lacking antimicrobial potential toward *S. aureus* had the largest scar areas and showed a significant presence of *S. aureus* in skin tissue. In contrast, NP-based treatments were reported to be potent bactericidal agents. Moreover, the sustained release of CGA-NPs from the microneedles further contributed to preventing the recurrence of *S. aureus* infections. This prolonged release ensured that the bacteria were not only killed initially but that any remaining bacteria were also continuously targeted, reducing the likelihood of reinfection and promoting more effective wound healing.

Hematoxylin and eosin staining of the affected tissue was conducted to further assess the wound-alleviating effects across different treatment groups (Fig. 7C). In the synthesized nanocomposite, the H&E staining results confirmed the superior healing outcomes, indicating successful re-epithelialization. Additionally, the formation of hair follicles and blood vessels was observed, suggesting that the underlying tissue structures were being effectively restored. These findings reinforced that the MN/PVP + Col III + CGA-NP treatment provided the best overall wound-healing effect among the groups studied.

4. Cancer treatment using smart nanomaterials

Cancer cells have quite a survival toolkit. Their ability to adjust and thrive under harsh conditions like low oxygen or limited nutrients is one reason why treating cancer can be so challenging.[108,109] The classification of cancer into solid and liquid tumours is indeed important, as it affects how they are diagnosed and treated. Traditional therapies like surgery, chemotherapy, and radiation therapy have been the mainstays for a long time, but they do come with limitations and potential side effects.[110] Theranostic nanomedicines, however, show great promise in cancer treatment. Their ability to detect specific cancer biomarkers and simultaneously deliver therapeutic agents can lead to more targeted and effective treatments. Nanotheranostics can combine multiple functionalities in a single nanosystem, such as drug delivery, imaging, and targeting, thus streamlining the treatment process, and reducing the need for multiple interventions.[111] This can be particularly beneficial for early-stage cancers or localized tumours where precise and localized treatment is crucial.

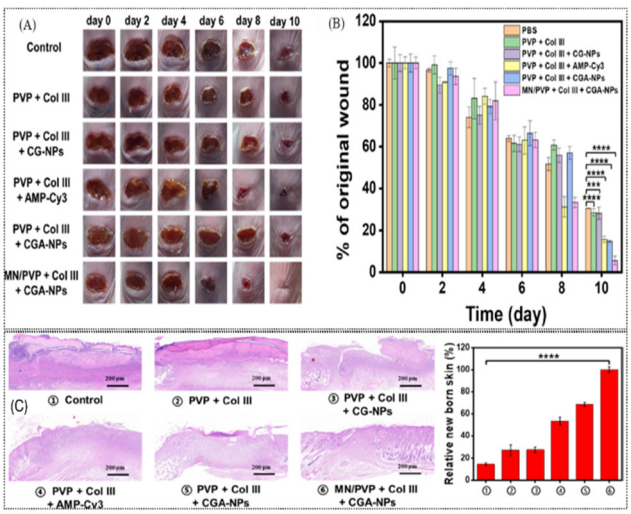

Fig. 7 Healing of wounds of mice over a period of ten days. (A) Wound pictures and (B) wound area quantification of infected mice for divergent treatment groups over a period of 10 days. (C) Pictures with H&E staining and quantification of data of the newborn skin of the wounded tissue of infected mice for divergent treatment groups on the 10th day. Reprinted with permission from ref. 107. Copyright 2023, American Chemical Society.

4.1. Advantage of smart nanomaterials over conventional nanomaterials in cancer therapeutics

Tumours often have an acidic microenvironment (pH ~ 6.5–6.8). Smart nanomaterials utilize acid-labile linkers (*e.g.*, hydrazone, imine, *etc.*) that break at tumour pH to release the encapsulated/tethered drug.[112] Intracellular GSH levels are 100–1000 times higher than extracellular ones. Smart nanomaterials with disulfide and diselenide linkers degrade in high-GSH environments, promoting intracellular drug release. Overexpressed enzymes like MMP-2 and cathepsin B in tumours can cleave the peptide and polymeric shells of smart nanomaterials, exposing the active core.[113] Photothermal agents (*e.g.*, GNRs, carbon nanodots, *etc.*) convert NIR light to heat, causing local hyperthermia for tumour ablation or drug release. Key advantages of smart nanomaterials over conventional nanomaterials utilized in cancer theranostics have been summarized in Table 5.

4.2. Cancer treatment using smart inorganic nanomaterials

Inorganic NMs, particularly metal (gold, iron, zinc, silver, *etc.*) and rare-earth metal NPs (*e.g.*, lanthanum oxide and ytterbium oxide), have garnered remarkable interest in biomedical applications owing to their distinct physical and chemical virtues at the nanoscale. Silica NPs are also widely used due to their biocompatibility, ease of functionalization, and low toxicity.

4.2.1. Cancer treatment using gold nanoparticles. The simple production, large surface area, high stability, surface plasmon resonance (SPR), multi-functionalization, and customizable surface chemistry of gold nanoparticles (AuNPs) makes them tremendously useful in the diagnosis of several malignancies and the delivery of medications. The exceptional optical and physical properties of GNRs, nanocubes, nanostars, nanospheres, and nanocages make them appealing for targeted delivery of drugs, photodynamic therapy (PDT), photothermal therapy (PTT), photoimaging, and biosensors to diagnose and treat tumours.[114,115]

Xu *et al.*[116] developed a sophisticated nanoplatform for targeted and combination therapy for breast cancer, incorporating GSH, hyaluronidase (HAase), and pH sensitivity. GNRs

Table 5 Summary of advantages of smart nanomaterials over conventional nanomaterials utilized in cancer therapy

S. no.	Feature	Conventional nanomaterials	Smart nanomaterials
1	Design philosophy	These are inert or passive carriers of therapeutic agents, generally lacking stimulus-responsive features	These are engineered with stimulus-responsive and multifunctional components that actively respond to tumour microenvironment (TME) or external signals
2	Targeting mechanism	These generally rely on passive targeting *via* the enhanced permeability and retention (EPR) effect	These use active targeting through ligand–receptor interactions (*e.g.*, folate), combined with stimulus-triggered release (*e.g.*, ROS, pH, enzymes, temperature, *etc.*)
3	Drug release kinetics	Uncontrolled release may result in premature drug leakage and systemic toxicity	Controlled and on-demand release triggered by tumour-specific stimuli, minimizing off-target effects
4	TME responsiveness	These lack sensitivity to tumour-specific features (*e.g.*, hypoxia, acidic pH, high GSH, MMPs, *etc.*)	These incorporate smart moieties (*e.g.*, redox-cleavable linkers, pH-sensitive bonds, enzyme-sensitive shells, *etc.*) to exploit TME characteristics for site-specific activation
5	Therapeutic modalities	These are primarily responsible for chemotherapeutic drug delivery. These have limited potential for combinatorial or synergistic effects	These are enabled with multimodal therapy (*e.g.*, chemotherapeutic-photothermal, chemotherapeutic-immunotherapeutic, PDT/PTT + gene therapy), boosting efficacy and overcoming resistance
6	Tumour penetration	Often limited due to size, lack of dynamic size/charge modulation	Smart systems can shrink, swell, and switch charge for deep tumour penetration and intracellular delivery
7	Biodistribution and clearance	Due to limited biodegradability there is a risk of accumulation in the reticuloendothelial system	Surface functionalization (*e.g.*, PEGylation) and biodegradable cores improve circulation and clearance, and reduce accumulation in the reticuloendothelial system
8	Therapeutic resistance management	Less capable of addressing MDR mechanisms	These can bypass MDR by targeting specific pathways (*e.g.*, endosomal escape, mitochondrial targeting, efflux pump inhibition, *etc.*)
9	Diagnostic integration	Rarely include imaging agents or real-time tracking capability	These are designed as theranostic platforms integrating imaging (*e.g.*, magnetic resonance imaging, computed tomography, fluorescence, *etc.*) for precision medicine
10	Clinical translation potential	These are easier to scale and standardize; several approved for clinical use (*e.g.*, Doxil)	These are more complex in design and regulation, but offer superior specificity, lower toxicity, and a higher therapeutic index in preclinical models

were initially encased with hydrazide and thiol di-functionalized hyaluronic acid (HA) *via* Au–S linkages. Cy7.5 imaging agent and 5-aminolevulinic acid (ALA) photosensitizer were then covalently conjugated onto the HA for fluorescence imaging and PDT, respectively. Anti-HER2 antibodies, being highly specific for HER2 receptors, were fixed onto the HA to get the multifunctional nanomaterial (Fig. 8). The NM is designed to exploit the dual receptor-mediated endocytosis of CD44 and HER2, leading to high tumour accumulation.

As all know, cancer cells typically exhibit a more acidic microenvironment and higher concentrations of HAase and GSH. This triggers the liberation of ALA and Cy7.5 within tumour cells. Intracellularly, the HA coating is degraded by the enzyme HAase and GSH, further enabling the release of Cy7.5 and ALA. Upon near-infrared (NIR) irradiation guided by fluorescence imaging, the dual-targeting and triple-responsive nanoframework (GNR-HA-ALA/Cy7.5-HER2) achieves superb remedial efficacy. The combination of PDT and PTT in a targeted manner enhanced treatment effects and minimized detrimental effects.

Recently, Liu *et al.*[117] presented an intriguing study that investigates how the surface chemistry of NPs can influence their behaviour in biological systems, particularly focusing on blood circulation time and targeting efficiency. The study involves AuNPs, a tumour-targeting peptide (Pep2), a zwitterionic peptide (for instance, EK), and fat (for instance, stearine) separately or in combination. The study presents a model system using Pep2-functionalized gold NPs (AuNPs-Pep2) that are designed to be similar in physical properties (size, shape, elasticity, *etc.*) but different in surface composition. The study further employs engineering strategies, such as modification of EK and EK-fat for modifying the surface of AuNPs-Pep2 nanoparticles. These modifications are designed to enhance the binding efficacy of the nanoparticles to tumorous cells and improve their targeting efficiency (Fig. 9). Preliminary results from *in vitro* experiments demonstrate that the modified nanoparticles exhibit higher binding affinity to tumour cells compared with unmodified AuNPs-Pep2 nanoparticles. Additionally, *in vivo* experiments show that the engineered AuNPs-Pep2-EK-fat nanoparticles achieve significantly higher rates of accumulation in tumourous areas of mice.

4.2.2. Cancer treatment using iron oxide nanoparticles. Iron oxide nanoparticles (IONPs) have enormous potential in theranostics due to their distinct characteristics like biocompatibility, magnetic properties, and tunable surface chemistry.[118,119] They can be coated with drugs and functionalized with targeting molecules (*e.g.*, antibodies, aptamers, *etc.*) that bind to cancer cells. Upon reaching the tumour site, the drug can be released in a controlled manner, reducing various systemic ramifications and ameliorating the therapeutic index.[120] They engender heat after exposure to a magnetic field.[121] This heat can be used to selectively demolish carcino-

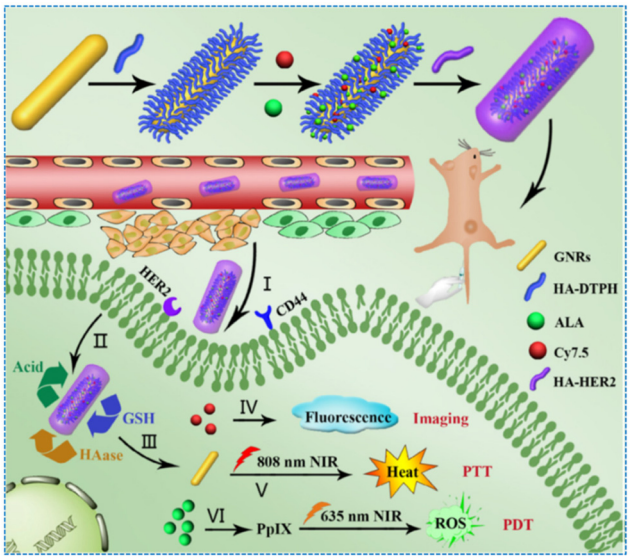

Fig. 8 Schematic depiction of GNRs and combination therapy for treating breast cancer. (I) The nanoplatform accumulates at the tumour area *via* the EPR (enhanced permeability and retention) effect, taking advantage of the leaky vasculature found in tumours. (II) The nanoplatform is identified by HER2 and CD44 receptors present on the tumour surface. Subsequently, it undergoes internalization into the tumour cells. (III) The acidic microenvironment of the tumour triggers the liberation of 5-aminolevulinic acid (ALA), a photosensitizer utilized in PDT. The hyaluronic acid (HA) coating on the nanoplatform is deteriorated by GSH and the enzyme hyaluronidase, further smoothing the liberation of Cy7.5 and ALA. Reprinted with permission from ref. 116. Copyright 2019, Elsevier.

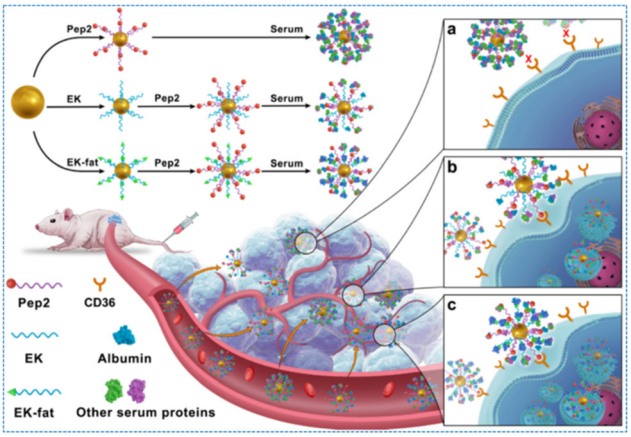

Fig. 9 The pictorial representation of fabrication of Pep2-functionalized gold NPs (AuNPs-Pep2) and their interaction with tumour cells highlights the importance of surface chemical properties in nanoparticle–cell interactions. (a) The AuNPs-Pep2 encounter a challenge in cell recognition because their surface becomes covered by a protein corona. This corona, composed of plasma proteins, can hinder the direct interaction between the nanoparticles and the CD36-overexpressing tumour cells. (b) To address the recognition blockade caused by the protein corona, EK peptides are added to the nanoparticle surface. These peptides help reduce the adsorption of plasma proteins on the NPs' surface. As a result, the nanoparticles become more accessible for correct recognition and internalization by the CD36-overexpressing tumour cells. (c) Further optimization is achieved by adding EK-fat peptides to the nanoparticle surface. These peptides alter the composition of the protein corona, leading to an increase in the amount of albumin while reducing the presence of other proteins. This compositional change in the protein corona facilitates the correct recognition and internalization of the nanoparticles by the tumour cells. Reprinted with permission from ref. 117. Copyright 2023, Elsevier.

genic cells together with not harming close healthy tissues. They are targeted to the tumour site, and when exposed to the magnetic field, they increase the temperature of the tumour cells to a level that induces apoptosis/necrosis. They also possess superparamagnetic properties, making them highly useful in MRI (magnetic resonance imaging) as contrast agents. Their magnetic behaviour can be exploited to guide nanoparticles to specific locations in the body using external magnetic fields, which is particularly useful in target-based drugs.[122,123] Recent reports have demonstrated that IONPs coated with responsive polymers exhibit different behaviours in response to variations in temperature and pH gradients.[124,125]

Recently, Li *et al.*[126] developed an impressive nanodrug called OPPL that combines oleic acid-amended superparamagnetic IONPs (O-SPIONs) with PPL polymer to deliver both a platinum prodrug and lauric acid for treating colorectal cancer (CRC), as shown in Fig. 10. OPPL demonstrates synergistic enhancement of biofilm disruption effects toward Fn (*Fusobacterium nucleatum*) when combined with the antimicrobial LA. This synergy is achieved through the production ROS *via* the nanodrug's peroxidase-like activity. OPPL increases intracellular ROS levels, promotes lipid peroxides, and depletes glutathione, ultimately leading to ferroptosis. This mechanism enhances the cytotoxicity of the nanodrug against CRC cells. *In vivo* studies demonstrate several favour-

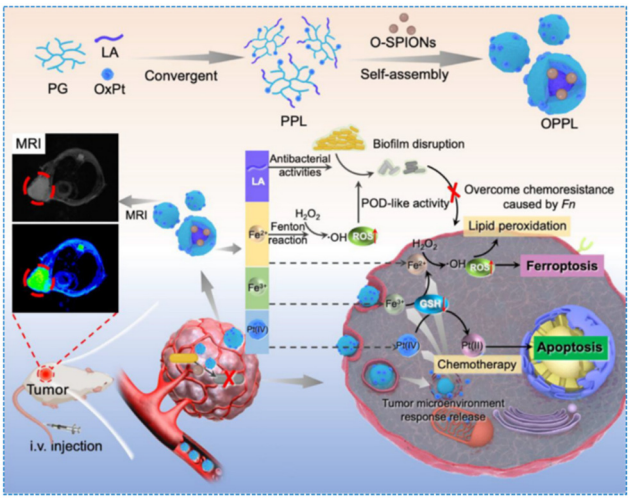

Fig. 10 Schematic illustration of development of the multifunctional nanodrug (OPPL), with integration of antimicrobial properties with targeted cancer therapy to address both the bacterial infection and the cancer cells, ultimately improving treatment outcomes for Fn-infected CRC. Reprinted with permission from ref. 126. Copyright 2024, Elsevier.

able outcomes: (i) OPPL shows increased accumulation at tumour sites, likely due to its design and magnetic properties. (ii) The nanodrug enables magnetic resonance imaging, furnishing a minimally intrusive means of monitoring tumour response and drug distribution. (iii) OPPL inhibits tumour growth effectively. (iv) The nanodrug also inhibits the growth of Fn within the tumour environment, which is crucial for CRC infected with this bacterium.

4.2.3. Cancer treatment using mesoporous silica nanoparticles (MSNs). According to IUPAC (International Union of Pure and Applied Chemistry), mesoporous materials are characterized by having pores of diameters ranging from 2 to 50 nm.[127] MSNs have gained extensive interest due to their tunable particle sizes (*e.g.*, 50 to 300 nm), large surface areas, homogeneous as well as adjustable pore sizes (*e.g.*, 2 to 6 nm), high pore volumes, and biocompatibility. MSNs are particularly valuable as smart nanocarriers in drug-releasing systems owing to their tunable particle size and configurable pore size, allowing the loading of drugs in divergent molecular forms. The high surface areas of both the interior pores and the external surfaces are ideal for grafting various functional groups, enhancing their functionality. MSNs are advantageous for cancer treatment as they can adhere to tumours by the EPR effect.[128] Their biocompatibility ensures minimal toxicity to healthy cells.

Conventional MSNs face several challenges, such as nonspecific binding to human serum proteins, hemolysis of RBCs, and phagocytosis by macrophages. These issues contribute to the short blood circulation half-lives of these conventional MSNs. However, various strategies can be employed to overcome these limitations and enhance their functionality as smart nanocarriers. Poly(ethylene glycol) (PEG) can be grafted onto the surface of MSNs to create a stealth layer, reducing immune recognition and clearance. This modification helps in prolonging the blood circulation time of MSNs by minimizing hemolysis, nonspecific protein binding, and phagocytosis.[129] Co-polymers can be grafted onto MSNs to control the pore openings of MSNs. For example, poly(*N*-isopropylacrylamide) fastened to hollow MSNs can switch the nanochannels between "open" as well as "closed" states in response to temperature changes, enabling on-demand loading and release of small molecules.[130] The surface of MSNs can be adjusted with targeting ligands, like folate, peptides, mannose, and transferrin protein. These modifications facilitate active targeting to cells and/or tissues, enhancing the therapeutic productiveness and eliminating off-target effects.[131,132] Smart MSNs are engineered to release their loaded drugs responding to various stimuli (*e.g.*, pH, redox reaction, magnetic field, temperature, light, *etc.*), enhancing their functionality and specificity in drug delivery.[133]

Zhang *at el.*[134] developed a redox and pH dual-responsive targeted drug release system employing hollow MSNs (HMSNs) grafted with bovine serum albumin–folic acid (BSA-FA), termed HBF, through imine bonds for the responsive and targeted delivery of doxorubicin (DOX) and methylene blue (MB), termed MD@HBF. The engineered HBF nanoparticle serves as a carrier for the drugs. This targeted delivery enhances the therapeutic effect while minimizing damage to healthy cells. The use of combination therapy is emphasized as an effective approach to address the limitations of monotherapy and enhance therapeutic efficacy. In this case, the combination involves both chemotherapy (DOX) and photodynamic therapy (MB), offering a synergistic effect against cancer cells. *In vitro* experiments, including cell uptake studies and toxicity assays, validate the efficacy and safety of MD@HBF. The *in vivo* study demonstrates the induction of apoptosis in cancerous cells (Fig. 11). The combination of chemophotodynamic therapy employing MD@HBF shows outstanding synergistic killing efficiency against cancer cells, as indicated by a low combination index (CI = 0.325).

4.2.4. Cancer treatment using quantum dots. Quantum dots (QDs) are semiconductor NPs that exhibit distinct optical and/or electronic characteristics, making them highly suitable for various biomedical applications, including cancer therapy.[135] QDs can be synthesized employing a top down/bottom-up scheme, each with its distinct techniques and advantages. Ion implantation, molecular beam epitaxy, and X-ray lithography are common top-down techniques to synthesize QDs.[136] In contrast, a bottom-up strategy involves the assembly of QDs from atomic or molecular precursors. This approach is often employed to create colloidal QDs. Chemical reduction, self-assembly, and surface passivation are the key steps in the bottom-up synthesis of colloidal QDs.[137] Due to their tunable fluorescence, high brightness, and stability, QDs have been explored for imaging, diagnosis, and cure of cancer. Commercially available QDs are typically composed of three main components: the core, the shell, and a capping sub-

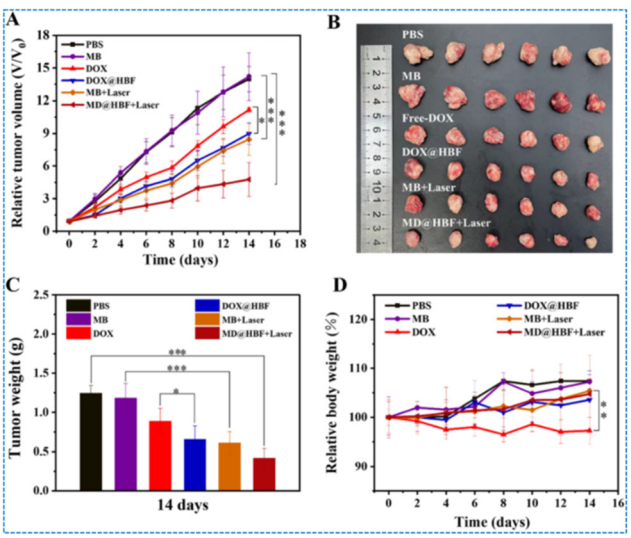

Fig. 11 (A) Variation of tumour volume with time. (B) Representative images of tumours of rats supplied with control (PBS), DOX, MB, MB + Laser, DOX@HBF, and MD@HBF + Laser. (C) Tumour weight variation after treatment over the period of 14 days. (D) Mouse weight variation during the treatment period of fourteen days. Reprinted with permission from ref. 134. Copyright 2023, Elsevier.

stance. The core of a QD is made from semiconductor materials and is primarily responsible for the QD's optical properties, such as fluorescence and emission wavelength. The choice of material and the size of the core determine the specific colour of light emitted by the QD when excited. Common semiconductor materials used for the core include cadmium selenide and telluride. The core's size and composition control the quantum confinement effect, which dictates the emission wavelength and brightness.

The shell is constructed around the semiconductor core to enhance the QD's optical properties and stability. The shell material (*e.g.*, zinc sulphide) is typically another semiconductor with a wider bandgap than the core. The shell passivates the core surface, reducing non-radiative recombination sites and thereby increasing the quantum yield (brightness) of the QDs. It protects the core from oxidation and other environmental factors, enhancing the stability and durability of the QDs. The shell can improve the biocompatibility of QDs for biological applications. Organic molecules, polymers, silica, *etc*. are used for capping. The capping layer stabilizes, solubilizes, and functionalizes the QDs. QDs functionalized by targeting ligands (*e.g.*, antibodies, peptides, proteins, and folate), can bind to cancer cells, enabling precise imaging and localization of tumours.[138] They can be conjugated with drugs or therapeutic agents for targeted delivery, reducing off-targets and enhancing therapeutic efficacy. They can also serve as photosensitizers, generating ROS upon light activation to kill cancer cells.

QDs, like many NPs, are taken up non-specifically by the reticuloendothelial system. They accumulate in tumour tissues due to the EPR effect. This phenomenon occurs because tumour vasculature is often more permeable than normal blood vessels, allowing nanoparticles to pass through and remain in the tumour environment. The fluorescence properties of QDs make them highly effective for visualizing cancer cells and tissues, providing several advantages over traditional imaging agents. For instance, QDs with a copper indium selenide (CISe) core and a zinc sulphide (ZnS) shell, doped with manganese (Mn) and functionalized with folic acid, were produced, which exhibited 31.2% fluorescence efficiency.[139]

4.3. Cancer treatment using polymer-based smart nanocarriers

Polymer-based smart nanocarriers are gaining significant attention for their potential in cancer treatment. These nanocarriers are designed to improve the targeted delivery of anticancer drugs, minimize side effects, and enhance therapeutic efficacy by exploiting the unique properties of polymers.[140,141]

4.3.1. Cancer treatment using polymeric nanomaterials. Polymeric NPs (PNPs) mark a significant advancement in biomedical applications, fostering collaboration among various disciplines like biology, chemistry, engineering, and medicine. This convergence has spurred a medical revolution, resulting in remarkable progress in medicine delivery, biomaterials, and tissue engineering.[142,143] The discovery of PNPs has paved the way for more effective treatments utilizing nucleic acids, proteins, and other active molecules.[144] This interdisciplinary approach has greatly enhanced our ability to deliver therapies with precision and efficacy, leading to transformative impacts in healthcare.

PNPs have a variety of advantages over traditional drug formulations in terms of stability, structural decomposition, premature release, and nonspecific release kinetics. Additionally, the ability to combine materials with divergent chemical compositions allows for the fabrication of nanoparticles with synergistic characteristics. The most employed techniques for preparing PNPs include emulsion polymerization, dialysis, solvent evaporation, *etc*. Incorporating biological response elements into polymer designs is a cutting-edge strategy. By leveraging biological cues or processes, such as specific enzyme activities or pH levels in different tissues, researchers can attune medicine release profiles for enhanced therapeutic outcomes. Polymers like poly(D,L-lactic-*co*-glycolic acid) (PLGA), being biodegradable as well as biocompatible, can be employed for controlled drug release. Its properties can be manipulated by adjusting factors like drug concentration and lactide to ethyl ester ratio, allowing for customized release kinetics. The hydrophobic nature of PLGA, in combination with methyl groups, influences water absorption and degradation rates. Increasing polylactic acid content typically reduces water absorption, slowing down degradation and prolonging the liberation of encased drugs.

Chansaenpak *et al.*[145] presented an aza-BODIPY derivative based nanosystem (AZB-CF3@DSPE-PEG NPs) for cancer treatment, which exhibited outstanding photostability as well as colloidal stability. The nanoparticles exhibited good biocompatibility both *in vitro* (cell cultures) and *in ovo* (chicken egg model). The nanoparticles demonstrated high PTT efficacy, suitable for cancer treatment. When tested on 4T1 breast cancer cells, the NPs (containing 20 μM AZB-CF3) combined with 5 minutes of 808 nm laser irradiation resulted in approximately 10% cell viability, indicating significant cancer cell death (Fig. 12). The NPs also showed properties that inhibit

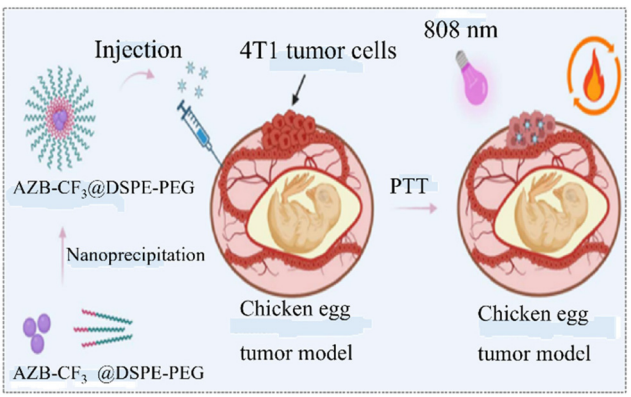

Fig. 12 Schematic representation of the synthesis of polymeric nanoparticles and their usage in the treatment of cancer based on the photothermal effect in the chicken egg tumour model. Reproduced with permission from ref. 145. Copyright 2024, Royal Society of Chemistry.

angiogenesis and metastasis. Approximately 40% vascular destruction was observed in the chicken egg tumour model.

4.3.2. Cancer treatment using dendrimers. Dendrimers have a nanoscale, spherical, and/or symmetrical make-up characterized by their tree-like branches or arms.[146] The outer layer is made up of functional groups employed for drug/medication conjugation and targeting, enhancing drug encasing efficacy, reducing drug toxicity, and facilitating controlled deliverance mechanisms within the inner layer.[147] Dendrimers can be customized and modified in various ways, leading to the creation of numerous molecules with specified characteristics and functions. In the divergent method, dendrimers grow from the inside out, with layers being added progressively from the core to the periphery. In contrast, the convergent method involves growth from the outside in, where dendritic branches are synthesized separately and then attached to a central core. These methods were originally developed to create dendrite structures.[148] The ability to control the properties of dendrimers during synthesis makes them highly promising for various pharmaceutical applications.[149]

Recio-Ruiz *et al.*[150] reported a carbosilane-based dendrimer that improves compatibility with lipophilic drugs and enhances nanostructures properties owing to the lipophilic, stable, and inert essence of the carbosilane scaffolds. For instance, delivering drugs to the central nervous system, which is typically hindered by the blood–brain barrier, can be obtained by linking the medication to a polyamidoamine dendrimer, allowing it to overcome this barrier.[151] Polylysine dendrimers show potential as biodegradable carriers that can deliver cytotoxic medications to solid tumours.[152]

Lee *et al.*[153] integrated an active therapeutic agents' delivery system with stimulus-controlled drug in a single nanocarrier, utilizing HA-modified dendrimers encasing gold NPs (AuDEN) for treating ovarian cancer (Fig. 13). HA was utilized due to its ability to target cluster determinant 44 (CD44)-overexpressing cancerous cells. DOX is loaded onto the nanocarriers by self-assembling thiolated DOX on the gold surface, resulting in high drug loading content and chemical stability. The high glutathione concentration and tumour acidic (pH 5.6) microenvironment control the release of the medications. In comparison with free DOX, the nanocarrier exhibited more cytotoxicity towards cancer cells.

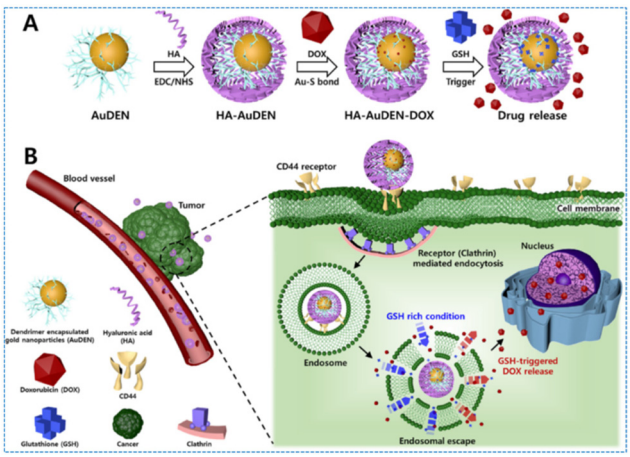

Fig. 13 Schematic representation of (A) the HA-AuDEN-DOX synthesis protocols; and (B) mechanisms of delivery of DOX, HA, and HA-AuDEN-DOX for treating ovarian cancer, facilitating a better understanding of the overall process and its therapeutic potential. Reprinted with permission from ref. 153. Copyright 2022, Elsevier.

4.3.3. Cancer treatment using micelles. Polymer micelles are fascinating nanostructures that have gained significant attention in biological applications owing to their distinct properties. Their size normally varies from 10 to 100 nm and they are composed of two distinct regions: the core part (being colloidally stable) and the outer part, also known as the shell or corona region, which consists of solvated hydrophilic polymer chains. In contrast, reverse micelles feature a hydrophobic corona and a hydrophilic core.[154] The unique structure and properties of micelles, particularly their corona–core arrangement, enhance the solubility of hydrophobic substances in water. Consequently, polymeric micelles can encapsulate amphipathic drugs, making them highly valuable in biomedical applications. Polymeric micelles are highly effective in encapsulating (solubilizing) hydrophobic drugs within their hydrophobic core. This physical encapsulation offers several significant advantages: (i) encapsulating hydrophobic drugs within the core of polymer micelles can help mitigate or eliminate adverse effects of the drugs, as the encapsulation can prevent direct interaction of the drug with healthy tissues; (ii) enhancement of water solubility of hydrophobic and insoluble drugs. This escalated solubility improves the bioavailability and therapeutic efficacy of these drugs; (iii) the tuned structure of polymer micelles provides control over the drug release rate precisely. This controlled release can be customized to accomplish sustained or targeted delivery, improving the therapeutic outcomes; and (iv) by encapsulating drugs within their core, polymer micelles protect drug molecules from degradation caused by ecological factors such as pH changes and temperature variations. This protection enhances the stability as well as shelf life of the drugs. Furthermore, advancements in synthetic chemistry have expanded the functionality of polymer micelles.[155]

The employment of long-established polymer micelles for targeting tumours in systemic cancer therapy is an innovative and promising strategy. These nanoscale vesicles, often modified on their surfaces for enhanced functionality, are designed to deliver small anti-tumour molecules, such as paclitaxel, directly to cancer cells. A previous report exhibited preferential accumulation of micelles in the leaky vasculature of tumours due to the EPR effect.[156] The extracellular microenvironment of the tumours was reported to be more acidic than normal tissues and blood due to the high metabolic activity of the cancer cells.[157] pH-Sensitive micelles can be designed to disassemble and release their drug payload in reaction to this acidic environment, providing targeted drug delivery to tumour sites. These smart nanoparticles can target transferrin receptors, which are often overexpressed in cancer cells, allow-

ing for more precise drug delivery.[158] Folate-modified micelles target folate receptors, which are frequently overexpressed in various cancers. This system can efficaciously reduce the systemic adverse effects of doxorubicin, particularly its cardiotoxicity and pulmonary toxicity, while enhancing its anti-tumour efficacy.[159] The pH-sensitive together with thermosensitive polymeric micelles can exploit the tumour's acidic environment and heat produced by PTT. This dual-responsive approach allows for controlled drug release, making it suitable for combined chemophotothermal cancer treatments.[160]

PLA-based micelles, particularly those composed of diblock copolymers, MPEG-SS-PMLA, represent a propitious technique for enhancing cancer therapy through the effective delivery and controlled release of ruthenium complexes.[161] Their high drug-loading capacity, sensitivity to the tumour microenvironment, and ability to induce targeted apoptosis *via* PDT highlight their potential in advancing cancer treatment strategies (Fig. 14). These micelles exemplify the integration of nanotechnology and smart drug delivery systems to improve the precision and efficacy of cancer therapies.

4.4. Cancer treatment using biomimetic smart nanocarriers

Biomimetic nanocarriers are designed to mimic natural biological structures and processes, enhancing their ability to specifically target cancer cells and deliver therapeutic agents effectively.[162]

4.4.1. Cancer treatment using liposomes. Liposomes are a type of amphipathic NP characterized by a membrane-like structure composed primarily of phospholipids. These phospholipids are made up of a phosphatic hydrophilic (water-attracting) head and a fatty acidic hydrophobic (water-repelling) tail. Liposomes have a fascinating cell-like structure that makes them versatile carriers for various types of drug, both lipid-soluble and water-soluble. This dual compatibility allows liposomes to carry a wide range of drugs. Multi-lamellar vesicles (MLVs) contain multiple lipid bilayers and are larger in size. They can carry a higher payload but may have slower release kinetics. Uni-lamellar vesicles (ULVs) have a single lipid bilayer and come in different sizes.[163] Liposomes can fuse with cell membranes, facilitating the delivery of encapsulated drugs directly into cells. This mechanism of cellular uptake is advantageous for targeted drug delivery and improving therapeutic efficacy.

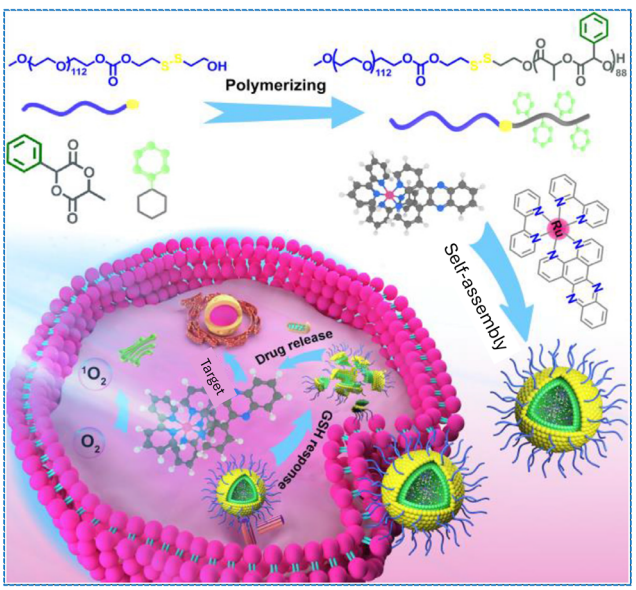

Fig. 14 Pictorial representation of biodegradable Ru-accommodating polylactide MPEG-SS-PMLA@Ru micelles for increased delivery of Ru(II) polypyridyl complexes and cancer phototherapy. The disulfide bonds in the micelles are sensitive to the reductive environment found in tumours, where the GSH concentration is significantly higher than in normal tissues. Reprinted with permission from ref. 161. Copyright, 2023, Elsevier.

While conventional techniques for liposome preparation have been widely used, they come with limitations such as solvent residues, heterogeneous size distribution, and scalability issues. Innovative technologies leveraging supercritical fluids offer potential solutions by providing more environmentally friendly, efficient, and scalable methods for liposome production.[164] By incorporating PEGylation, stimulus-responsiveness, and radiolabelling, the smart liposomes provide improved stability, targeted delivery, and multifunctional capabilities, enhancing their potential for effective drug delivery, diagnostics, and therapeutic applications.[165–167]

Lee *et al.*[168] generated liposomes by combining DSPE and DSPE-PEG-2k lipids, loaded them with DOX and PTX (commonly used chemotherapeutic agents), and explored the effects of LED (light-emitting diode) irradiation on their structure and drug-loading capability. LsLipo (LED-irradiated liposomes) displayed rougher and more irregular surfaces than NsLipo (non-irradiated liposomes). LED irradiation increased the loading efficiency of PTX and DOX in the liposomes. The structural changes, for instance reduced membrane rigidity, likely facilitated better encapsulation of the drugs. Additionally, in a breast cancer mouse model, these LED-irradiated liposomes demonstrated a therapeutic effect by effectively reducing the size and weight of the tumours (Fig. 15B–G). Fig. 15A shows the injection of LsLipo and NsLipo into nude mice tumours. The tumours treated with LsLipo were smaller compared with the bigger NsLipo-treated tumours (Fig. 15B). As compared with conventional liposomes, LsLipo treatment caused a huge decrease in growth rate of the tumours (Fig. 15C). LsLipo@N holding greater amounts of PTX and DOX led to a larger *in vivo* anticancer effect and smaller tumour growth compared with NsLipo and LsLipo@B (Fig. 15D and E). The very few body weight differences between the different groups show the non-toxic nature of the liposomes, which caused no side effects in the mice (Fig. 15F). Tumour tissue analysis results showed the highly porous appearance of the liposome-treated tumour tissues due to increased tumour cell death compared with the dense tumour tissues of control mice (Fig. 15G).

4.4.2. Cancer treatment using protein nanoparticles. Protein NPs have transpired as a propitious strategy for cancer treatment, offering targeted delivery, controlled release, and

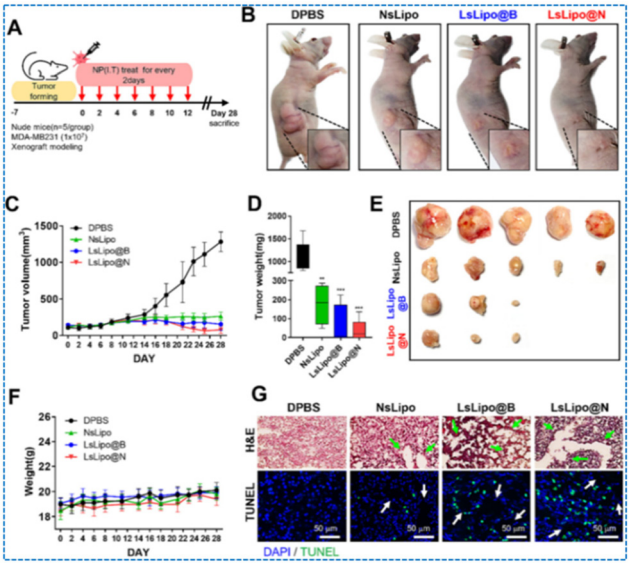

Fig. 15 (A) Injection of LsLipo and NsLipo into nude mice tumours; (B) LsLipo-treated tumours were reported to be smaller than the NsLipo treated tumours; (C) as compared with conventional liposomes, LsLipo treatment caused a huge decrease in growth rate of the tumours; (D and E) LsLipo@N holding greater amounts of PTX and DOX led to a larger *in vivo* anticancer effect and smaller tumour growth compared with NsLipo and LsLipo@B; (F) the very small body weight differences between the different groups show the non-toxic nature of liposomes, which cause no side effects in the mice; (G) tumour tissue analysis results showed a highly porous appearance of liposome-treated tumour tissues due to increased tumour cell death compared with the dense tumour tissues of control mice. Reprinted with permission from ref. 168. Copyright 2024, Elsevier.

reduced side effects compared with conventional treatments. They are simple to synthesize, non-immunogenic, non-toxic, biodegradable, and biocompatible, and have high binding potential with various drugs/medications.[169] The presence of functional groups on protein surfaces allows for easy modification with targeting polymers, ligands, and other molecules, enabling the creation of smart nanoparticles for targeted drug delivery.[170] Albumin, one of the most abundant proteins in plasma, has been widely employed to create NPs for therapeutic systems due to its biocompatibility, non-immunogenicity, and ability to bind various drugs. Doxorubicin-loaded HSA (human serum albumin) NPs have shown more advancements in *in vitro* anticancer potential toward neuroblastoma cell lines compared with the pure drug.[171] PTX-loaded BSA (bovine serum albumin) NPs decorated with folic acid have demonstrated great potential in targeting prostate cancer.[172] This targeted approach increases the uptake of the NPs by cancer cells, enhancing the therapeutic effect of paclitaxel.[173] Abraxane, with a diameter of approximately 130 nm, is the first commercially available nanoparticle drug approved by the FDA. It has shown remarkable effectuality in treating breast cancer and represents a significant advancement in nanoparticle-based drug delivery systems.[174,175]

Recently, Meng *et al.*[176] hypothesized an innovative and promising approach to target tumour cells by leveraging the natural properties of active HSA to deliver the PTEN (phosphate and tensin homology) protein. Leveraging active HSA can facilitate the delivery of PTEN protein into tumour cells *via* Gp60 (albondin)- and SPARC (osteonectin/BM40)-mediated pathways, thereby restoring the tumour suppressor function of PTEN and offering a novel anti-tumour strategy (Fig. 16). The Gp60-mediated pathway leverages the high expression of Gp60 in endothelial cells to facilitate transcytosis and tumour cell targeting. The SPARC-mediated pathway exploits SPARC's overexpression in tumour cells for enhanced albumin binding and internalization.

4.4.3. Cancer treatment using cell membrane nanomaterials. Conventional NPs for cancer therapy face significant challenges, including rapid clearance from the bloodstream, easy recognition and neutralization by the immune system, and insufficient accumulation at target sites.[177] Cell membrane-coated NPs (CMCNPs) are potent bio-inspired NMs to address these issues. The presence of numerous proteins on cell membranes allows CMCNPs to dodge the immune system and enhance the circulation period and target specificity.[177–179] The preparation of CMCNPs involves isolation of cell membranes from the chosen cell source (*e.g.*, cancer cells, platelets, *etc.*) and encapsulation of core nanoparticles within the isolated membrane vesicles, forming CMCNPs.

Liu *et al.*[180] developed core–shell NPs, comprising upconversion NPs (UCNPs) as the core and $Zn_xMn_{1-x}S$ (ZMS) as the shell, coated with BxPC-3 pancreatic cancer cell membranes,

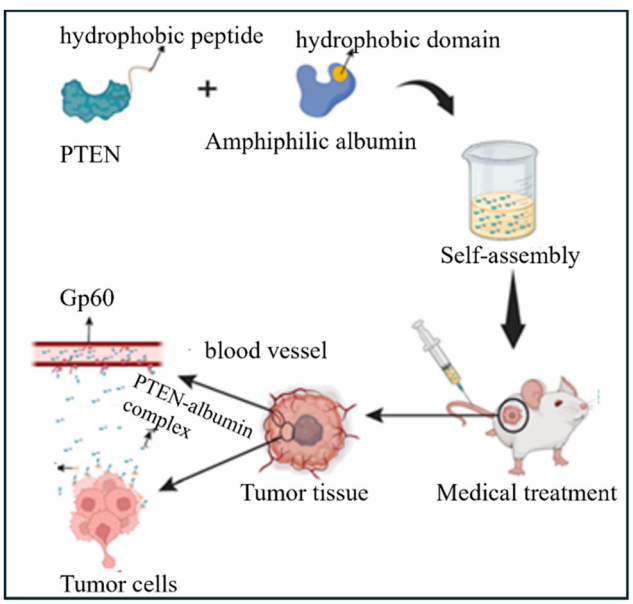

Fig. 16 Schematic illustration of the hypothesis from the formation of PTEN–albumin complexes to their targeted delivery to tumour cells *via* the Gp60 and SPARC pathways, ultimately aiming to restore the tumour-suppressing functions of PTEN within the tumour environment. Reprinted with permission from ref. 176. Copyright 2024, Elsevier.

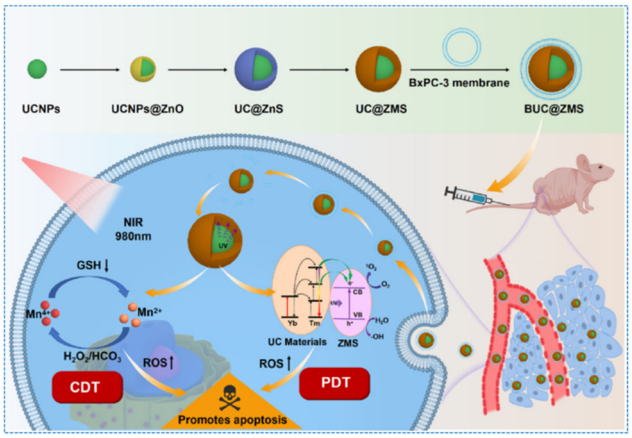

Fig. 17 Schematic representation of the design and functionality of BUC@ZMS core–shell nanoparticles, highlighting their components, mechanisms of action, and therapeutic potential for pancreatic cancer treatment. Reprinted with permission from ref. 180. Copyright 2023, Elsevier.

abbreviated as BUC@ZMS, to enhance homologous targeting and provide a synergistic treatment approach combining CDT and PDT for pancreatic ductal adenocarcinoma (PDAC) (Fig. 17). In the presence of NIR, UCNPs cause ROS generation. Mn ions in ZMS catalyze the Fenton-like reaction, converting hydrogen peroxide (H_2O_2) into hydroxyl radicals ($^{\bullet}OH$), further increasing ROS levels and enhancing the sensitivity of tumour cells to oxidative stress. *In vitro* study confirmed high levels of ROS production in pancreatic cancer cells treated with BUC@ZMS nanoparticles as well as a significant reduction in intracellular GSH levels. *In vivo* study showed that BUC@ZMS nanoparticles accumulate in tumour sites and suppress the growth of PDAC, with minimal observed toxicity to healthy tissues.

4.5. Cancer treatment using carbon-based nanomaterials

Carbon-based NMs have garnered significant attention in cancer treatment owing to their distinct characteristics, like high surface area, chemical versatility, and functionalization with targeting ligands for targeted therapy.[181,182] Graphene's excellent photothermal conversion efficiency makes it suitable for PTT. Upon exposure to near-infrared (NIR) light, graphene can generate localized heat to kill cancer cells. Graphene-based materials can also generate ROS under light irradiation, contributing to PDT. This section provides an overview of the essence of divergent carbon NMs, together with graphene, graphdiyne, fullerenes, carbon nanotubes (CNTs), and carbon quantum dots (CQDs), in anticancer strategies.[181–183]

Being inherently hydrophobic, these carbon NMs are suitable for loading drugs *via* π–π bonding or hydrophobic interactions.[184] Due to their versatile functionalization possibilities, these NMs can be amended with divergent biomolecules covalently as well as non-covalently, which enhances their biocompatibility, water solubility, and biosafety.[185] Moreover, various targeting ligands or functional molecules can be encased into carbon NMs to escalate their targetability.[186] This approach can significantly alter the electronic, mechanical, and chemical properties of NMs. Covalent functionalization involves oxidation, halogenation, amination, click chemistry, nitrene addition, Bingel reactions, addition reactions, cyclopropanations, *etc*. Non-covalent functionalization involves weaker interactions inclusive of van der Waals interactions, π–π stacking interactions, hydrogen bonding, host–guest chemistry, and electrostatic interactions (Fig. 18).[187]

Wu *et al.*[188] developed a nanohybrid drug delivery system sensitive to redox conditions, pH, and enzymatic activity. This system was fabricated *via* assembling GSH-sensitive BSA-encased DOX and MMP-2-sensitive gelatine onto graphene oxide (GO) nanosheets for attaining controlled drug release (Fig. 19). In the TME, which has high levels of proteases, the nanosystem released 5 nm nano-units enveloping DOX. Upon reaching the reductive, acidic, and enzymatic conditions of the tumour tissue, the system enables a synergistic therapeutic effect. This is achieved through the switchable release of DOX, which can be controlled by an irradiating NIR laser. *In vitro* observations showed that the nanosystem could heat up to 45.6 °C after 5 minutes of NIR laser irradiation, ablating MCF-7 cancer cells.

Recently, Zhao *et al.*[189] demonstrated the potential of carbon nanoparticle suspension injection (CNSI) in cancer treatment through the photothermal effect under NIR irradiation. This method effectively eliminates primary tumours and induces immunogenic cell death (ICD). Additionally, when combined with anti-programmed cell death protein 1 (aPD-1) therapy, CNSI under irradiation spurs an immune response that inhibits the growth of distal tumours.

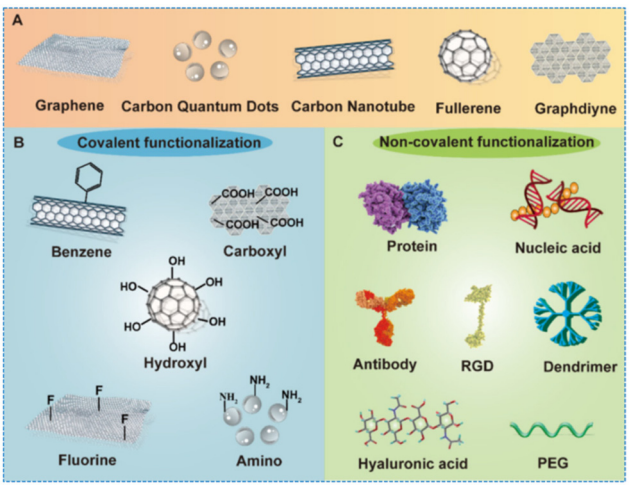

Fig. 18 Schematic showing divergent carbon NMs and strategies of functionalization. Carbon NMs can be functionalized with both covalent and non-covalent methods employing different biomolecules and chemical groups. The functionalized carbon NMs play an exuberant role in targeted drug delivery in cancer treatment. Reprinted from ref. 187. Copyright 2022, The Author(s). This is an open access article distributed under the terms of the Creative Commons Attribution License (https://creativecommons.org/licenses/by/4.0/).

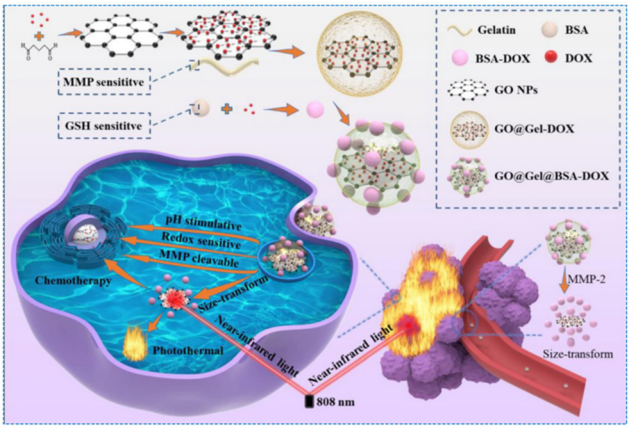

Fig. 19 Schematic illustration of the construction and functional mechanism of GO@Gel@BSA-DOX nanohybrids designed for TME-responsive drug release and cancer treatment. Reprinted with permission from ref. 188. Copyright 2021, Royal Society of Chemistry.

The study also explored the use of phototherapy to treat metastatic lymph nodes. NIR irradiation of CNSI in these nodes eradicates cancer cells and activates the immune response within the lymphatic system. The synergy between CNSI-mediated PTT and aPD-1 therapy significantly boosts the overall antitumour effect (Fig. 20), demonstrating the potential to control and eliminate metastatic disease.

4.6. Cancer treatment using advanced nanomaterials

BP and MOF both represent the forefront of advanced NMs, each offering unique properties and vast potential across various applications.[190] In this section, I have discussed the anticancer applications of BP and MOF.

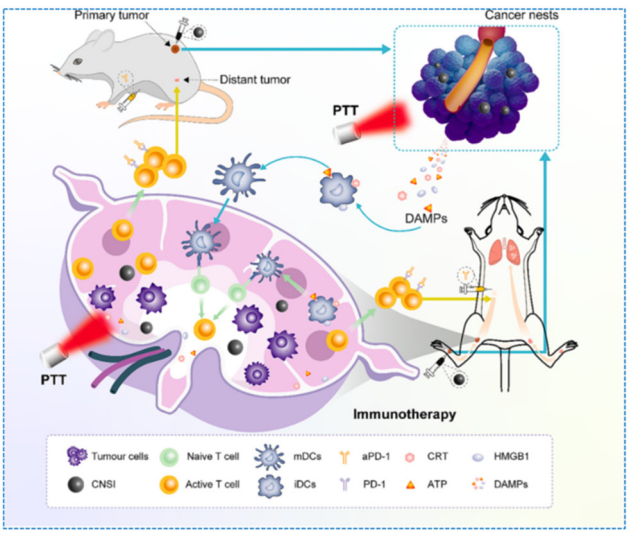

Fig. 20 Schematic representation of carbon nanoparticle suspension injection (CNSI)-mediated PTT and immunotherapy toward cancer metastasis. Reprinted with permission from ref. 189. Copyright 2024, Elsevier.

4.6.1. Cancer treatment using black phosphorus. BP has emerged as a propitious material in cancer treatment, particularly in drug delivery systems and tumour microenvironment modulators, potentially enhancing the immune response against cancer cells.[191,192] It can be used in combination with chemotherapy/radiotherapy to enhance overall treatment efficacy. PEGylated BP nanoparticles are particularly promising as a novel nanotheranostic agent due to their ability to: (i) generate heat from NIR light, which can be used for photothermal therapy to ablate cancer cells; and (ii) provide enhanced contrast for photoacoustic imaging, facilitating better visualization and targeting tumours.[193]

Geng *et al.*[194] reported a significant advancement in the field of pancreatic cancer treatment through the development of an innovative combination chemotherapeutic approach leveraging gemcitabine (GEM) and bioactive black phosphorus. GEM triggers blockage of the cell cycle in the G0/G1 phase. The co-loading of iRGD-amended zein NPs with GEM and BP quantum dots (BPQDs), termed BP-GEM@NPs, ensured direct delivery of the chemotherapeutic agents at the tumour site and enhanced their effectiveness. After intravenous injection, BP-GEM@NPs demonstrated marvellous tumour targeting proficiency, allowing for more sustained therapeutic effects, and a higher rate of pancreatic tumour cell apoptosis (Fig. 21).

4.6.2. Cancer treatment using MOF nanomaterials. MOFs are one- to three-dimensional porous materials made up of

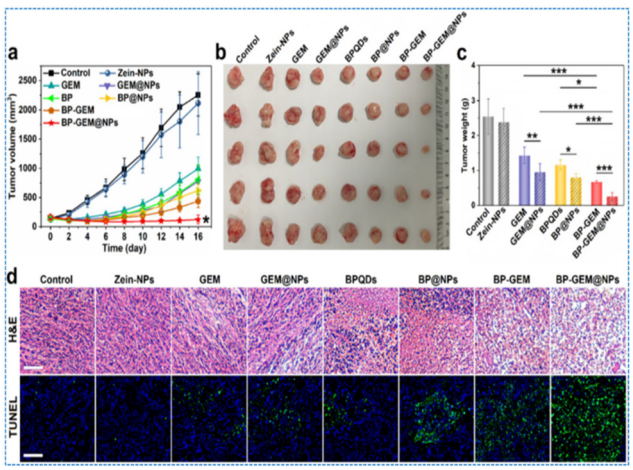

Fig. 21 Synergistic anticancer results of BP-GEM@NPs on tumour bearing mice *in vivo*. (a) Profiles of tumour growth. All the treatments show a clear inhibition of growth of tumour compared with the blank Zein-NPs and control groups, showing chemotherapeutic impacts of GEM and BPQDs toward pancreatic carcinoma. The BP-GEM@NPs averted the tumour growth completely. (b) Photographs showing maximum inhibition of tumour growth by the BP-GEM@NPs. (c) The tumour weights of the BP-GEM@NPs groups are much lower due to prolonged blood circulation and targeted drug delivery effects. (d) Hematoxylin & eosin staining and TUNEL assay show that BP-GEM@NPs cause severe nucleus shrinkage, karyorrhexis, plasmatorrhexis, and a larger degree of apoptosis. Reprinted with permission from ref. 194. Copyright 2023, Elsevier.

metal ions coordinating to organic ligands.[195] Due to their versatile chemical composition and structure, MOFs have gained significant attention in gas storage, separation, catalysis, and biomedical applications. The prominent types of MOF include: (i) zeolitic imidazolate frameworks (ZIFs). ZIFs use imidazole or its derivatives as ligands; (ii) materials of Institute Lavoisier (MIL), for example, MIL-53, MIL-88, and MIL-101; (iii) MOFs with alkaline earth post metals (AEPFs). Metal centers consist of alkaline earth metals such as calcium, strontium, and magnesium; (iv) MOFs with rare earth post metals (RPFs). Metal centers include rare earth elements like lanthanides and benzenecarboxylated acids as ligands; (v) HKUST-1 (Hong Kong University of Science and Technology). Copper ions coordinated with benzenetricarboxylate (BTC); (vi) UiO series (University of Oslo). These are zirconium-based MOFs. Examples include UiO-66 and UiO-67; (vii) IRMOF (isoreticular MOFs). Composition involves zinc ions with terephthalate linkers. Examples include IRMOF-1 to IRMOF-16; (viii) PCN (porous coordination networks). Composition involves metal ions with various organic linkers; and (ix) post-synthetic modified MOFs.[196]

MOFs have garnered noteworthy attention as hybrid crystalline porous biomaterials, distinctly in the realm of DDS. Their unique characteristics such as adjustable pore sizes and shapes, ultrahigh surface areas, and versatile functionalities can be tuned for developing advanced drug delivery systems.[197] However, challenges such as physiological instability and cytotoxicity owing to toxic metal ions have limited their applications, However, this approach enhances the stability, biocompatibility, and therapeutic efficacy of MOFs.

The multifunctional hybrid systems can be employed to generate ROS upon light irradiation, effectively killing cancer cells. MOFs with photothermal properties can absorb NIR light and convert it into heat, destroying cancer cells with localized hyperthermia. They can encapsulate chemotherapeutic drugs, providing targeted and controlled release, minimizing side effects on healthy tissues. Combining different therapeutic modalities (*e.g.*, PDT, PTT, chemotherapy) within a single MOF platform can produce synergistic effects, improving overall treatment outcomes.[198] A recent study demonstrated the use of an endogenous copper MOF nanozyme therapy for colon cancer treatment. This innovative approach leverages endogenous biomarkers to trigger the "turn-on" production of drugs *in situ*, simplifying the creation of nanomedicine and enhancing the targeting of cancer treatment.[199]

Ji *et al.*[200] have developed an innovative multifunctional copper-based MOF (Cu-MOF) nanoparticle, loaded with mitoxantrone (MTO) and azobenzene (AXB) and decorated with a tumour cell membrane (TCM) to form M/A@MOF@CM. This hybrid system is designed for a synergistic anticancer therapy that induces cuproptosis, ferroptosis, and apoptosis (Fig. 22). TCM provides a homologous targeting mechanism, enhancing cellular uptake through membrane-mediated endocytosis. It helps evade immune detection, improving biocompatibility and reducing off-target effects. The mechanism of action involves depletion of GSH through reduction of Cu^{2+} to Cu^{+}.

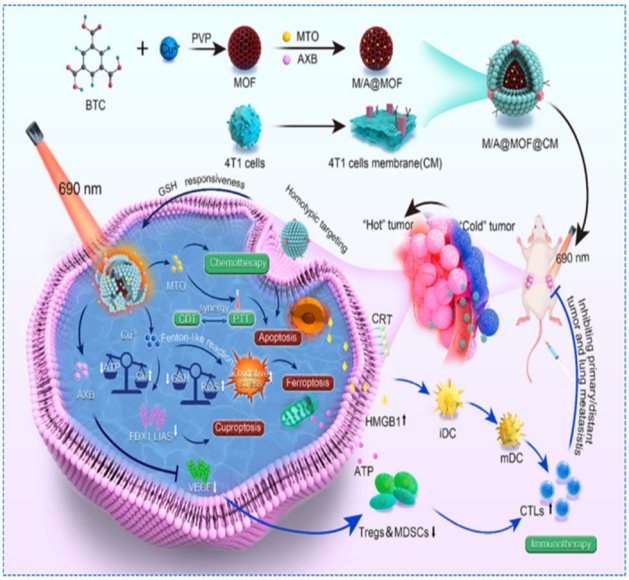

Fig. 22 Schematic showing synthesis and anticancer mechanism of the MOF-based nanosystem in mice. Reprinted with permission from ref. 200. Copyright 2024, Elsevier.

Disruption of cellular energy metabolism increases cytoplasmic copper concentration, which is conducive to the production of hydroxyl radicals (˙OH). High copper ion concentrations cause the loss of ferredoxin 1 (FDX1) and lipoylated proteins (LIAS), leading to cell death through a process known as cuproptosis. Increased ROS levels cause lipid peroxidation, damaging cell membranes. Glutathione peroxidase 4 (GPX4) deactivation further enhances ferroptosis. MTO directly intercalates DNA, triggering apoptosis through DNA damage and cell cycle arrest. The combination of cuproptosis, ferroptosis, and MTO-induced apoptosis leads to robust and efficient tumour cell elimination. The treatment induces severe ICD, distinguished by the liberation of damage-associated molecular patterns (DAMPs) and tumour-associated antigens (TAAs). The release of DAMPs and TAAs elicits strong systemic immune responses, enhancing the ability to inhibit distant (abscopal) tumours and reduce metastasis, particularly in the lungs. M/A@MOF@CM combines chemotherapy, CDT, and PTT, providing a broad range of therapeutic activities. TCM decoration enhances tumour-specific targeting and uptake, ameliorating remedy proficiency and lessening side effects.

4.6.3. Cancer treatment using MXenes. The properties of MXenes have been discussed in the wound healing section. In this section, applications of MXenes in cancer treatment have been discussed.

Wu *et al.*[201] reported a smart responsive $Ti_3C_2T_x$ nano-drug delivery system. The exceptional properties of $Ti_3C_2T_x$ MXenes inclusive of functional group accessibility, negatively charged surface, and photothermal effect played an outstanding role in the construction of a smart $Ti_3C_2T_x$-DOX-PMAsh-Tf nanoplatform by assembling positively charged DOX, a PMAsh (sulfhydryl-modified polymethacrylic acid) shell and the Tf protein

layer. The carboxyl groups in PMAsh are protonated in acidic domains, leading to partial cleavage of the shell, while excessive GSH can break the disulfide bonds, resulting in disintegration and controlled release of the drug. The addition of a tumour-targeting Tf layer ensures that the smart material is preferentially directed towards tumour cells, enhancing the specificity and reducing off-target effects.

An MTT assay was used to evaluate the effectiveness of a nanomedicine release system in killing human hypopharyngeal carcinoma cells (FaDu) *in vitro*. Various treatment groups, including normal saline (NS), $Ti_3C_2T_x$, free DOX, $Ti_3C_2T_x$-DOX, $Ti_3C_2T_x$-DOX-PMAsh, and $Ti_3C_2T_x$-DOX-PMAsh-Tf, were employed for the purpose. Free DOX exhibited higher cytotoxicity than $Ti_3C_2T_x$-DOX-PMAsh-Tf (Fig. 23A). The lower cytotoxicity of $Ti_3C_2T_x$-DOX-PMAsh-Tf than free DOX was attributed to incomplete drug release from the nanocarrier platform within the 24-hour culture period. This suggested a lower drug concentration delivered to cells than the originally loaded concentration. The survival rate of cells treated with $Ti_3C_2T_x$ alone was 97.9% without NIR irradiation, indicating good biocompatibility of the $Ti_3C_2T_x$ nanomaterial. In the presence of $Ti_3C_2T_x$, laser irradiation reduced the viability of tumour cells, demonstrating the effectiveness of the photothermal effect in inducing cell death. The cytotoxicity of $Ti_3C_2T_x$-DOX-PMAsh and $Ti_3C_2T_x$-DOX was similar, but both exhibited higher cytotoxicity than that of $Ti_3C_2T_x$ alone. $Ti_3C_2T_x$-DOX-PMAsh-Tf had a lower cytotoxicity than free DOX but was more cytotoxic than the other NM groups. $Ti_3C_2T_x$-DOX-PMAsh-Tf was shown to effectively target tumour cells expressing the Tf receptor. Upon entering the cancer cells, the GSH cleaved the disulfide bond present in the nanocarrier which led to drug release and subsequent cell death. The IC_{50} (half maximal inhibitory concentration) of $Ti_3C_2T_x$-DOX-PMAsh-Tf + NIR, $Ti_3C_2T_x$-DOX-PMAsh-Tf, and DOX were reported as 0.22, 1.26, and 0.41 μg mL^{-1}, respectively (Fig. 23B). The decrease in IC_{50} value under NIR indicates enhanced cytotoxicity and confirms that photothermal therapy can markedly improve therapeutic efficacy.

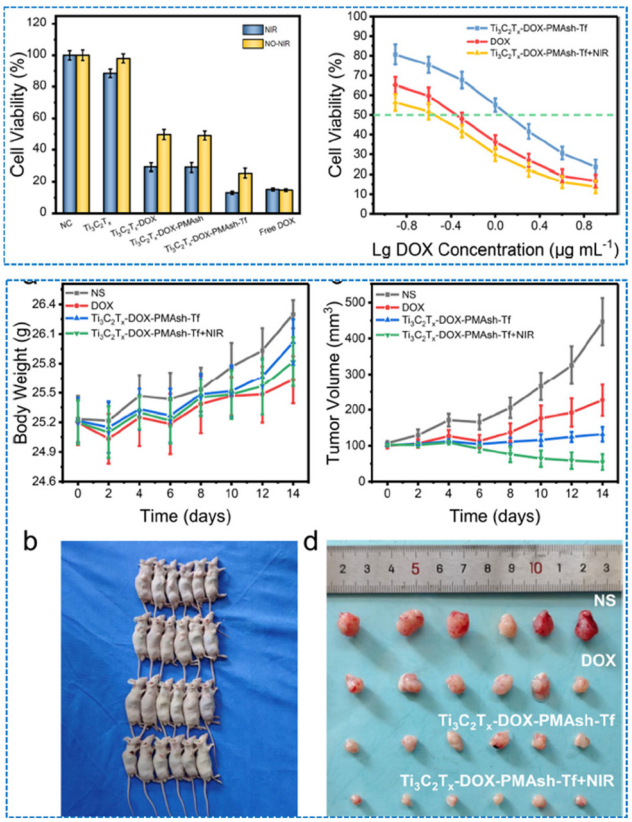

Fig. 23 The MTT assay providing insights into the cytotoxic effects of different treatment groups on FaDu cells, both with and without NIR laser irradiation. Enhanced cytotoxicity was observed due to the photothermal effect of $Ti_3C_2T_x$ MXene, which led to increased cell death, either through enhanced drug release or direct thermal damage. (B) IC_{50} value of different treatment groups. $Ti_3C_2T_x$-DOX-PMAsh-Tf + NIR likely has a lower IC_{50} than treatment without NIR, indicating enhanced cytotoxicity due to the combined chemophotothermal therapy. (C–F) *In vivo* investigation of anticancer activity in mice with different treatment groups. (C) Changes in the body weight of tumour-bearing mice over treatment of fourteen days. (E) Post-treatment digital images of the mice. (D) Curve showing the change in tumour volume during a treatment period of fourteen days. (F) Post-treatment digital images of tumours. Reprinted with permission from ref. 201. Copyright 2023, American Chemical Society.

They further conducted an *in vivo* examination to evaluate the effectiveness of a $Ti_3C_2T_x$-DOX-PMAsh-Tf nanomaterial as a drug release system for treating FaDu tumours in mice. The experiment compared the effects of different treatment groups, including a control group, a group treated with free DOX, a group treated with the nanomaterial ($Ti_3C_2T_x$-DOX-PMAsh-Tf), and a group treated with the nanomaterial plus NIR irradiation. Mice were injected with 5 mg kg^{-1} DOX on days 0 and 5. In the case of the NIR group, nine hours after injection, the tumour region was treated with radiation for ten minutes at 1 W cm^{-2}. This irradiation raised the tumour area temperature from 30° centigrade to 46.3° centigrade, inducing a photothermal effect. The body weight and survival of all the mice was reported to be stable after treatment for fourteen days (Fig. 23C). Tumour volume measurements and post-treatment tumour extraction indicated that the $Ti_3C_2T_x$-DOX-PMAsh-Tf + NIR group exhibited the most significant inhibition of tumour growth (Fig. 23D–F). Overall, this study showed significant efficacy of the $Ti_3C_2T_x$-DOX-PMAsh-Tf composite material in killing carcinogenic cells *in vitro* and inhibiting tumour growth *in vivo* when exposed to 808 nm laser irradiation. The combination of targeted drug delivery and photothermal effects resulted in enhanced therapeutic outcomes.

Dai *et al.*[202] showcased a significant advancement in the field of cancer nanotheranostics by modifying the surface of Ta_4C_3 MXenes with manganese oxide nanoparticles (MnOx). They combined multiple imaging and therapeutic modalities into a single platform and enhanced both the diagnostic and treatment capabilities in cancer therapy. The tantalum in Ta_4C_3 MXenes acted as a high-performance contrast agent for contrast-enhanced CT imaging. This made it easier to visualize tumours with greater clarity and detail using CT scans. The manganese oxide nanoparticles incorporated into the MXene

structure were responsive to the tumour microenvironment, making them effective contrast agents for *T*1-weighted MRI. This responsiveness allowed for better imaging of tumours, particularly in distinguishing them from surrounding healthy tissues.

5. Tissue engineering and regeneration applications of smart nanomaterials

NM-based drug delivery systems are crucial components in TER, offering targeted, controlled, and sustained release of drugs. These systems can enhance tissue regeneration by releasing drugs, growth factors, and genes directly to disease sites.[203,204]

5.1. Bone tissue engineering and regeneration applications of smart nanomaterials

Bone is an intricate and dynamic tissue essential for structural support, protection of vital organs, and haematopoiesis. However, bones can be damaged due to various reasons such as disease (osteosarcoma, osteoarthritis, and bone metastasis in cancer), trauma, congenital abnormalities, aging, *etc*. In one study, Liu *et al.*[205] loaded bone morphogenetic protein-2 (BMP-2) into adhesive liposomes which were then incorporated into the hydrogel to develop antibacterial and self-healing multifunctional DDSs for injection into osteoporotic cracks and bone marrow cavity. The results showed better osteogenic differentiation and rapid bone remodeling of osteoporotic fractures.

5.1.1. Bone tissue engineering and regeneration applications of polymeric micelles. Polymeric micelle-based nanocarrier systems are widely employed for targeted drug delivery in TER due to their great loading efficiency, controlled release, low CMC, enhanced stability, and improved solubility of hydrophobic drugs. Lima *et al.*[206] delineated a sophisticated drug release system utilizing polymeric micelle-based nanocarriers specifically fabricated for the low-level release of the anti-inflammatory drug dexamethasone (Dex) for arthritic disease (Fig. 24A). This innovative approach leveraged the elevated activity of the glutathione reductase (GR) enzyme present in inflamed joints to create a system that is sensitive to GR enzyme activity, thereby enabling efficient and targeted delivery of Dex in the treatment of arthritic diseases. The micelles limited the exposure of non-target tissues to Dex, decreasing the risk of adverse effects.

In another study, Long *et al.*[207] developed an innovative polymeric micelle system designed to respond to hypoxic conditions and target bone metastasis for the treatment of bone metastatic prostate cancer efficiently (Fig. 24B). The system exploited the unique microenvironment created during bone metastasis, particularly the hypoxic conditions, to ensure targeted and efficient delivery of DOX medication. Alendronate was incorporated into the micelles to confer bone-targeting properties whereas azobenzene was used as a hypoxia-sensitive linker which undergoes structural changes in response to hypoxic conditions, triggering the release of the encapsulated drugs. *In vivo* study confirmed the selective accumulation of micelles in metastatic bone, hypoxia-triggered release of DOX at the metastatic site, suppression of tumour growth in bone, and inhibition of bone destruction by a reduction of osteoclast activity and promotion of osteoblast activity.

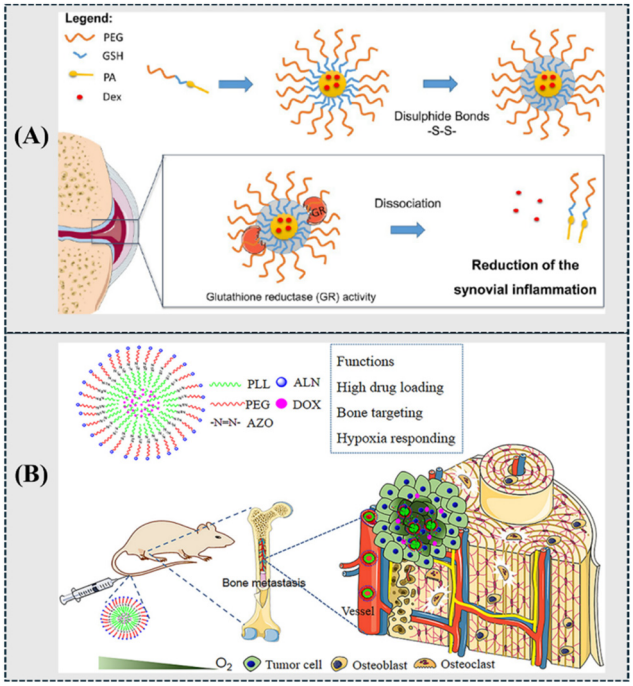

Fig. 24 (A) Schematic representation of the usage of glutathione reductase (GR)-sensitive polymeric micelles for arthritis treatment. Reprinted with permission from ref. 206. Copyright 2021, American Chemical Society; (B) schematic illustration of the applicability of hypoxia-responsive and bone tissue-targeting polymeric micelles for targeted treatment of bone metastatic prostate cancer. Reprinted with permission from ref. 207. Copyright 2021, Elsevier.

5.1.2. Bone tissue engineering (BTE) and regeneration applications of polymeric nanomaterials. Polymeric NPs, specifically PLGA and chitosan, are increasingly being utilized in BTE for targeted drug delivery owing to their notable biodegradability, non-immunogenicity, and ability to liberate medications directly to the targeted sites. These NPs can be easily engineered to intensify bone regeneration and mending by imparting controlled growth factors, medications, and divergent bioactive molecules.[208,209] Chitosan NPs have emerged as highly effective nanocarriers in BTE, primarily due to their intrinsic osteoinductive and antibacterial properties. These characteristics not only facilitate bone regeneration but also help mitigate the risk of infections, which is a significant challenge post-bone grafting.[210]

5.1.3. Bone tissue engineering and regeneration applications of smart nanofibers. Nanofibers represent an advanced and versatile class of nanofibrous materials that are increas-

ingly being explored for their applications in BTE and guided bone regeneration. These nanofibers can respond to various physical, chemical, and biological stimuli, making them highly suitable for creating dynamic and responsive environments conducive to bone healing and regeneration. One such example of smart nanofibers in BTE is a nano- or microfibrous composite consisting of polycaprolactone (PCL) and silk fibroin.[211] This composite has demonstrated enhanced functionality in promoting bone regeneration and can be tailored by adjusting the nanofiber content within the scaffold. Additionally, hybrid scaffolds composed of nano- or microfibrous mats have shown increased cellular responses, particularly with MC3T3-E1 cells, compared with individual scaffolds.[212] Electroconductive composite nanofibers represent a cutting-edge approach in BTE, offering a combination of electroactivity, biomimetic properties, and controlled growth factor delivery.[213] These scaffolds have demonstrated the ability to promote osteoinductivity, osteoconductivity, and biocompatibility, making them highly promising for enhancing the healing process in bone defects.[214] With ongoing advancements in materials science and tissue engineering, the electroconductive nanofibers hold great potential for clinical translation and ameliorating patient outcomes in bone regeneration therapies.

5.2. Cartilage tissue engineering and regeneration applications of smart nanomaterials

Cartilage-targeting nanoplatforms have been extensively researched and developed, showing great promise in overcoming the dense type II collagen barriers in cartilage and serving as effective drug carriers. These nanoplatforms utilize various materials and strategies to enhance their targeting, penetration, and therapeutic efficacy within the challenging environment of cartilage tissue.

Bajpayee *et al.*[215] demonstrated a novel approach for the intra-articular (IA) treatment of osteoarthritis (OA) employing a DEX-loaded avidin nanoplatform. The approach leveraged the small size and positive charge characteristics of avidin to achieve rapid and effective penetration into cartilage tissue. The positive charge of avidin improved its retention within the cartilage, ensuring sustained release of DEX and prolonged anti-inflammatory effects. Hu *et al.*[216] developed an advanced cartilage-targeting drug, termed CAP-PEG-PAMAM, employing a partly PEGylated polyamidoamine (PAMAM) dendrimer, for the efficacious delivery of drugs to articular cartilage, addressing several challenges associated with cartilage-targeting drug delivery. The chondrocyte-affinity peptide (CAP) peptide specifically binds to chondrocytes, enhancing the targeting and uptake of the nanocarrier in cartilage tissue. The study revealed efficient delivery and rapid penetration of the nanocarrier into the deep zones of the cartilage, ensuring that therapeutic agents reach their target cells effectively.

Recently, Xue *et al.*[217] reported a twofold drug delivery system using an MOF-furbished mesoporous polydopamine (MPDA) structure. The development of the system involved loading rapamycin (Rap) and bilirubin (Br) into the mesopores

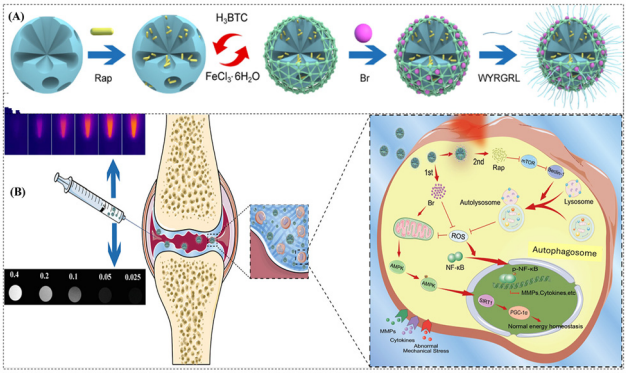

Fig. 25 Schematic illustration of (A) fabrication of the RB@MPMW nanoplatform; (B) cartilage-targeting dual drug delivery mechanism as well as NIR laser response of the nanoplatform in osteoarthritis therapy. Reprinted with permission from ref. 217. Copyright 2021, Elsevier.

and shell of the MOF, respectively. To target collagen II in cartilage, they conjugated a collagen II-directing peptide (WYRGRL) onto the nanocarrier, resulting in the RB@MPMW nanoplatform (Fig. 25A). The results displayed back-to-back release of Br and Rap from the nanoplatform in the presence of NIR light. Br's rapid release from the MOF shell showed outstanding ROS scavenging potency and anti-apoptotic effects, albeit reducing autophagy activity to some extent. The presence of NIR light caused the quick release of Rap from the MOF-based nanosystem and elevated activation of autophagy and protection of the chondrocytes (Fig. 25B).

5.3. Tissue engineering and regeneration applications of smart nanomaterial-based 3D bioprinting

3D bioprinting has emerged as the utmost additive biomanufacturing technology, revolutionizing the field of TER medicine. This advanced technology, boosted with outstanding bioinks and sophisticated bioprinters, enables the construction of functional tissues and organs, potentially eliminating the need for artificial organs. Moreover, the integration of NMs into bioink platforms represents a significant advancement in this technology. Various research groups recently explored how NMs can enhance the properties and functionalities of bioinks, making them more suitable for creating complex tissue structures and promoting tissue regeneration.[218,219] Recently, Rizwana *et al.*[219] made a notable stride in regenerative medicines by developing NM-based multimodal bioink designed for the treatment of peripheral nerve injuries. This innovative bioink serves dual purposes: it acts as a carrier for cells and functions as a free radical scavenger (Fig. 26A). The bioink formulation consists of PVA and cerium oxide NPs (NC), employing a novel dual crosslinking method with citric acid and NaOH.

Digital light processing (DLP) printing technology has emerged as a significant tool in BTE, allowing the fabrication of complex and highly precise polymeric scaffolds. It offers significant benefits in terms of material handling, cell viability, structural complexity, printing speed, and resolution, making

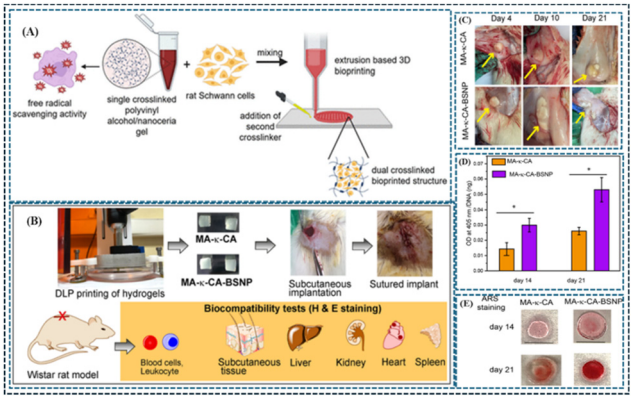

Fig. 26 Schematic representation of (A) cerium oxide nanoparticles (nanoceria) based multimodal bioink serving as both a cell carrier as well as free radical scavenger for the treatment of peripheral nerve injury. Reprinted with permission from ref. 219. Copyright 2023, American Chemical Society; (B) schematics of *in vivo* biocompatibility of DLP-printed MA@k@CA@BSNP and MA@k@CA hydrogels after subcutaneous implantation inside laboratory Wistar rats. No symptoms of skin inflammation, illness/mortality, and adverse effects on the liver, kidneys, spleen, and heart were observed; (C) digital images showing subcutaneously implanted MA@k@CA@BSNP, and MA@k@CA hydrogels on days 4, 10, and 21; (D) assessment of osteogenic differentiation in DLP-printed-osteoblast-laden MA-k@CA@BSNP, and MA@k@CA hydrogels employing the alkaline phosphatase (ALP) activity assay. The assessment showed a remarkable enhancement in ALP activity by the MA@k@CA@BSNP composite hydrogels compared with native MA-k-CA hydrogels; (E) digital images demonstrating deposition of calcium in the Alizarin Red S-stained MA@k@CA@BSNP composite hydrogels (deep brick orange-red colour) compared with native MA@k@CA hydrogels on days 14 and 21. Reprinted with permission from ref. 220. Copyright 2024, Royal Society of Chemistry.

it a powerful technique for fabricating complex tissue engineering scaffolds. Recently, Kumari *et al.*[220] combined methacrylate-k-carrageenan (MA@k@CA) with bioactive SNPs (BSNPs) using DLP printing, achieving high precision and resolution in creating complex bone structures (Fig. 26B–E). The incorporated BSNPs improved the osteogenic properties (*i.e.*, mechanical strength, viscosity, rheological properties, *etc.*) of the hydrogel, promoting bone growth and regeneration. An *in vitro* study was executed with pre-osteoblast-loaded scaffolds of MA@k@CA-BSNP and the results manifested a fostering of cell proliferation, mass transfer, and osteogenesis by the DLP-fabricated porous structures, showing bone ingrowth. An *in vivo* study of the hydrogel scaffold was conducted on Wistar rats and the results manifested slow degradation of the MA@k@CA@BSNP hydrogels and good biocompatibility (no inflammation of subcutaneous tissue, kidneys, liver, spleen, and heart tissues) over the study period.

5.4. Tissue engineering and regeneration applications of smart nanomaterial-based hybrid bioinks

NM-based hybrid bioinks furnish a propitious approach to enhancing the performance of bioinks in 3D bioprinting. By exploiting the distinct properties of both natural and synthetic NMs, these hybrid bioinks provide improved biocompatibility, mechanical strength, and functionalization, making them highly suitable for advanced tissue engineering applications.

Zhang *et al.*[221] produced NM-based bioink using a GO/alginate/gelatine composite to construct 3D bone-mimicking scaffolds employing a 3D bioprinting technique. This bioink was laden with human mesenchymal stem cells (hMSCs). The findings reported that while higher GO concentrations (0.5GO, 1GO, and 2GO) generally improved the initial performance of bioinks, the 1GO concentration maintained the best balance, providing high scaffold fidelity, bioprintability, cell viability, mechanical strength, and osteogenic differentiation, making it the most promising concentration for BTE applications. The integration of graphene, CNTs, nanoclay, transition metal dichalcogenides, polymeric NPs, and magnetic and MOF NMs into polymeric hydrogels enhances their mechanical strength, biocompatibility, and functionality, providing advanced materials for 3D bioprinting and proliferating their applications in TER medicine.[222–224]

5.5. Soft tissue engineering and regeneration applications of smart nanomaterials

Smart NMs hold vast potential in soft tissue engineering and regeneration, offering innovative solutions for creating tissue scaffolds, enhancing cell growth, and delivering bioactive compounds precisely. These materials respond to distinct stimuli, balance with physiological conditions, and mimic natural tissue properties, which are all critical in soft tissue applications like skin, muscle, nerve, and cartilage regeneration.[225]

5.5.1. Muscle tissue engineering. The integration of various NMs and cells in the development of implantable 3D muscle tissue is a significant area of research in TER medicines. NMs based on CNTs, chitosan, fibrin, PEG, HA, collagen, alginate, decellularized extracellular matrix (dECM), hyaluronic acid (HA), poly(oligo ethylene glycol) methacrylate/cellulose nanocrystal (POEGMA/CNC), polycaprolactone (PCL), and keratin play an important role in the manufacture of implantable 3D muscle tissue.[226] A variety of cells such as hMPC (human muscle progenitor cells), HUVEC (human umbilical vein endothelial cells), and C2C12 (mouse myoblasts) cells are utilized in conjunction with the nanomaterial-based bioinks.[226]

NM-infused bioinks present significant advancements in muscle tissue engineering by overcoming some of the key limitations of traditional bioinks. These limitations include challenges in balancing the printability of the bioink with crucial cellular requirements such as absorbability, adhesion, and support for cell growth and differentiation.[227] Conventional bioinks often struggle to achieve this balance, which can impede the effectiveness of tissue engineering efforts. The infusion of NMs into bioinks addresses these challenges by enhancing the mechanical properties and biocompatibility of the constructs. These nanomaterial-infused bioinks are particularly effective in crafting tissue constructs that closely mimic the natural muscle tissue.[228] They offer improved cellular adhesion and absorption, better mechanical strength, and enhanced support to cell proliferation. This

makes them highly suitable for engineering functional muscle tissues that can integrate well with the body's natural systems, thereby improving the potential for successful tissue regeneration and repair. Thus, the integration of NMs into bioinks for muscle TER provides improvements in various critical aspects, such as biocompatibility, cell viability, printability, and muscle regeneration. Researchers have observed that these bioinks, when combined with cells, not only support the creation of complex tissue structures but also promote the alignment of cells, which is essential for functional muscle tissue.[226,228]

One of the most significant benefits of incorporating NMs into 3D bioprinted constructs is their ability to enhance myoblast cell differentiation, for instance C2C12 cells, into mature skeletal muscle cells.[228] This process is typically challenging and often requires additional myogenic agents to achieve it. However, with NM-infused bioinks, the differentiation occurs more naturally, eliminating the need for these extra agents and simplifying the tissue engineering process. One of the key innovations in 3D bioprinting for muscle tissue engineering is the incorporation of microchannel structures within the printed constructs. By optimizing the initial cell density and ensuring a more even distribution of nutrients, these microchannels help construct a more conducive environment for tissue growth and maturation.[229]

5.5.2. Skin appendages and other tissue engineering/regeneration/vascularization. Skin appendages including sweat glands, hair follicles, and nails play crucial roles in sensation, thermoregulation, and skin homeostasis.[230,231] Engineering or regenerating these structures along with their vascularization is an advanced field in regenerative medicine and tissue engineering. NMs based on CNTs, alginate, and gelatine have transformative potential in tissue engineering, especially for regenerating skin appendages and promoting vascularization, which are critical for the functionality and longevity of engineered tissues.[232] Combining gene therapy with skin appendage engineering to activate or repress certain pathways could yield more reliable appendage regeneration. Smart biomaterials that can dynamically respond to the needs of regenerating tissues (*e.g.*, releasing growth factors in response to local cues) are being explored for skin and appendage regeneration.

The usage of NM-based hybrid bioinks has opened exciting possibilities in the bioprinting and manufacturing of various tissues and organs inclusive of the kidneys, spleen, heart,[233] liver,[234] and pancreas, porous tissues, and even 3D tumour models,[235] for evaluating the efficacy of NMs. Nanocomposite and nanocolloidal hydrogels represent an exciting approach to recreating ECM-like environments due to their customizable properties, including tunable mechanical properties, nanoscale features, bioactive cues, fibre alignment, porosity, and surface roughness.[236]

6. Nanotoxicity assessment

Nanotoxicity assessment is a complex and evolving field that is indispensable for confirming the safety and application of NMs.[237–242] By combining advanced experimental techniques, computational models,[243–245] and regulatory frameworks, researchers can better understand and mitigate the potential risks associated with NMs, ultimately leading to safer and more sustainable technologies.

6.1. *In vitro* toxicity assessment

Advances in personalized medicine and related technologies are further fuelling the demand for *in vitro* toxicology testing, as these methods can provide more relevant and specific insights into how NMs and other substances can affect human cells.[246] The market based on *in vitro* toxicity testing is expected to grow to USD 17.1 billion up to 2028, manifesting a total annual growth rate of 9.5% from 2023–2028.[247] Guidelines for evaluating *in vitro* nanotoxicity proposed by ISO/TC 229, ASTM, and OECD have been recapitulated in Table 6. *In vitro* assays employing divergent cell line models of various organs are widely used to assess the potency and toxicity of NPs. These cell lines are typically chosen based on the organs where NPs are most likely to accumulate such as the lungs, kidneys, brain, *etc*.[248,249]

Lo Giudice *et al.*[250] reported the usage of immortalized cell lines to examine the effects of metal nanoparticles (MNPs) on the immune system. A549 cells were employed to assess how exposure to silica nanoparticles (SiNPs) triggers innate immune responses, including the production of inflammatory cytokines (Fig. 27A). They provided valuable insights into how different metal nanoparticles can influence immune system functions. This is critical for assessing the safety and potential health impacts of nanoparticles, guiding their safe use in medical and industrial applications.

Clift and colleagues[251] studied the interactions between AuNPs and B lymphocytes. They treated human B lymphocytes with AuNPs of divergent shapes and surface properties (Fig. 27B). The coated AuNPs had minimal interaction with B lymphocytes compared with uncoated ones. Importantly, even at a high concentration of 20 μg mL^{-1} over 24 hours, none of the AuNPs affected cell viability. Furthermore, the coated nanospheres did not impact on the expression of activation markers or cause an increase in pro-inflammatory cytokine secretion by naive B lymphocytes. However, uncoated nanospheres and rod-shaped AuNPs led to decreased IL-6 cytokine generation by activated B lymphocytes, indicating a functional impairment.

Duan *et al.*[252] advanced the understanding of how ENPs (engineered nanoparticles) affect macrophage functions through oxidative stress and SSG (*S*-glutathionylation protein) modifications (Fig. 27C), offering valuable information for the development of safer NMs. Their study provided insights into protein signatures and pathways that serve as ROS sensors, facilitating cellular adaptation to ENPs, and identifying targets of ENP-induced oxidative stress that led to irreversible cell damage. Understanding these mechanisms can aid in designing safer ENPs that minimize adverse effects on immune functions, which is crucial for their biomedical applications.

In vitro platforms play a decisive role in various aspects of biomedical research, including drug discovery and toxicity testing.

Table 6 Summary of *in vitro* toxicity of NMs

Mode of toxicity assessment	Objective	Method/s	Remarks	Standard ID	Pros	Cons	Ref.
Cytotoxicity	Study of metabolic activity	MTT assay	Assessment of cytotoxicity of NPs employing human hepatocarcinoma cells and porcine kidney cells	ASTM E2526-08 (201)	Simple and rapid	Insufficient sensitivity to detect the number of viable cells and interference of dye with NPs	253–255
Cytotoxicity		3D cells	Assessing toxicity of NPs with the possibility of allocating high-throughput screening analysis	ISO/AWI TS 22455			256
Cytotoxicity	To examine the toxicity of NMs and determine possible risks associated with human health	LDH and MTS assay	Measurement of the cytotoxicity of NPs	ISO 19007:2018	Widely employed for characterizing NMs for medical devices	No detailed testing protocols	254 and 256
Cell uptake	To quantify absolute particle number or/ and surface per cell	Transmission electron microscopy (TEM)	To examine the uptake and intracellular outcome of NPs. Imparts signal of electron-dense NPs and biological situation within one channel, which needs analysis before quantification	Nature protocol	NPs tracking without linking to a probe	Observer effects can significantly impact the accuracy of the interpretation	257 and 258
Cell uptake	Quantification of NPs' uptake	Flow cytometry	Quality nano-SOP		Fluorescent NP uptake measurement in individual cells and production of high-quality content data with ease	To ensure accurate measurements and avoid interference from residual free or labile dye, careful characterization, and stability assessment of the starting dispersion of carbon nanomaterials in cell culture media is essential	259
Cell uptake	Quick detection and characterization of the NPs internalized and trafficked organelles		Production of quantitative data on NPs' intracellular distribution, colocalization, and trafficking kinetics, employing a combination of advanced microscopy techniques and image analysis tools		Provide fast, high-throughput, and quantitative space- and time-resolved information on NP numbers and their distribution across different organelles	Imaging methods can be employed for more detailed information on intracellular outcomes	260
Hemolysis	To evaluate biocompatibility and hemolytic response/ properties	*In vitro* blood biocompatibility test	To assess NPs' hemolysis rate	ASTM E25 24-08(201)	Simple	Limited to RBCs	253
Chemoattractant	To measure the chemoattractant capacity		*In vitro* measurement of chemoattractant capacity of NPs	ASTM WK60373			253 and 256
Immunological response	To observe the host's immune reaction	Colony assay	To evaluate if NPs initiate the formation of mouse granulocyte-macrophage colonies	ASTM E25 25-08(2013)		Counting colonies that grow close together can indeed be challenging	253 and 256
Endotoxin	Contamination by endotoxin	*Limulus* amoebocyte lysate test	For *in vitro* systems, endotoxin test on NM samples	EN ISO 29701:2010	Applied to NMs studied for *in vitro* tests		256
Oxidative stress	Removal of antioxidant capacity	Nanotechnologies-5-(and 6)-chloromethyl-2′,7′-dichloro-dihydrofluorescein diacetate (CM)	To evaluate if NPs induce ROS generation, employing RAW 264.7 macrophage cell line	ISO/TS 19006:2016			254 and 256

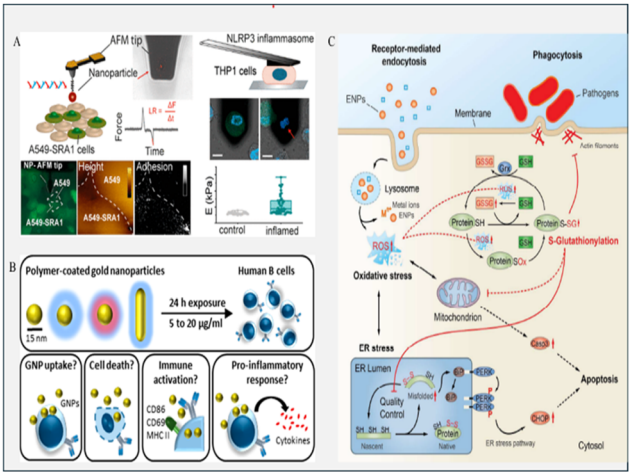

Fig. 27 Schematic illustration of the feasible applicability of immortalized cell lines to examine the effect of MNPs on the immune system. (A) Schematic representation of the interaction of SiNPs with SRA1 (scavenger receptor A1) on A549 cells and their subsequent effects on inflammasome activation, helping to elucidate the immune responses triggered by nanoparticle exposure. Reprinted with permission from ref. 250. Copyright 2022, American Chemical Society. (B) Schematic representation of how AuNPs with different surface coatings (PVA/PEG) and shapes (rods and spheres) affect B lymphocyte immune function. Polymer-coated AuNPs interacted poorly with B lymphocytes compared with uncoated AuNPs. Reprinted with permission from ref. 251. Copyright 2019, American Chemical Society. (C) Illustration of participation of the suggested pathways and organelles in the initiation of oxidative stress or *S*-glutathionylation of proteins. It also highlights the potential influence on phagosome function, endoplasmic reticulum (ER) stress, and cell survival engendered by ENPs (engineered nanoparticles). Reprinted with permission from ref. 252. Copyright 2016, American Chemical Society.

However, despite their importance, these platforms have significant limitations, particularly in the assessment of pharmacokinetic (PK) and toxicokinetic (TK) parameters. The dynamic and complex nature of these processes in a whole organism cannot be fully replicated *in vitro*, which often leads to an incomplete understanding of a compound's behaviour in the body.

As a result, *in vivo* models, which appertain to the utilization of live animals, remain the gold standard for laboratory examination to deduct toxicities[261,262] and other critical pharmacological properties. *In vivo* testing provides a comprehensive view of how a substance interacts with various biological systems, offering invaluable insights that are not possible to obtain through *in vitro* methods alone.[263] However, the use of *in vivo* models raises ethical concerns and is subject to stringent regulatory and ethical guidelines.

6.2. *In vivo* toxicity assessment

The *in vivo* toxicology market, which involves studying the effects of chemicals on living organisms, is projected to grow from USD 5.0 billion in 2020 to USD 6.6 billion by 2025.[264] This represents a CAGR of 5.5% over the forecast period. The *in vivo* toxicology market is expected to experience steady growth, slightly slower than the rapid advancements and adoption seen in the *in vitro* market. This reflects a balanced approach in the industry, leveraging the strengths of both methodologies.

The selection of appropriate animal models for toxicological assessment is critical for obtaining relevant and reliable data. While no single model perfectly replicates human biology, a combination of traditional animal models, emerging technologies, and alternative methods can provide comprehensive insights into toxicological effects. Careful consideration of the study objectives, ethical implications, and specific advantages and limitations of each model is essential for effective toxicological research.[265]

Nonmammalian models like *Caenorhabditis elegans* (*C. elegans*, a nematode) and *Drosophila melanogaster* (*D. melanogaster*, a fruit fly) are valuable tools in the field of nanotoxicology. They provide important preliminary data on the safety and potential biological impacts of NMs, helping to identify hazards before advancing to more complex mammalian models. Their ability to reveal toxicity related to both the active components and the structural materials of nanocarriers is particularly beneficial in the development of safer nanomedicines. *In vivo* studies based on *C. elegans* revealed that polymeric NPs and unloaded solid lipid NPs exhibit higher toxicity, manifesting as increased mortality rates, reduced reproduction rates, and delayed development compared with tripolyphosphate/chitosan carriers.[266,267] *D. melanogaster* is a validated model for monitoring genotoxicity endpoints and has been utilized to test the safety of polymeric and solid lipid-based nanocarriers. For example, a study based on *D. melanogaster* demonstrated that near-lethal doses of PLA NPs trigger oxidative stress as well as cell cycle arrest at G1.[268] Additionally, aquatic models like *Danio rerio* (zebrafish), *Artemia salina*, and *Daphnia magna* have proved highly valuable for assessing the safety of polymeric NMs.[269–271] These alternative *in vivo* models serve as excellent tools for screening initial toxicity or as complementary steps. However, it is important to note that each nonmammalian model has its limitations compared with more complex models like rodents.

Mice are widely employed in preclinical as well as nanotoxicity examinations since their genomes closely resemble the human genome. *In vivo* evaluation in these models typically involves examining apoptosis and inflammation in primary target organs such as the spleen, lung, kidneys, heart, and brain, as well as other systems that may accumulate NPs. For example, Kupffer and hepatic sinusoids cells are crucial for liver functions in metabolism and detoxification, where NPs tend to concentrate. Relevant assessment models for drug nanocarriers should mimic the exposure route (injection, ingestion, inhalation, and transdermal delivery) and the intended applications to ensure accurate safety and efficacy evaluations.[265]

Different studies based on *in vivo* toxicity assessment of NMs have been incorporated in Table 7. Many of the incorporated studies have focused on the assessment of the toxicity of the NPs with the purpose of employing them as future nanomedicines for cancer[289] and infections.[290,291] Polymer-coated nanoparticles reduced the associated toxicities and enhanced their systemic circulation time.[258,259] The usage of nonmam-

Table 7 Summary of *in vivo* toxicity of nanomaterials

NPs	Type of NPs	Animal Model	Age (weeks)	Gender	Remarks	Ref.
AgNPs	Inorganic	Balb/c mice	6–8	Female	Caused toxicity based on cell-/organ-type-, particle-type- and dose-dependent manner	272
AgNPs	Inorganic	Zebrafish (*Danio rerio*)			Caused toxicity based on size and concentration of AgNPs	273
Silica nanoparticles (SiNPs)	Inorganic	C57BL/6 mice	6–8	Female	SiNPs cause acute reproductive toxicity	274
Bioinspired Ag and Se NPs	Inorganic	Swiss albino mice	Adult	Female	The bioinspired synthesized NPs did not cause a remarkable toxic effect at a higher therapeutic effect	275
Ultrasmall superparamagnetic iron oxide nanoparticles (USPIONs) with/without ibuprofen	Inorganic	Balb/c mice		Male	No systemic toxicity but unexpected anti-inflammatory effect of ibuprofen-carrying USPIONs	276
Zirconia nanoparticles (ZrO_2NPs)	Inorganic	Wistar rats	Adult	Male	The ZrO_2NPs caused hepatotoxicity	277
Titanium dioxide nanoparticles (TiO_2NPs) with/without eugenol	Inorganic	Wistar rats	Adult	Male	TiO_2NPs cause oxidative damage to the kidneys and liver However, co-administration of NPs with eugenol mitigates the induced toxicity	278
Poly(thioether-ester) (PTEe) nanoparticles	Polymeric	Swiss mice		Male	No acute toxicity was caused	279
β-Cyclodextrin chitosan with/without epalrestat (EPL)	Polymeric	Albino rabbits			Caused acute oral toxicity	280
Supramolecular polyamine phosphate nanoparticles (PANs) with/without PEG	Polymeric	BALB/cJRj	10	Female	Reduction in toxicity of PANs was observed due to PEGylation. PEGylation alters the charge of PANs and increases their circulation half-time	281
Silk nanoparticles	Polymeric	Mice			Systemic administration of silk nanospheres caused no toxicity	282
Cyclodextrins (CDs) with/without docetaxel	Polymeric	Healthy rabbits		Male	No toxic effects were reported on the major organs of the rabbits	283
Polylactic acid-polyethylene glycol (PLAPEG) with/without encapsulated biosurfactant	Polymeric	Balb/c mice	4–6	Female	Biosurfactants loaded in PLA-PEG copolymeric NPs were observed to be nontoxic	284
Chitosan-coated lignin NPs	Polymeric	Embryonic zebrafish (*Danio rerio*)			Compared with plain lignin NPs, engineered Ch-LNP formulations were observed to be more toxic at higher concentrations	285
Polyacrylic acid-coated cobalt ferrite core–shell magnetic NPs (PAA@CF-NPs)		Sprague–Dawley rat	Adult	Male	Injected PAA@CF-NPs appeared to be renally/hepatically biocompatible. However, more studies are required to evaluate their biodistribution, homeostatic conditions, and chronic toxicity	286
IONPs/haematite nanoparticles with/without PEG or citrate	Inorganic and polymeric	Albino rats			Small inflammatory changes were observed in normal parenchymal tissues of the spleen, kidneys, and liver, while no acute damage was observed. PEG-modified NPs exhibited better biocompatibility compared with bare and citrate-coated NPs	287
GONPs	Carbon-based	Nematodes – *Caenorhabditis elegans*	—	—	Long exposure to low doses of GONPs may cause issues in locomotion and reproduction as well as induction of oxidative stress	288

malian models like *Daphnia magna*, *Danio rerio*, *Drosophila*, and *Caenorhabditis elegans* (a type of roundworm) imparted insights into the effects of NPs on various aspects, including health, environmental impact, reproductive systems, and behavioural changes,[273,285,288,292,293] hence providing valuable information about the potential risks associated with NP exposure without using mammalian subjects.

6.3. *In silico* toxicity assessment

Nanoinformatics, a burgeoning field at the intersection of nanotechnology and informatics, employs various computational and predictive modelling approaches to enhance the understanding and assessment of NMs' safety.[294,295] The study aims to predict NMs' properties, interaction of NMs with cells and biomolecules, transformation of NMs by divergent stimuli or biotransformation, and toxicity of byproducts of the transformed NMs as compared with their original forms.[296] Various computational models and tools[297] used to predict the toxicity of NMs used in biomedical/biological/environmental applications have been presented in Fig. 28.

The establishment of predictive models for the potential adverse effects of NPs relies on the encoding of their physicochemical properties as mathematical entities called descriptors.[298] These descriptors capture the size, chemical compo-

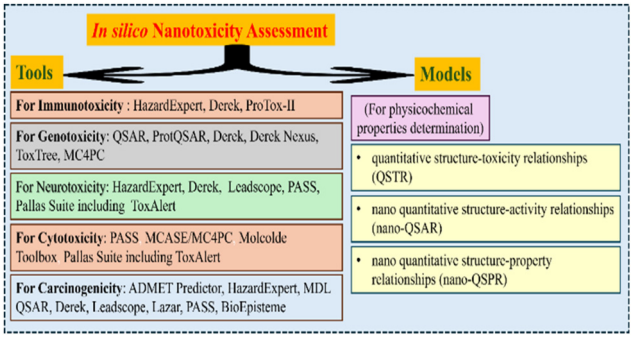

Fig. 28 Different computational models and tools used for nano/toxicological study.

sition, shape, and surface charge of the NPs. Artificial intelligence (AI), machine learning (ML), and deep learning (DL) methods play a critical role in generating predictive models based on these descriptors.[299] ML methods can significantly reduce the time and labour required for material testing by automating the analysis process. These methods enable the handling of large datasets and the screening of numerous materials simultaneously, facilitating the rapid identification of promising candidates. By analysing large volumes of data, AI and ML can uncover patterns and relationships that inform the design of new NMs with desired properties.[300–302] Singh *et al.*[303] utilized a machine learning-based approach to study how various physicochemical descriptors (like zeta-potential, size, shape, concentration, polydispersity, and diffusion coefficients) of NMs influence their interactions with cell membranes and intracellular uptake at sublethal concentrations. Specifically, their ML algorithm identified the cell shape index and nuclear area as critical descriptors associated with alterations induced by NMs in the Madin–Darby canine kidney (MDCK) epithelial cell line model. This finding suggests that NMs capable of inducing changes in cell and nuclear shape at subtoxic levels may trigger epigenetic modifications that control epithelial to mesenchymal transition processes.

Quantitative structure–activity relationship (QSAR) and quantitative structure–toxicity relationship (QSTR) approaches have increasingly been recognized as valuable tools for safety and risk assessment in various fields, including nanotechnology.[304,305] Some guidelines have been proposed to navigate the regulatory challenges associated with the development and application of QSAR/QSTR models.[306] Modern 3D QSAR (3D-QSAR) and molecular docking techniques are particularly useful for predicting molecular characteristics as well as biological interactions in pharmaceuticals.[307] Nonetheless, these 3D-QSAR and traditional molecular descriptors often fall short in capturing the unique properties of NPs. To address the specificity of NMs, quantitative nanostructure–activity relationship (QNAR) models, also known as nano-QSAR models, have been developed.[299] These models are designed to account for the unique descriptive properties of NMs, providing a more accurate prediction of their behaviour and interactions in biological and environmental systems.[308,309] The NanoTox platform, developed under the GNU General Public License (https://github.com/NanoTox), is an open-source and freely available tool that provides access to nanotoxicology reports and offers a definite feature space for modelling NM toxicity.[302] This feature space incorporates both external and internal physicochemical properties of NMs, and periodic table properties, and correlates these with cell type, cell line, and assay methods.

AuNPs have been considerably examined owing to their distinct characteristics and potent applicability in divergent fields inclusive of electronics, medicine, and biological sustainability.[310] However, understanding their potential toxic effects is crucial for their safe use. *In silico* profiling has been conducted on various AuNPs, leading to the design of geometrical nanodescriptors. These descriptors are essential for quantitative modelling and virtual screening of AuNPs. Quantitative nanostructure–activity relationship (QNAR) modelling has demonstrated high predictability for certain physicochemical characteristics, particularly hydrophobicity (log *P*) and zeta-potential. The QNAR models also show strong predictive power for simple biological activities, such as the uptake of AuNPs by human kidney epithelial cells (HEK293 cells) and lung cells (A549 cells). However, the accuracy of these models decreases for more complex bioactivities. For instance, moderate accuracy was observed for predicting the binding of AuNPs to the acetylcholinesterase enzyme and the induction of ROS in HEK293 cells.[311] This indicates that while the models are useful for certain applications, they may need further refinement for more complex biological interactions. Generation of ROS (the byproducts of cellular oxidative metabolism, primarily produced by the mitochondria) is a critical endpoint in nanotoxicity assessments. Elevated levels of ROS disrupt cellular functions, damage proteins, nucleic acids, and lipids, and ultimately lead to apoptosis or necrosis.[312] This underlines the importance of monitoring ROS production when assessing the toxicity of NPs, including metal and carbon-based NPs, as excessive ROS generation can have severe biological consequences.

CNTs, particularly single-walled CNTs (SWCNTs), are widely utilized in biomedical applications but are also known to pose some hazardous effects.[313] One of the notable toxic effects of SWCNTs is their ability to induce mitochondrial nanotoxicity, leading to bioenergetic dysfunction. Interestingly, this property can be exploited as a potential mechanism for cancer treatment, where disrupting cancer cell bioenergetics could be beneficial. Nanoinformatic tools that utilize quantitative structure–binding relationship (QSBR) models are being developed to better understand and predict the mitotropic behaviour of SWCNTs. These models use optimal structural nanodescriptors to predict how SWCNTs interact with mitochondria. By accurately modelling these interactions, QSBR models can help assess the risk or benefit relationships of SWCNTs in various applications, including their potential use in targeted cancer therapies.[314] This approach aims to balance the beneficial effects of SWCNTs in medical treatments with their potential risks, ensuring safer and more effective use of these NMs.

González-Durruthy *et al.*[315] reported a significant advancement in the assessment of nanotoxicity and therapeutic potential of CNT-based NMs. They employed molecular docking and molecular dynamic (MD) simulations to investigate the interactions between SWCNTs and mitochondrial channels, specifically focusing on the human mitochondrial voltage-dependent anion-selective channel (hVDAC1). The simulations demonstrated that zigzag-SWCNTs could selectively block the ATP-entry-point in hVDAC1 (Fig. 29), potentially disrupting mitochondrial function by inhibiting ATP transport. These findings validated the usage of *in silico* strategies, such as molecular docking and MD simulations, to predict the interactions and potential toxic effects of NMs on cellular components.

MoS_2 NMs have gained attention for their capability in biological applications owing to their properties like carbon-based NMs. They are promising candidates for drug release applications toward microorganisms suitable for cancer theranostics. However, their applications are not without concerns. The findings from MD simulations and electrophysiology experiments have highlighted a potential concern regarding the interaction of MoS_2 nanoflakes with the voltage sensor domain of potassium channels.[316] This interaction could interfere with the proper functioning of these channels, which are critical for the electrical activity of cells, including nerve and muscle cells.

6.4. Mechanism of toxicity of nanomaterials

The mechanism of toxicity of nanomaterials in biomedical applications is complex and depends on various physicochemical properties such as size, surface charge, shape, composition, and surface functionalization.[317,318] Understanding these mechanisms is critical to mitigate adverse biological effects and ensure safe clinical translation. The evaluation of mechanism of toxicity of nanomaterials in biological system involves different steps (Fig. 30) as follows.

(I) Cellular uptake and bioavailability: due to their small size nanomaterials enter cells directly by membrane penetration or indirectly *via* endocytosis (clathrin/caveolae-mediated, macropinocytosis, phagocytosis, *etc.*) (Fig. 30I_1).

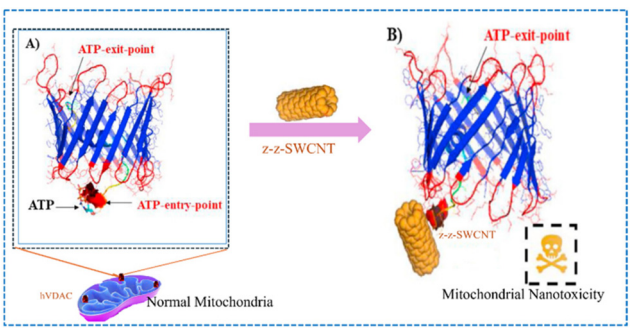

Fig. 29 Computational modelling showing mitochondrial channel nanotoxicity by zigzag-SWCNT NMs; (A) strong affinity of ATP molecules for the ATP-entry-points; (B) the z-z-SWCNT selectively weaken/block the ATP-entry-point in hVDAC1 cells, potentially disrupting mitochondrial function by inhibiting ATP transport. Reprinted with permission from ref. 315. Copyright 2020, Elsevier.

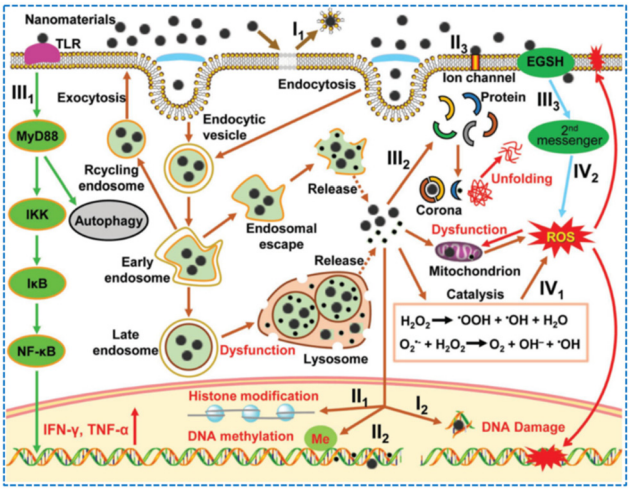

Fig. 30 Different pathways for potential mechanisms of toxicity of nanomaterials in biological systems. (I_1) Shows direct physical destruction of the biomembrane. (I_2) Shows direct destruction of DNA. (II_1 and II_2) Show epigenetic effects induced by nanomaterials. (II_3) Shows nanomaterial-induced blockage of ion channels. (III_1) Shows interaction between nanomaterials and biomolecules, leading to the activation of inflammasome responses (*e.g.*, TLRs) and autophagy. (III_2 and III_3) Show interaction of nanomaterials with proteins, leading to the formation of a corona that alters their functionality, and cellular uptake immune responses. (IV_1) Direct generation of ROS from catalytic reactions. (IV_2) Shows indirect production of ROS by the activation of ROS-related signaling pathways. Reprinted with permission from the ref. 23. Copyright 2019, WILEY-VCH Verlag GmbH & Co. KGaA, Weinheim.

After cellular uptake, they accumulate in organelles (*e.g.*, mitochondria, lysosomes, *etc.*), interfere with cellular homeostasis, and trigger stress signalling pathways.[317]

(II) Oxidative stress and ROS generation: many nanomaterials (*e.g.*, metal oxides like TiO_2, ZnO, *etc.*) catalyze the formation of ROS (Fig. 30IV_1, IV_2), leading to DNA damage, lipid peroxidation, protein denaturation/aggregation, and apoptosis/necrosis.[318]

(III) Inflammatory responses: sometimes nanomaterials activate innate immune receptors like Toll-like receptors (TLRs) and the NOD-like receptor protein 3 (NLRP3) inflammasome (Fig. 30III_1), resulting in the release of pro-inflammatory cytokines (*e.g.*, IL-6, TNF-α, IL-1β), recruitment of immune cells, and chronic inflammation/tissue damage.[319]

(IV) Genotoxicity and DNA damage: genotoxicity occurs *via* direct interaction of nanomaterials with DNA (*e.g.*, intercalation, strand breaks, *etc.*), indirect damage through ROS, chromosomal aberrations and micronucleus formation (Fig. 30I_2). It leads to mutagenesis and carcinogenesis.[320]

(V) Protein corona formation: when nanomaterials enter biological fluids, proteins adsorb to their surface and form a "protein corona" that alters surface identity, cellular uptake profile, and immune recognition (Fig. 30III_2). This may lead to unexpected toxicity and immune activation.[321]

(VI) Lysosomal dysfunction: nanomaterials can accumulate in lysosomes (Fig. 30I_1), causing lysosomal membrane permeabilization, and release of cathepsins leading to cell death.[322]

(VII) Disruption of mitochondrial function: nanomaterials damage mitochondrial functions (Fig. 30IV$_1$, IV$_2$) like impaired mitochondrial membrane potential, ATP depletion, release of pro-apoptotic factors, and enhanced ROS generation.[323]

(VIII) Autophagy dysregulation: nanomaterials can both induce and inhibit autophagy (Fig. 30III$_1$). Disruption of autophagy can exacerbate inflammation and neurotoxicity.[324]

(IX) Epigenetic alterations: some nanomaterials have been shown to alter DNA methylation, histone modifications, and miRNA expression (Fig. 30II$_1$ and II$_2$). These changes can have long-term effects on gene expression and cell behaviour.[325]

7. Clinical trials of smart nanomaterials

Clinical trials involving smart nanomaterials are advancing in various medical or biological fields, including diagnostic imaging, targeted drug delivery, and cancer therapy. These materials are designed to respond to specific biological signals and/or environmental conditions, inclusive of temperature, magnetic fields, and pH, allowing for precise control over therapeutic actions. Smart nanomaterials like liposomes, dendrimers, and polymer-based NPs are being employed to encapsulate drugs and release them at targeted sites, minimizing side effects. These trials often focus on cancer treatments where drugs need to be released to tumour cells while sparing healthy cells.

Liposomes, as pioneering drug delivery systems, have remained prevalent due to their unique advantages. They offer flexibility in composition, are biocompatible and biodegradable, and have low immunogenicity.[326,327] Structurally, liposomes are artificially constructed phospholipid vesicles that can be single or/and multilamellar and are typically between 50–100 nm in size. They contain a central aqueous core where hydrophilic drugs can be encapsulated, although hydrophobic drugs may also be incorporated within the lipid bilayer or chemically attached to the liposome surface. The key distinction between liposomes and micelles, despite both being composed of phospholipids, lies in their structures and applications. While liposomes have an aqueous core suitable for hydrophilic drugs, micelles have a hydrophobic core, making them more suited for encapsulating hydrophobic drugs. Both systems are utilized to achieve targeted delivery, thus minimizing systemic toxicity.[328] Traditional liposomes, known as the "first generation", showed limitations in circulation time due to rapid clearance by the mononuclear phagocyte system, leading to an accumulation mainly in organs like the spleen and liver rather than in tumour tissues. To overcome this, new lipid formulations and modifications were developed, such as sterically stabilized liposomes containing sphingomyelin and choline or pegylated liposomes. These modifications led to extended circulation time and reduced uptake by the reticuloendothelial system (RES), and allowed passive targeting to tumour tissues through the EPR effect.[329] Doxil™, a PEGylated liposomal formulation, was first approved by the FDA in 1995.[330] Like Doxil™, Caelyx™ also uses PEGylation and was approved in 1996 by the European Medicines Agency (EMA). Myocet™ is a non-PEGylated liposomal formulation and was approved in 2000 by the EMA. All these medications (Doxil™, Caelyx™, and Myocet™) represent significant milestones in the field of nanopharmaceuticals, especially in oncology treatment, due to their ability to improve the safety and efficacy of doxorubicin. By encapsulating doxorubicin within liposomal nanocarriers, these formulations reduce the cardiotoxicity linked with the free drug and improve its targeting capabilities.[330,331] Doxil™ and Caelyx™ have versatile indications across several cancer types due to their modified release profile and reduced toxicity. Both Caelyx™ and Doxil™ are used to treat ovarian cancer, particularly in patients whose disease has progressed after platinum-based chemotherapy. These formulations are also indicated for treating Kaposi's sarcoma in patients with AIDS, providing an option that targets the tumours with minimized systemic toxicity. Caelyx™ and Myocet™ are approved for treating metastatic breast cancer, addressing the need for less cardiotoxic options in this patient population.[329]

Mepact™ (mifamurtide) medication is a liposomal formulation containing muramyl tripeptide phosphatidylethanolamine, an immunomodulator. It works by activating monocytes and macrophages to enhance the immune response in paediatric and young adult patients for the treatment of bone cancer.[332] Marqibo™ medication is a nanoparticle formulation containing vincristine encapsulated in cholesterol- and sphingomyelin-based liposomes. Vincristine itself is a potent antineoplastic drug with a multitude of activities, particularly effective against haematological cancers. However, traditional vincristine administration is associated with side effects such as neurotoxicity and/or peripheral neuropathy, which occur in a dose-dependent manner.[333,334]

Protein-based nanoparticles (PrNPs) are also advantageous in drug release systems owing to their biocompatibility and biodegradability. Unlike many synthetic NPs, PrNPs can be formulated without organic solvents or toxic chemicals.[335,336] Oncaspar™ is a PEGylated form of the asparaginase enzyme, employed in treating acute lymphoblastic leukaemia (ALL) in both adults and children. This formulation functions by depleting the blood levels of asparagine, an amino acid vital for the growth and division of tumour cells. Since these cancer cells cannot produce their own asparagine, its reduction leads to their death. Healthy cells, however, are less impacted as they can synthesize asparagine independently. The PEG modification helps reduce hypersensitivity, which is a common side effect in non-PEGylated asparaginase formulations. Moreover, PEGylation increases the enzyme's stability and duration in the bloodstream, allowing for less frequent dosing.[337,338]

Abraxane™ and Pazenir™ are albumin-bound forms of paclitaxel (Taxol), which were approved by the FDA in 2005 and by the EMA in 2008. Paclitaxel, a pioneering member of the taxane family, is widely employed in cancer chemotherapy for its cytotoxic effects. It works by stabilizing microtubules, arresting cells in the G2/M phase of the cell cycle, which pre-

vents them from forming a normal mitotic apparatus, leading to apoptosis. These formulations have shown efficacy toward solid tumours, inclusive of breast, lung, and pancreatic cancers.[339]

Kadcyla™ (also known as ado-trastuzumab emtansine or T-DM1) is a pioneering antibody–drug conjugate that was the first of its kind approved by the FDA and the EMA in 2013. This innovative formulation combines trastuzumab, a humanized monoclonal antibody targeting the HER2 receptor, with emtansine (DM-1), an antimicrotubular agent that interferes with cellular division.[340] DM-1, once internalized, disrupts microtubule function, leading to cell cycle arrest and apoptosis in cancer cells.[341,342]

As of now, in addition to Kadcyla™, a total of 11 other antibody–drug conjugates (ADCs) have received approval from the FDA and EMA.[330] NanoTherm™ is a groundbreaking technology, specifically as the only metallic-based nanoparticle therapy for cancer to receive both EMA and FDA approval.[343] Developed by MagForce AG in Berlin, Germany, NanoTherm™ relies on iron oxide nanoparticles with an amino silane coating, designed to form a colloidal suspension of particles approximately 15 nm in size. These nanoparticles are injected directly into the tumour or its surrounding cavity and subsequently heated through an alternating magnetic field, allowing for localized hyperthermia. This heating either destroys cancer cells directly or sensitizes them to radiotherapy or chemotherapy, which can help prevent recurrence. The primary clinical indications for NanoTherm™ are prostate cancer and glioblastoma multiforme.[344] While nanotechnology holds tremendous potential for advancing cancer therapies, several challenges such as toxicity and biocompatibility, targeting and specificity, clearance and degradation, manufacturing and scalability, regulatory and approval pathways, cost and accessibility, and personalization and patient-specific variability need to be tackled to make sure safe and effective clinical use.[345–355]

7.1. Key challenges in the clinical translation of smart nanomaterials

Despite successful laboratory demonstrations, clinical adoption of smart nanomaterials remains low due to a series of interconnected translational challenges, many of which are under-addressed in the current literature.[356] In this section, we discuss some of the critical challenges that need to be addressed.

1. Manufacturing scale-up and reproducibility

Scaling up the synthesis of smart nanomaterials from lab-scale experiments to industrial-level manufacturing is highly challenging. The synthesis of these materials generally relies on multistep fabrication procedures, involving surface functionalization, ligand attachment, and core–shell layer engineering.[357] These techniques are highly sensitive to reaction conditions. Batch-to-batch variations arises due to inconsistent shape, size, and surface chemistry. These variations particularly arise in black phosphorus and MXenes, which degrade and oxidize readily during processing. Maintaining functional stimulus-responsiveness (*e.g.*, GSH- and pH-sensitive drug release) under good manufacturing practice (GMP) conditions is a difficult task because industrial undertakings usually prioritize stability and simplicity over complexity. In addition, equipment employed at industrial scale may not replicate the fine-tuned parameters of small-scale synthesis. This leads to a loss of biofunctionality and performance of smart nanomaterials.

2. Regulatory frameworks and approval pathways

Smart nanomaterials transcend conventional classifications of drugs, devices, and biologics, leading to a hybrid identity that introduces regulatory ambiguities and hinders their timely clinical translation.[358] In addition to that, regulatory bodies like the EMA and FDA lack established guidelines specific to stimulus-responsive systems. In continuation, the smart materials usually undergo dynamic transformations *in vivo* (*e.g.*, change in charge, shape, *etc.*), complicating their toxicological analysis and long-term safety evaluation.

Moreover, the absence of standardized characterization protocols (*e.g.*, for degradation kinetics, adaptive behaviour, stimulus-response, *etc.*) make it difficult to produce and submit reproducible data for regulatory approval.

3. Long-term toxicity and biocompatibility

Preclinical studies typically assess short-term toxicity. However, for clinical applications, long-term biocompatibility and immunological responses are critical. Smart nanomaterials which switch their properties inside the body may produce unknown degradation products. These unknown products could accumulate and interact unpredictably with biological systems.[359] Moreover, chronic toxicity, immunogenicity, organ-specific accumulation, and interference with cellular pathways are insufficiently studied. For example, black phosphorus degrades into phosphate ions. However, its impact on cellular calcium signaling and potential calcification is still under investigation.[360] Likewise, graphene and metallic hybrid systems may accumulate in the liver, lymph nodes, and spleen, raising concerns about long-term clearance and systemic burden.[361]

4. Economic and scalability barriers

Smart nanomaterials usually require complex, high-cost manufacturing operations, involving cleanroom environments, rare materials, and multistage purification steps. The financial practicability of scaling up these platforms for routine clinical usage is rarely discussed in academic research. Cost-efficacy is essential for acquisition in healthcare systems, particularly in low-resource settings.[362] If smart nanomaterials fail to deliver significantly improved outcomes at a reasonable cost, they risk being overlooked in favor of simpler and more traditional alternatives.

5. Stability, shelf-life, and storage issues

Many smart nanomaterials, especially 2D materials (*e.g.*, MXenes, black phosphorus, *etc.*) and hydrogels, are intrinsically unstable.[363] Their responsiveness to environmental signals is therapeutically advantageous but they are vulnerable to degradation during storage and transportation. Light, humidity, oxygen, and temperature can trigger premature

degradation and loss of functionality. These factors complicate the logistics of packaging, sterilization, and storage under clinical settings.

8. Conclusions and future perspectives

Smart NMs hold transformative potential in wound healing, cancer theranostics, TER, and beyond, offering advanced solutions for targeted therapy and diagnostics. They have transfigured wound treatment through targeted and accelerated healing processes. NMs can deliver drugs directly to infected sites, promote tissue regeneration, and reduce infection. They enhance cell proliferation and differentiation, leading to ameliorated wound closure and reduced scarring.

NM-based wound healing future perspectives involve: (i) personalized medicine: development of smart NMs tailored to individual patients' needs, considering genetic and environmental factors; (ii) advanced biocompatibility: enhancing the biocompatibility of NMs to minimize immune response and adverse reactions; (iii) integration with smart devices: combining NMs with wearable devices for real-time monitoring and controlled release of therapeutics; and (iv) regenerative medicine: exploring the potential of NMs in promoting stem cell remedy and tissue engineering for more complex wound healing applications. Future research should continue to focus on enhancing the biocompatibility and specificity of the smart NMs used in wound healing applications.

In cancer theranostics, smart NMs offer a dual approach of diagnosis and therapy, ameliorating the effectiveness of drugs while inhibiting side effects. NMs can be manipulated to attack specified cancer cells, deliver drugs, and provide imaging contrast, allowing for timely diagnosis and precise treatment.

The future perspectives of NM-based cancer theranostics involve: (i) development of multifunctional NMs: development of NMs that combine multiple curative and diagnostic functions within a single platform is essential; (ii) advanced targeting mechanisms: enhancing targeting mechanisms for improving explicitness and reducing off-target effects, possibly through advanced ligand–receptor interactions, should be increased; (iii) advanced non-invasive techniques: refining non-invasive diagnostic techniques using NMs, such as liquid biopsies, will boost cancer theranostics; these techniques enhance diagnostic accuracy and therapeutic precision in cancer therapy; and (iv) advanced therapeutic monitoring: real-time monitoring of treatment responses using NMs to adjust therapy dynamically. Smart NMs enable sophisticated, real-time, non-invasive monitoring of therapeutic responses in cancer therapy. By integrating diagnostic and therapeutic functions, these materials provide valuable insights into drug delivery, efficacy, and resistance. Future developments in this field aim to enhance the sensitivity, specificity, and multifunctionality of NMs, ultimately improving personalized cancer treatment and patient outcomes. The continuous advancement of nanotechnology will likely lead to more precise, efficient, and safer therapeutic monitoring strategies.

Nanotechnology offers a promising strategy for TER. Nanoscale scaffolds provide outstanding advantages over traditional therapies by closely mimicking native ECM. This creates an ideal environment for cell proliferation, adhesion, and differentiation. Key nanostructures, for example, nanotubes, nanofibers, polymeric nanoparticles, and nanocomposites, contribute to controlled degradation rates, enhanced mechanical strength, and improved bioactivity. They also have the capability to encapsulate small molecules, genetic materials, and growth factors, protecting these agents and allowing for their sustained release at the injury site. 3D bioprinting holds considerable potential to meet the demand for biomimetic artificially regenerated tissues for transplantation in patients with damaged organs. The review also examines the use of hybrid bioinks made up of synthetic and natural NMs with various printers. However, the fabrication of inner tissues/organs may lead to biological safety and liability concerns, presenting another obstacle that needs to be addressed.

While smart NMs hold great promise, their potential toxicity remains a critical concern. Nanotoxicity studies have revealed that certain NMs can induce cytotoxicity, genotoxicity, and dysfunction of the heart, kidneys, spleen, liver, *etc*. by accumulating in them. The toxicity of NMs is affected by both the NMs' shape, composition, size, and coatings as well as the biological system with which they interact. Understanding and mitigating these effects are essential for safe clinical applications.

The future perspectives of nanotoxicity involve: (i) comprehensive toxicity profiling: development of standardized methods for comprehensive toxicity profiling of NMs is essential; (ii) advanced green nanotechnology: advancing green synthesis methods to produce environmentally benign and biocompatible NMs is the need of the moment to overcome nanotoxicity; (iii) robust regulatory frameworks: establishment of robust regulatory frameworks and guidelines for the safe use of NMs in medical applications will help in reducing nanotoxicity; and (iv) long-term and comprehensive studies: conducting long-term and comprehensive *in vivo* studies to understand the chronic effects and biodistribution of NMs would help in understanding and overcoming nanotoxicity.

Hence, smart NMs represent a remarkable furtherance in biomedical applications, offering innovative solutions for wound healing, cancer theranostics, tissue engineering and regeneration, and other medical challenges. However, their successful implementation requires careful consideration of their biocompatibility and potential toxic effects.

Taken together, smart nanomedicine-based future research should focus on the following key areas: (i) standardization and scalability of synthesis protocols; (ii) comprehensive toxicological profiling; (iii) multifunctionality and stimulus-responsiveness in complex microenvironments; (iv) integration with digital health and theranostics; (v) overcoming regulatory and ethical barriers; (vi) application-specific innovations; and (vii) real-world validation and clinical trials.

Hence, the future of smart nanomaterials in biomedicine lies in interdisciplinary convergence, regulatory reform, and patient-centric design. By integrating continued advances in materials science, systems biology, and digital health, smart nanomaterials are poised to revolutionize diagnostics, therapy, and regenerative medicine if safety, scalability, and societal acceptance are comprehensively addressed.

Author contributions

Manoj Kumar Goshisht: idea conceptualization, writing original draft, methodology, and editing. Ashu Goshisht: idea conceptualization, writing original draft, methodology, editing and reviewing. Animesh Bajpai: writing – original draft and reviewing. Abheshek Bajpai: writing – original draft and methodology.

Conflicts of interest

The authors declare that they have no known competing financial interests or personal relationships that could have appeared to influence the work reported in this paper.

Data availability

No primary research results, software or code have been included, and no new data were generated or analyzed as part of this review.

References

1 M. Yoshida and J. Lahann, Smart Nanomaterials, *ACS Nano*, 2008, **2**(6), 1101–1107, DOI: 10.1021/nn800332g.
2 B. K. Kashyap, V. V. Singh, M. K. Solanki, A. Kumar, J. Ruokolainen and K. K. Kesari, Smart nanomaterials in cancer theranostics: challenges and opportunities, *ACS Omega*, 2023, **8**(16), 14290–14320, DOI: 10.1021/acsomega.2c07840.
3 A. K. Dąbrowska, F. Spano, S. Derler, C. Adlhart, N. D. Spencer and R. M. Rossi, *Skin Res. Technol.*, 2018, **24**, 165–174.
4 S. K. Nethi, S. Das, C. R. Patra and S. Mukherjee, *Biomater. Sci.*, 2019, **7**, 2652–2674.
5 S. F. Spampinato, G. I. Caruso, R. De Pasquale, M. A. Sortino and S. Merlo, *Pharmaceuticals*, 2020, **13**, 60.
6 H. N. Wilkinson and M. J. Hardman, *Open Biol.*, 2020, **10**, 200223.
7 H. Singh, M. Dhanka, I. Yadav, S. Gautam, S. M. Bashir, N. C. Mishra, T. Arora and S. Hassan, *Tissue Eng., Part B*, 2024, **30**, 230–253.
8 R. Mu, S. Campos de Souza, Z. Liao, L. Dong and C. Wang, *Adv. Drug Delivery Rev.*, 2022, **185**, 114298.
9 C. K. Sen, G. M. Gordillo, S. Roy, R. Kirsner, L. Lambert, T. K. Hunt, F. Gottrup, G. C. Gurtner and M. T. Longaker, *Wound Repair Regen.*, 2009, **17**, 763–771.
10 M. Wang, X. Huang, H. Zheng, Y. Tang, K. Zeng, L. Shao and L. Li, *J. Controlled Release*, 2021, **337**, 236–247.
11 M. M. Mihai, M. B. Dima, B. Dima and A. M. Holban, *Materials*, 2019, **12**, 2176.
12 D. K. Chandra, R. L. Reis, S. C. Kundu, A. Kumar and C. Mahapatra, *ACS Biomater. Sci. Eng.*, 2024, **10**(7), 4145–4174.
13 H. Sung, J. Ferlay, R. L. Siegel, M. Laversanne, I. Soerjomataram, A. Jemal and F. Bary, *CA: Cancer J. Clin.*, 2021, **71**, 209–249.
14 F. Bray, J. Ferlay, I. Soerjomataram, R. L. Siegel, L. A. Torre and A. Jemal, *CA: Cancer J. Clin.*, 2018, **68**, 394–424.
15 Y. Hosomi, S. Morita, S. Sugawara, T. Kato, T. Fukuhara, A. Gemma, K. Takahashi, Y. Fujita, T. Harada, K. Minato, K. Takamura, K. Hagiwara, K. Kobayashi, T. Nukiwa and A. Inoue, *J. Clin. Oncol.*, 2020, **38**, 115–123.
16 R. Baghban, L. Roshangar, R. Jahanban-Esfahlan, K. Seidi, A. Ebrahimi-Kalan, M. Jaymand, S. Kolahian, T. Javaheri and P. Zare, *Cell Commun. Signaling*, 2020, **18**, 59.
17 P. K. Gupta, *J. Pharm. Sci.*, 1990, **79**, 949–962.
18 R. Tenchov, R. Bird, A. E. Curtze and Q. Zhou, *ACS Nano*, 2021, **15**, 16982–17015.
19 M. J. Mitchell, M. M. Billingsley, R. M. Haley, M. E. Wechsler, N. A. Peppas and R. Langer, *Nat. Rev. Drug Discovery*, 2021, **20**, 101–124.
20 J. Liu, Z. Liu, Y. Pang and H. Zhou, *J. Nanobiotechnol.*, 2022, **20**, 127.
21 Y. Herdiana, N. Wathoni, S. Shamsuddin and M. Muchtaridi, *Heliyon*, 2022, **8**, e08674.
22 D. Peer, J. M. Karp, S. Hong, O. C. Farokhzad, R. Margalit and R. Langer, *Nat. Nanotechnol.*, 2007, **2**, 751–760.
23 L. Yan, F. Zhao, J. Wang, Y. Zu, Z. Gu and Y. Zhao, *Adv. Mater.*, 2019, **31**, 1805391, DOI: 10.1002/adma.201805391.
24 P. C. Ray, H. Yu and P. P. Fu, Toxicity and Environmental Risks of Nanomaterials: Challenges and Future Needs, *J. Environ. Sci. Health, Part C: Environ. Carcinog. Ecotoxicol. Rev.*, 2009, **27**, 1–35.
25 Mamata, A. Agarwal, A. Awasthi, K. Awasthi and A. Dutta, Antibacterial activities of GO–Ag nanocomposites with various loading concentrations of Ag nanoparticles, *Appl. Phys. A*, 2023, **129**, 838, DOI: 10.1007/s00339-023-07115-w.
26 A. Agrawal, R. Sharma, A. Sharma, K. C. Gurjar, S. Kumar, S. Chatterjee, H. Pandey, K. Awasthi and A. Awasthi, Antibacterial and antibiofilm efficacy of green synthesized ZnO nanoparticles using Saraca asoca leaves, *Environ. Sci. Pollut. Res. Int.*, 2023, **30**, 86328–86337, DOI: 10.1007/s11356-023-28524-7.
27 S. K. Sohaebuddin, P. T. Thevenot, D. Baker, J. W. Eaton and L. Tang, *Part. Fibre Toxicol.*, 2010, **7**, 22.
28 V. A. Senapati, A. Kumar, G. S. Gupta, A. K. Pandey and A. Dhawan, *Food Chem. Toxicol.*, 2015, **85**, 61–70.
29 X. Yuan, W. Nie, Z. He, J. Yang, B. Shao, X. Ma, X. Zhang, Z. Bi, L. Sun, X. Liang, Y. Tie, Y. Liu, F. Mo, D. Xie, Y. Wei and X. Wei, *Theranostics*, 2020, **10**, 4589–4605.

30 V. Ramalingam, S. Revathidevi, T. Shanmuganayagam, L. Muthulakshmi and R. Rajaram, *RSC Adv.*, 2016, **6**, 20598–20608.
31 L. Zhang, L. Wu, Y. Mi and Y. Si, *Bull. Environ. Contam. Toxicol.*, 2019, **103**, 181–186.
32 T. H. Shin, C. Seo, D. Y. Lee, M. Ji, B. Manavalan, S. Basith, S. K. Chakkarapani, S. H. Kang, G. Lee, M. J. Paik and C. B. Park, *Arch. Toxicol.*, 2019, **93**, 1201–1212.
33 M. K. Goshisht, P. Kaur and M. S. Bakshi, *ACS Appl. Nano Mater.*, 2024, **7**(14), 16949–16963, DOI: 10.1021/acsanm.4c03061.
34 F. Farjadian, S. Rezaeifard, M. Naeimi, S. Ghasemi, S. Mohammadi-Samani, M. E. Welland and L. Tayebi, *Int. J. Nanomed.*, 2019, **14**, 6901–6915, DOI: 10.2147/IJN.S214467.
35 H. M. El-Husseiny, E. A. Mady, L. Hamabe, A. Abugomaa, K. Shimada, T. Yoshida, T. Tanaka, A. Yokoi, M. Elbadawy and R. Tanaka, *Mater. Today Bio*, 2022, **13**(2022), 100186, DOI: 10.1016/j.mtbio.2021.100186.
36 M. Moniruzzaman, S. D. Dutta, K.-T. Lim and J. Kim, *ACS Omega*, 2022, **7**(42), 37388–37400, DOI: 10.1021/acsomega.2c04130.
37 M. S. Bakshi, *Acc. Mater. Res.*, 2024, **5**(8), 1000–1012, DOI: 10.1021/accountsmr.4c00151.
38 M. Aflori, *Nanomaterials*, 2021, **11**, 396, DOI: 10.3390/nano11020396.
39 G. E. Yılmaz, I. Göktürk, M. Ovezova, F. Yılmaz, S. Kılıç and A. Denizli, *Hygiene*, 2023, **3**, 269–290, DOI: 10.3390/hygiene3030020.
40 S. K. Mondal, S. Chakraborty, S. Manna and S. M. Mandal, *RSC Pharm.*, 2024, **1**, 388–402, DOI: 10.1039/D4PM00032C.
41 A. B. Khiabani and M. Gasik, *Int. J. Mol. Sci.*, 2022, **23**, 3665, DOI: 10.3390/ijms23073665.
42 K. M. Fahy, M. K. Eiken, K. V. Baumgartner, K. Q. Leung, S. E. Anderson, E. Berggren, E. Bouzos, L. R. Schmitt, P. Asuri and K. E. Wheeler, *ACS Omega*, 2023, **8**(3), 3310–3318, DOI: 10.1021/acsomega.2c06882.
43 M. K. Goshisht, R. Kaur and M. S. Bakshi, *Langmuir*, 2025, **41**(12), 8214–8227, DOI: 10.1021/acs.langmuir.4c05340.
44 A. Lamoot, A. Uvyn, S. Kasmi and B. G. De Geest, *Angew. Chem., Int. Ed.*, 2021, **60**, 6320, DOI: 10.1002/anie.202015625.
45 J. Zhang, L. Mou and X. Jiang, *Chem. Sci.*, 2020, **11**, 923–936, DOI: 10.1039/C9SC06497D.
46 X.-P. Li, D.-Y. Hou, J.-C. Wu, P. Zhang, Y.-Z. Wang, M.-Y. Lv, Y. Yi and W. Xu, *ACS Biomater. Sci. Eng.*, 2024, **10**(9), 5474–5495, DOI: 10.1021/acsbiomaterials.4c00388.
47 M. Guo, Y. Yan, H. Zhang, H. Yan, Y. Cao, K. Liu, S. Wan, J. Huang and W. Yue, *J. Mater. Chem.*, 2008, **18**, 5104–5112, DOI: 10.1039/B810061F.
48 T. Fuoco, D. Pappalardo and A. Finne-Wistrand, *Macromolecules*, 2017, **50**(18), 7052–7061, DOI: 10.1021/acs.macromol.7b01318.
49 J. Wen, J. Xu, M. Hong, W. Li and T. Li, *J. Drug Delivery Sci. Technol.*, 2025, **105**, 106638, DOI: 10.1016/j.jddst.2025.106638.
50 A. Joorabloo and T. Liu, *J. Controlled Release*, 2023, **356**, 463–480.
51 E. Kolanthai, Y. Fu, U. Kumar, B. Babu, A. K. Venkatesan, K. W. Liechty and S. Seal, *Wiley Interdiscip. Rev.: Nanomed. Nanobiotechnol.*, 2021, e1741.
52 M. K. Goshisht, L. Moudgil, M. Rani, P. Khullar, G. Singh, H. Kumar, N. Singh, G. Kaur and M. S. Bakshi, *J. Phys. Chem. C*, 2014, **118**(48), 28207–28219, DOI: 10.1021/jp5078054.
53 X. Chen, D. Wu and Z. Chen, *MedComm*, 2024, **5**(8), e643, DOI: 10.1002/mco2.643.
54 U. Havelikar, K. B. Ghorpade, A. Kumar, A. Patel, M. Singh, N. Banjare and P. N. Gupta, *Discover Nano*, 2024, **19**, 165, DOI: 10.1186/s11671-024-04118-1.
55 G. Gaucher, M.-H. Dufresne, V. P. Sant, N. Kang, D. Maysinger and J.-C. Leroux, *J. Controlled Release*, 2005, **109**(1–3), 169–188, DOI: 10.1016/j.jconrel.2005.09.034.
56 A. Crintea, A. C. Motofelea, A. S. Şovrea, A.-M. Constantin, C.-B. Crivii, R. Carpa and A. G. Duțu, *Pharmaceutics*, 2023, **15**(5), 1406, DOI: 10.3390/pharmaceutics15051406.
57 M. Vallet-Regí, F. Schüth, D. Lozano, M. Colilla and M. Manzano, *Chem. Soc. Rev.*, 2022, **51**, 5365–5451, DOI: 10.1039/D1CS00659B.
58 A. Vashist, G. P. Alvarez, V. A. Camargo, A. D. Raymond, A. Y. Arias, N. Kolishetti, A. Vashist, P. Manickam, S. Aggarwal and M. Nair, *Biomater. Sci.*, 2024, **12**, 6006–6018, DOI: 10.1039/D4BM00224E.
59 P. Makvandi, C. Y. Wang, E. N. Zare, A. Borzacchiello, L. N. Niu and F. R. Tay, *Adv. Funct. Mater.*, 2020, **30**, 1910021.
60 Y. Zheng, M. Wei, H. Wu, F. Li and D. Ling, *J. Nanobiotechnol.*, 2022, **20**, 328.
61 D. Franco, G. Calabrese, S. P. Guglielmino and S. Conoci, *Microorganisms*, 2022, **10**, 1778.
62 I. X. Yin, J. Zhang, I. S. Zhao, M. L. Mei, Q. Li and C. H. Chu, *Int. J. Nanomed.*, 2020, **15**, 2555–2562.
63 G. R. Tortella, O. Rubilar, N. Durán, M. C. Diez, M. Martínez, J. Parada and A. B. Seabra, *J. Hazard. Mater.*, 2020, **390**, 121974.
64 S. Sathiyaraj, G. Suriyakala, A. Dhanesh Gandhi, R. Babujanarthanam, K. S. Almaary, T. W. Chen and K. Kaviyarasu, *J. Infect. Public Health*, 2021, **14**, 1842–1847.
65 Sonia, A. Singh, Shivangi, R. Kukreti, S. Kukreti and M. Kaushik, *Biomater. Adv.*, 2022, **134**, 112678.
66 A. S. Abu Lila, B. Huwaimel, A. Alobaida, T. Hussain, Z. Rafi, K. Mehmood, M. H. Abdallah, T. A. Hagbani, S. M. D. Rizvi, A. Moin and A. F. Ahmed, *Materials*, 2022, **15**, 5709.
67 L. Wang, W. Zheng, S. Li, Q. Hou and X. Jiang, *Chem. Commun.*, 2022, **58**, 7690–7693.
68 L. Qiu, C. Wang, M. Lan, Q. Guo, X. Du, S. Zhou, P. Cui, T. Hong, P. Jiang, J. Wang and J. Xia, *ACS Appl. Bio Mater.*, 2021, **4**, 3124–3132.
69 Y. Hu, J. Shao, H. Dong, D. Yang and X. Dong, *ACS Mater. Lett.*, 2024, **6**(9), 4209–4229, DOI: 10.1021/acsmaterialslett.4c01165.

70 B. Singh, J. Kim, N. Shukla, J. Lee, K. Kim and M.-H. Park, *ACS Appl. Bio Mater.*, 2023, **6**(6), 2314–2324, DOI: 10.1021/acsabm.3c00178.
71 T. A. Singh, A. Sharma, N. Tejwan, N. Ghosh, J. Das and P. C. Sil, *Adv. Colloid Interface Sci.*, 2021, **295**, 102495.
72 A. Naskar, S. Lee and K. S. Kim, *RSC Adv.*, 2020, **10**, 1232–1242.
73 O. R. Abbasabadi, M. R. Farahpour and Z. G. Tabatabaei, *Int. J. Biol. Macromol.*, 2022, **217**, 42–54.
74 H. Zhang, X. Zhang, Q. Cao, S. Wu, X.-Q. Wang, N. Peng, D. Zeng, J. Liao and H. Xu, *Biomater. Sci.*, 2022, **10**, 5888–5899.
75 M. K. Goshisht, *APMIS*, 2025, **133**(7), e70050, DOI: 10.1111/apm.70050.
76 R. Sharma, N. Gupta, V. Kumar, S. Pal, V. Kaundal and V. Sharma, *Int. Surg. J.*, 2017, **4**(8), 2627–2631, DOI: 10.18203/2349-2902.isj20173401.
77 D. Patel, R. Maisuria, J. Manza, D. Chaudhari and D. Dave, *Int. Surg. J.*, 2019, **6**(2), 508–511, DOI: 10.18203/2349-2902.isj20190393.
78 Y. Tajdar, S. Singh, A. Raj, A. Raj and V. Bhushan, *Turk. J. Surg.*, 2024, **40**(1), 28–35, DOI: 10.47717/turkjsurg.2024.6168.
79 Bheemya, A. I. Peter and V. Kalyanpur, *AJ J. Med. Sci.*, 2025, **2**(1), 11–16, DOI: 10.71325/ajjms.v2i1.25.5.
80 G. Borkow, T. Roth and A. Kalinkovich, *Microbiol. Res.*, 2022, **13**, 366–376, DOI: 10.3390/microbiolres13030029.
81 E. Melamed, J. Dabbah, T. Israel, I. Kan, M. S. Pinzur, T. Roth and G. Borkow, *Adv. Wound Care*, 2025, DOI: 10.1089/wound.2024.0273.
82 N. Chauhan, K. Saxena and U. Jain, *Biomed. Mater. Devices*, 2023, **1**, 108–121.
83 D. K. Shanmugam, Y. Madhavan, A. Manimaran, G. S. Kaliaraj, K. G. Mohanraj, N. Kandhasamy and K. K. Amirtharaj Mosas, *Gels*, 2023, **9**, 22.
84 C. Xie, Y. Xu, Y. Liu, M. Chen, P. Du, Y. Zhang, X. Ma and S. Yang, *Chem. Eng. J.*, 2023, **477**, 146997.
85 P. Bridgman, *J. Am. Chem. Soc.*, 1914, **36**, 1344–1363.
86 M. Fojtů, X. Chia, Z. Sofer, M. Masařík and M. Pumera, *Adv. Funct. Mater.*, 2017, **27**, 1701955.
87 X. W. Huang, J. J. Wei, M. Y. Zhang, X. L. Zhang, X. F. Yin, C. H. Lu, J. B. Song, S. M. Bai and H. H. Yang, *ACS Appl. Mater. Interfaces*, 2018, **10**, 35495–35502.
88 S. Huang, S. Xu, Y. Hu, X. Zhao, L. Chang, Z. Chen and X. Mei, *Acta Biomater.*, 2022, **137**, 199–217.
89 B. Anasori, M. R. Lukatskaya and Y. Gogotsi, *Nat. Rev. Mater.*, 2017, **2**, 16098.
90 V. M. Hong Ng, H. Huang, K. Zhou, P. S. Lee, W. Que, J. Z. Xu and L. B. Kong, *J. Mater. Chem. A*, 2017, **5**, 3039–3068.
91 K. Rasool, M. Helal, A. Ali, C. E. Ren, Y. Gogotsi and K. A. Mahmoud, *ACS Nano*, 2016, **10**, 3674–3684.
92 O. S. Lee, M. E. Madjet and K. A. Mahmoud, *Nano Lett.*, 2021, **21**, 8510–8517.
93 Y. Gao, Y. Dong, S. Yang, A. Mo, X. Zeng, Q. Chen and Q. Peng, *J. Colloid Interface Sci.*, 2022, **617**, 533–541.
94 C. Yu, S. Sui, X. Yu, W. Huang, Y. Wu, X. Zeng, Q. Chen, J. Wang and Q. Peng, *Colloids Surf., B*, 2022, **217**, 112663.
95 G. P. Lim, C. F. Soon, N. L. Ma, M. Morsin, N. Nayan, M. K. Ahmad and K. S. Tee, *Environ. Res.*, 2021, **201**, 111592.
96 X. Zhao, A. Vashisth, E. Prehn, W. Sun, S. A. Shah, T. Habib, Y. Chen, Z. Tan, J. L. Lutkenhaus, M. Radovic and M. J. Green, *Matter*, 2019, **1**, 513–526.
97 H. Park, J.-U. Kim, S. Kim, N. S. Hwang and H. D. Kim, *Mater. Today Bio*, 2023, **23**, 100881, DOI: 10.1016/j.mtbio.2023.100881.
98 X. Li, J. Shan, W. Zhang, S. Su, L. Yuwen and L. Wang, *Small*, 2017, **13**, 1602660.
99 S. Bharti, S. K. Tripathi and K. Singh, *Anal. Biochem.*, 2024, **685**, 115404.
100 A. S. Sethulekshmi, A. Saritha, K. Joseph, A. S. Aprem and S. B. Sisupal, *J. Controlled Release*, 2022, **348**, 158–185.
101 W. Yin, J. Yu, F. Lv, L. Yan, L. R. Zheng, Z. Gu and Y. Zhao, *ACS Nano*, 2016, **10**, 11000–11011.
102 F. Cao, E. Ju, Y. Zhang, Z. Wang, C. Liu, W. Li, Y. Huang, K. Dong, J. Ren and X. Qu, *ACS Nano*, 2017, **11**, 4651–4659.
103 W. Duan, K. Xu, S. Huang, Y. Gao, Y. Guo, Q. Shen, Q. Wei, W. Zheng, Q. Hu and J.-W. Shen, *Int. J. Pharm.*, 2024, **659**, 124247.
104 A. Joorabloo and T. Liu, *J. Nanobiotechnol.*, 2022, **20**, 407.
105 A. T. Yayehrad, E. A. Siraj, M. Matsabisa and G. Birhanu, *Regen. Ther.*, 2023, **24**, 361–376.
106 L. Mao, L. Wang, M. Zhang, M. W. Ullah, L. Liu, W. Zhao, Y. Li, A. A. Q. Ahmed, H. Cheng, Z. Shi and G. Yang, *Adv. Healthcare Mater.*, 2021, **10**, 2100402.
107 B. Wang, D. Zhao, Y. Li, X. Zhou, Z. Hui, X. Lei, L. Qiu, Y. Bai, C. Wang, J. Xia, Y. Xuan, P. Jiang and J. Wang, *ACS Appl. Nano Mater.*, 2023, **6**(8), 6891–6900.
108 S. C. Owen, D. P. Y. Chan and M. S. Shoichet, *Nano Today*, 2012, **7**, 53–65.
109 R. Solanki and D. Bhatia, Stimulus-Responsive Hydrogels for Targeted Cancer Therapy, *Gels*, 2024, **10**, 440, DOI: 10.3390/gels10070440.
110 N. Zhang, Z. Wang and Y. Zhao, *Cytokine Growth Factor Rev.*, 2020, **55**, 80–85.
111 Y. H. A. Hussein and M. Youssry, *Materials*, 2018, **11**, 688.
112 O. Gutiérrez Coronado, C. Sandoval Salazar, J. L. Muñoz Carrillo, O. A. Gutiérrez Villalobos, M. d. l. L. Miranda Beltrán, A. D. Soriano Hernández, V. Beltrán Campos and P. T. Villalobos Gutiérrez, *Int. J. Mol. Sci.*, 2025, **26**, 2633, DOI: 10.3390/ijms26062633.
113 M. Puzzo, M. De Santo, C. Morelli, A. Leggio and L. Pasqua, *Small Sci.*, 2024, **4**, 2400113, DOI: 10.1002/smsc.202400113.
114 P. Singh, S. Pandit, V. R. S. S. Mokkapati, A. Garg, V. Ravikumar and I. Mijakovic, *Int. J. Mol. Sci.*, 2018, **19**, 1979.
115 P. Singh, H. Singh, Y. J. Kim, R. Mathiyalagan, C. Wang and D. C. Yang, *Enzym. Microb. Technol.*, 2016, **86**, 75–83.

116 W. Xu, J. Qian, G. Hou, Y. Wang, J. Wang, T. Sun, L. Ji, A. Suo and Y. Yao, *Acta Biomater.*, 2019, **83**, 400–413, DOI: 10.1002/adhm.202100402.
117 M. Liu, W. Lai, M. Chen, P. Wang, J. Liu, X. Fang, Y. Yang and C. Wang, *Colloids Surf., A*, 2023, **662**, 131016, DOI: 10.1021/acsanm.2c05467.
118 F. Soetaert, P. Korangath, D. Serantes, S. Fiering and R. Ivkov, *Adv. Drug Delivery Rev.*, 2020, **163–164**, 65–83, DOI: 10.1016/j.addr.2020.06.025.
119 T. Vangijzegem, V. Lecomte, I. Ternad, L. Van Leuven, R. N. Muller, D. Stanicki and S. Laurent, *Pharmaceutics*, 2023, **15**(1), 236, DOI: 10.3390/pharmaceutics15010236.
120 S. Chung, R. A. Revia and M. Zhang, *Nanoscale Horiz.*, 2021, **6**, 696–717, DOI: 10.1039/D1NH00179E.
121 C. A. Quinto, P. Mohindra, S. Tong and G. Bao, *Nanoscale*, 2015, **7**, 12728–12736, DOI: 10.1039/C5NR02718G.
122 V. Sachdeva, A. Monga, R. Vashisht, D. Singh, A. Singh and N. Bedi, *J. Drug Delivery Sci. Technol.*, 2022, **74**, 103585, DOI: 10.1016/j.jddst.2022.103585.
123 M. V. Shestovskaya, A. L. Luss, O. A. Bezborodova, V. V. Makarov and A. A. Keskinov, *Pharmaceutics*, 2023, **15**(10), 2406, DOI: 10.3390/pharmaceutics15102406.
124 Z. Zhao, M. Li, J. Zeng, L. Huo, K. Liu, R. Wei, K. Ni and J. Gao, *Bioact. Mater.*, 2022, **12**, 214–245.
125 P. Rani, J. U. Rahim, S. Patra, R. Gupta, M. Gulati and B. Kapoor, *J. Drug Delivery Sci. Technol.*, 2024, **96**, 105715.
126 X. Li, J. Niu, L. Deng, Y. Yu, L. Zhang, Q. Chen, J. Zhao, B. Wang and H. Gao, *Acta Biomater.*, 2024, **173**, 432–441, DOI: 10.1016/j.actbio.2023.11.019.
127 D. Brühwiler, *Nanoscale*, 2010, **2**, 887–892.
128 F. Tang, L. Li and D. Chen, *Adv. Mater.*, 2012, **24**, 1504–1534.
129 Q. He, J. Zhang, J. Shi, Z. Zhu, L. Zhang, W. Bu, L. Guo and Y. Chen, *Biomaterials*, 2010, **31**, 1085–1092.
130 X. Liu, W. Chen, D. Zhao, X. Liu, Y. Wang, Y. Chen and X. Ma, *ACS Nano*, 2022, **16**, 10354–10363.
131 Y. Cai, T. Deng, Y. Pan and J. I. Zink, *Adv. Funct. Mater.*, 2020, **30**, 2002043.
132 S. Yang, L. Chen, X. Zhao, P. Sun, L. Fu, F. You, M. Xu, Z. You, G. Kai and C. He, *Chem. Eng. J.*, 2019, **378**, 122171.
133 Y. Wang, Q. Zhao, N. Han, L. Bai, J. Li, E. Che, L. Hu, Q. Zhang, T. Jiang and S. Wang, *Nanomedicine*, 2015, **11**, 313–327.
134 Y. Zhang, Z. Ye, R. He, Y. Li, B. Xiong, M. Yi, Y. Chen, J. Liu and B. Lu, *Colloids Surf., B*, 2023, **224**, 113201, DOI: 10.1016/j.colsurfb.2023.113201.
135 P. Zrazhevskiy, M. Sena and X. Gao, *Chem. Soc. Rev.*, 2010, **39**, 4326–4354.
136 M. F. Bertino, R. R. Gadipalli, L. A. Martin, L. E. Rich, A. Yamilov, B. R. Heckman, N. Leventis, S. Guha, J. Katsoudas, R. Divan and D. C. Mancini, *Nanotechnology*, 2007, **18**, 315603.
137 A. R. C. Osypiw, S. Lee, S.-M. Jung, S. Leoni, P. M. Smowton, B. Hou, J. M. Kim and G. A. J. Amaratunga, *Mater. Adv.*, 2022, **3**, 6773–6790.
138 S. Sun, Q. Guan, Y. Liu, B. Wei, Y. Yang and Z. Yu, *Chin. Chem. Lett.*, 2019, **30**, 1051–1054.
139 Y. Li, P. Zhang, W. Tang, K. J. McHugh, S. V. Kershaw, M. Jiao, X. Huang, S. Kalytchuk, C. F. Perkinson, S. Yue, Y. Qiao, L. Zhu, L. Jing, M. Gao and B. Han, *ACS Nano*, 2022, **16**, 8076–8094.
140 L. Karthikeyan, P. A. Rasheed, Y. Haldorai and R. Vivek, *ACS Appl. Polym. Mater.*, 2023, **5**(9), 7167–7179, DOI: 10.1021/acsapm.3c01148.
141 T. G. Katmerlikaya, B. C. Ersen, A. Dag, B. Sancakli, P. S. O. Ozgen, E. K. Yalcin and B. Avci, *ACS Appl. Polym. Mater.*, 2024, **6**(7), 4149–4163, DOI: 10.1021/acsapm.4c00238.
142 M. He, L. Yu, Y. Yang, B. Zou, W. Ma, M. Yu, J. Lu, G. Xiong, Z. Yu and A. Li, *Chin. Chem. Lett.*, 2020, **31**, 3178–3182.
143 Z. Hong, X. Zan, T. Yu, Y. Hu, H. Gou, S. Zheng, X. Gao and P. Zhou, *Chin. Chem. Lett.*, 2023, **34**, 107603.
144 N. Kamaly, B. Yameen, J. Wu and O. C. Farokhzad, *Chem. Rev.*, 2016, **116**, 2602–2663.
145 K. Chansaenpak, G. Y. Yong, A. Prajit, P. Hiranmartsuwan, S. Selvapaandian, B. Ouengwanarat, T. Khrootkaew, P. Pinyou, C. S. Kue and A. Kamkaew, *Nanoscale Adv.*, 2024, **6**, 406–417, DOI: 10.1039/D3NA00718A.
146 A. P. Singh, A. Biswas, A. Shukla and P. Maiti, *Signal Transduct. Target. Ther.*, 2019, **4**, 33.
147 Z. Mhlwatika and B. A. Aderibigbe, *Molecules*, 2018, **23**, 2205.
148 S. García-Gallego, G. Franci, A. Falanga, R. Gómez, V. Folliero, S. Galdiero, F. J. de la Mata and M. Galdiero, *Molecules*, 2017, **22**, 1581.
149 A. Santos, F. Veiga and A. Figueiras, *Materials*, 2019, **13**, 65.
150 J. Recio-Ruiz, R. Carloni, S. Ranganathan, L. Muñoz-Moreno, M. J. Carmena, M. F. Ottaviani, F. J. de la Mata and S. García-Gallego, *Chem. Mater.*, 2013, **35**, 2797–2807.
151 B. Srinageshwar, S. Peruzzaro, M. Andrews, K. Johnson, A. Hietpas, B. Clark, C. McGuire, E. Petersen, J. Kippe, A. Stewart, O. Lossia, A. Al-Gharaibeh, A. Antcliff, R. Culver, D. Swanson, G. Dunbar, A. Sharma and J. Rossignol, *Int. J. Mol. Sci.*, 2017, **18**, 628.
152 L. M. Kaminskas, B. D. Kelly, V. M. McLeod, G. Sberna, D. J. Owen, B. J. Boyd and C. J. H. Porter, *J. Controlled Release*, 2011, **152**, 241–248.
153 C.-S. Lee, T. W. Kim, Y. Kang, Y. Ju, J. Ryu, H. Kong, Y.-S. Jang, D. E. Oh, S. J. Jang, H. Cho, S. Jeon, J. Kim and T. H. Kim, *Mater. Today Chem.*, 2022, **26**, 101083, DOI: 10.1016/j.mtchem.2022.101083.
154 S. Perumal, R. Atchudan and W. Lee, *Polymers*, 2022, **14**, 2510.
155 Y. H. A. Hussein and M. Youssry, *Materials*, 2018, **11**, 688.
156 Z. Cong, F. Yang, L. Cao, H. Wen, T. Fu, S. Ma, C. Liu, L. Quan and Y. Liao, *Int. J. Nanomed.*, 2018, **13**, 8549.
157 Z. Yang, R. Cheng, C. Zhao, N. Sun, H. Luo, Y. Chen, Z. Liu, X. Li, J. Liu and Z. Tian, *Theranostics*, 2018, **8**, 4097–4115.

158 W. Gao, G. Ye, X. Duan, X. Yang and V. C. Yang, *Int. J. Nanomed.*, 2017, **12**, 1047.
159 X. Li, X. Yang, Z. Lin, D. Wang, D. Mei, B. He, X. Wang, X. Wang, Q. Zhang and W. Gao, *Eur. J. Pharm. Sci.*, 2015, **76**, 95–101.
160 H. Shan, W. Yin, L. Wen, A. Mao and M. Lang, *Eur. Polym. J.*, 2023, **195**, 112214.
161 M. He, Z. Zhang, Z. Jiao, M. Yan, P. Miao, Z. Wei, X. Leng, Y. Li, J. Fan, W. Sun and X. Peng, *Chin. Chem. Lett.*, 2023, **34**, 107574, DOI: 10.1016/j.cclet.2022.05.088.
162 S. Sun, R. Han, Y. Sun, W. Chen, L. Zhao, X. Guan and W. Zhang, *Colloids Surf., B*, 2024, **238**, 113909.
163 A. Akbarzadeh, R. Rezaei-Sadabady, S. Davaran, S. W. Joo, N. Zarghami, Y. Hanifehpour, M. Samiei, M. Kouhi and K. Nejati-Koshki, *Nanoscale Res. Lett.*, 2013, **8**, 102.
164 K. Otake, T. Shimomura, T. Goto, T. Imura, T. Furuya, S. Yoda, Y. Takebayashi, H. Sakai and M. Abe, *Langmuir*, 2006, **22**, 2543–2550.
165 T. M. Allen and P. R. Cullis, *Adv. Drug Delivery Rev.*, 2013, **65**, 36–48.
166 Q. Xiao, X. Li, C. Liu, Y. Yang, Y. Hou, Y. Wang, M. Su and W. He, *Chin. Chem. Lett.*, 2022, **33**, 4191–4196.
167 B. Børresen, J. R. Henriksen, G. Clergeaud, J. S. Jørgensen, F. Melander, D. R. Elema, J. Szebeni, S. A. Engelholm, A. T. Kristensen, A. Kjær, T. L. Andresen and A. E. Hansen, *ACS Nano*, 2018, **12**, 11386–11398.
168 S. Lee, H. J. Kim, J.-H. Choi, H. J. Jang, H. B. Cho, H.-R. Kim, J.-I. Park, K.-S. Park and K.-H. Park, *J. Controlled Release*, 2024, **368**, 756–767, DOI: 10.1016/j.jconrel.2024.03.027.
169 G. Yang, S. Kim, J. Y. Oh, D. Kim, S. Jin, E. Choi and J.-H. Ryu, *J. Colloid Interface Sci.*, 2023, **649**, 1014–1022.
170 M. G. M. Ghazy and N. A. N. Hanafy, *Int. J. Biol. Macromol.*, 2024, **260**, 129338.
171 M. Sun, H. Hu, L. Sun and Z. Fan, *Chin. Chem. Lett.*, 2020, **31**, 1729–1736.
172 J. Iglesias, *Breast Cancer Res.*, 2009, **11**, S21.
173 M. J. Hawkins, P. Soon-Shiong and N. Desai, *Adv. Drug Delivery Rev.*, 2008, **60**, 876–885.
174 A. T. Guduru, A. Mansuri, U. Singh, A. Kumar, D. Bhatia and S. V. Dalvi, *Biomater. Adv.*, 2024, **161**, 213886, DOI: 10.1016/j.bioadv.2024.213886.
175 Y. Xu, Y. Liu, T. He, Y. Zhang, M. Wang, H. Yuan and M. Yang, *Colloids Surf., B*, 2021, **207**, 112020, DOI: 10.1016/j.colsurfb.2021.112020.
176 R. Meng, L. Zuo and X. Zhou, *Med. Hypotheses*, 2024, **184**, 111271, DOI: 10.1016/j.mehy.2024.111271.
177 X. Zhen, P. Cheng and K. Pu, *Small*, 2019, **15**, 1804105.
178 M. K. Goshisht, N. Tripathi, G. K. Patra and M. Chaskar, *Chem. Sci.*, 2023, **14**, 5842–5871.
179 X. Wei, J. Gao, R. H. Fang, B. T. Luk, A. V. Kroll, D. Dehaini, J. Zhou, H. W. Kim, W. Gao, W. Lu and L. Zhang, *Biomaterials*, 2016, **111**, 116–123.
180 X. Liu, Z. Chu, B. Chen and Y. Ma, *Mater. Today Bio*, 2023, **22**, 100765, DOI: 10.1016/j.mtbio.2023.100765.
181 K. Brindhadevi, H. A. Garalleh, A. Alalawi, E. Al-Sarayreh and A. Pugazhendhi, *Biochem. Eng. J.*, 2023, **192**, 108828.
182 A. Sharma, P. Vaswani and D. Bhatia, *Nanoscale Adv.*, 2024, **6**, 3714–3732, DOI: 10.1039/D4NA00145A.
183 M. F. Naief, S. N. Mohammed, H. J. Mayouf and A. M. Mohammed, *J. Organomet. Chem.*, 2023, **999**, 122819.
184 H. Cabral, K. Miyata, K. Osada and K. Kataoka, *Chem. Rev.*, 2018, **118**, 6844–6892.
185 M. He, L. Yu, Y. Yang, B. Zou, W. Ma, M. Yu, J. Lu, G. Xiong, Z. Yu and A. Li, *Chin. Chem. Lett.*, 2020, **31**, 3178–3182.
186 Z. Hong, X. Zan, T. Yu, Y. Hu, H. Gou, S. Zheng, X. Gao and P. Zhou, *Chin. Chem. Lett.*, 2023, **34**, 107603.
187 L. Tang, J. Li, T. Pan, Y. Yin, Y. Mei, Q. Xiao, R. Wang, Z. Yan and W. Wang, *Theranostics*, 2022, **12**, 2290–2321, DOI: 10.7150/thno.69628.
188 B. Wu, M. Li, L. Wang, Z. Iqbal, K. Zhu, Y. Yang and Y. Li, *J. Mater. Chem. B*, 2021, **9**, 4319–4328, DOI: 10.1039/D1TB00396H.
189 M. Zhao, Z. Li, C. Yu, Q. Sun, K. Wang and Z. Xie, *Chem. Eng. J.*, 2024, **482**, 149039, DOI: 10.1016/j.cej.2024.149039.
190 J. Wang, S. Zhou, F. Lu, S. Wang and Q. Deng, *Food Chem.*, 2024, **451**, 139451.
191 X. Zhang, J. Tang, C. Li, Y. Lu, L. Cheng and J. Liu, *Bioact. Mater.*, 2021, **6**(2), 472–489, DOI: 10.1016/j.bioactmat.2020.08.024.
192 L. Sun, Y. Han, Y. Zhao, J. Cui, Z. Bi, S. Liao, Z. Ma, F. Lou, C. Xiao, W. Feng, J. Liu, B. Cai and D. Li, *Front. Pharmacol.*, 2024, **15**, 1396975, DOI: 10.3389/fphar.2024.1396975.
193 C. Sun, L. Wen, J. Zeng, Y. Wang, Q. Sun, L. Deng, C. Zhao and Z. Li, *Biomaterials*, 2016, **91**, 81–89.
194 S. Geng, X. Zhang, T. Luo, M. Jiang, C. Chu, L. Wu, P. Gong and W. Zhou, *J. Controlled Release*, 2023, **354**, 889–901, DOI: 10.1016/j.jconrel.2022.12.054.
195 U. T. Uthappa, M. Suneetha, S. M. Ji, H.-H. Jeong and S. S. Han, *Microporous Mesoporous Mater.*, 2023, **362**, 112795.
196 S. Senapati, A. K. Mahanta, S. Kumar and P. Maiti, *Signal Transduct. Target. Ther.*, 2018, **3**, 7.
197 H. Zhang, X. Liu, Y. Wu, C. Guan, A. K. Cheetham and J. Wang, *Chem. Commun.*, 2018, **54**, 5268–5288.
198 X. Lin, H. Wu, J. Zhang, X. Chen and X. Gao, *Chem. Eng. J.*, 2024, **480**, 147865.
199 Y. Li, J. Zhou, L. Wang and Z. Xie, *ACS Appl. Mater. Interfaces*, 2020, **12**, 30213–30220.
200 M. Ji, H. Liu, X. Liang, M. Wei, D. Shi, J. Gou, T. Yin, H. He, X. Tang and Y. Zhang, *Chem. Eng. J.*, 2024, **485**, 149640, DOI: 10.1016/j.cej.2024.149640.
201 M. Wu, J. Yang, T. Ye, B. Wang, Y. Tang and X. Ying, *ACS Appl. Mater. Interfaces*, 2023, **15**(25), 29939–29947, DOI: 10.1021/acsami.3c03928.
202 C. Dai, Y. Chen, X. Jing, L. Xiang, D. Yang, H. Lin, Z. Liu, X. Han and R. Wu, *ACS Nano*, 2017, **11**(12), 12696–12712, DOI: 10.1021/acsnano.7b07241.

203 D. Prakashan, A. Kaushik and S. Gandhi, *Chem. Eng. J.*, 2024, **497**, 154371, DOI: 10.1016/j.cej.2024.154371.
204 N. Singh, K. P. Srikanth, V. Gopal, M. Rajput, G. Manivasagam, K. G. Prashanth, K. Chatterjee and S. Suwas, *J. Mater. Chem. B*, 2024, **12**, 5982–5993, DOI: 10.1039/D4TB00379A.
205 L. Liu, Y. Xiang, Z. Wang, X. Yang, X. Yu, Y. Lu, L. Deng and W. Cui, *NPG Asia Mater.*, 2019, **11**, 81, DOI: 10.1038/s41427-019-0185-z.
206 A. C. Lima, R. L. Reis, H. Ferreira and N. M. Neves, *ACS Biomater. Sci. Eng.*, 2021, **7**(7), 3229–3241, DOI: 10.1021/acsbiomaterials.1c00412.
207 M. Long, X. Liu, X. Huang, M. Lu, X. Wu, L. Weng, Q. Chen, X. Wang, L. Zhu and Z. Chen, *J. Controlled Release*, 2021, **334**, 303–317, DOI: 10.1016/j.jconrel.2021.04.035.
208 T. Kulsirirat, K. Sathirakul, N. Kamei and M. Takeda-Morishita, *Int. J. Pharm.*, 2021, **602**, 120618, DOI: 10.1016/j.ijpharm.2021.120618.
209 Z. Liu, K. Wang, X. Peng and L. Zhang, *Eur. Polym. J.*, 2022, **166**, 110979, DOI: 10.1016/j.eurpolymj.2021.110979.
210 X. Shi, B. Ma, H. Chen, W. Tan, S. Ma and G. Zhu, *Biosensors*, 2022, **12**(10), 847.
211 W. H. Park, B. S. Kim, K. E. Park, H. K. You, J. Lee and M. H. Kim, *Int. J. Nanomed.*, 2015, **10**, 485–502.
212 S. Kwak, A. Haider, K. C. Gupta, S. Kim and I.-K. Kang, *Nanoscale Res. Lett.*, 2016, **11**, 323, DOI: 10.1186/s11671-016-1532-4.
213 H. Samadian, H. Mobasheri, M. Azami and R. Faridi-Majidi, *Sci. Rep.*, 2020, **10**, 1–14.
214 T. Gong, T. Liu, L. Zhang, W. Ye, X. Guo, L. Wang, L. Quan and C. Pan, *ACS Biomater. Sci. Eng.*, 2018, **4**, 240–247.
215 A. G. Bajpayee, R. E. De la Vega, M. Scheu, N. H. Varady, I. A. Yannatos, L. A. Brown, Y. Krishnan, T. J. Fitzsimons, P. Bhattacharya, E. H. Frank, A. J. Grodzinsky and R. M. Porter, *Eur. Cells Mater.*, 2017, **34**, 341–364.
216 Q. Hu, Q. Chen, X. Yan, B. Ding, D. Chen and L. Cheng, *Nanomedicine*, 2018, **13**, 749–767.
217 S. Xue, X. Zhou, W. Sang, C. Wang, H. Lu, Y. Xu, Y. Zhong, L. Zhu, C. He and J. Ma, *Bioact. Mater.*, 2021, **6**, 2372–2389, DOI: 10.1016/j.bioactmat.2021.01.017.
218 D. K. Chandra, R. L. Reis, S. C. Kundu, A. Kumar and C. Mahapatra, *ACS Biomater. Sci. Eng.*, 2024, **10**, 4145–4174, DOI: 10.1021/acsbiomaterials.4c00166.
219 N. Rizwana, K. Maslekar, K. Chatterjee, Y. Yao, V. Agarwal and M. Nune, *ACS Appl. Nano Mater.*, 2024, **7**, 18177–18188, DOI: 10.1021/acsanm.3c02962.
220 S. Kumari, P. Mondal, S. Tyeb and K. Chatterjee, *J. Mater. Chem. B*, 2024, **12**, 1926, DOI: 10.1039/d3tb02179c.
221 J. Zhang, H. Eyisoylu, X.-H. Qin, M. Rubert and R. Müller, *Acta Biomater.*, 2021, **121**, 637–652, DOI: 10.1016/j.actbio.2020.12.026.
222 N. Marovič, I. Ban, U. Maver and T. Maver, *Nanotechnol. Rev.*, 2023, **12**, 20220570, DOI: 10.1515/ntrev-2022-0570.
223 A. Chakraborty, A. Roy, S. P. Ravi and A. Paul, *Biomater. Sci.*, 2021, **9**, 6337–6354, DOI: 10.1039/D1BM00605C.
224 S. Nasra, D. Bhatia and A. Kumar, *Adv. Healthcare Mater.*, 2024, **13**, 2400679, DOI: 10.1002/adhm.202400679.
225 A. Halim, K.-Y. Qu, X.-F. Zhang and N.-P. Huang, *ACS Biomater. Sci. Eng.*, 2021, **7**(8), 3503–3529, DOI: 10.1021/acsbiomaterials.1c00490.
226 P. Zhuang, J. An, C. K. Chua and L. P. Tan, *Mater. Des.*, 2020, **193**, 108794, DOI: 10.1016/j.matdes.2020.108794.
227 E. Fornetti, F. De Paolis, C. Fuoco, S. Bernardini, S. M. Giannitelli, A. Rainer, D. Seliktar, F. Magdinier, J. Baldi, R. Biagini, S. Cannata, S. Testa and C. Gargioli, *Biofabrication*, 2023, **15**(2), 025009, DOI: 10.1088/1758-5090/acb573.
228 H. J. Jo, M. S. Kang, H. J. Heo, H. J. Jang, R. Park, S. W. Hong, Y. H. Kim and D.-W. Han, *Int. J. Biol. Macromol.*, 2024, **265**, 130696, DOI: 10.1016/j.ijbiomac.2024.130696.
229 J. H. Kim, Y.-J. Seol, I. K. Ko, H.-W. Kang, Y. K. Lee, J. J. Yoo, A. Atala and S. J. Lee, *Sci. Rep.*, 2018, **8**, 12307, DOI: 10.1038/s41598-018-29968-5.
230 M. Hosseini, K. R. Koehler and A. Shafiee, *Adv. Healthcare Mater.*, 2022, **11**(22), e2201626, DOI: 10.1002/adhm.202201626.
231 C. Mazio, I. Mavaro, A. Palladino, C. Casale, F. Urciuolo, A. Banfi, L. D'Angelo, P. A. Netti, P. de Girolamo, G. Imparato and C. Attanasio, *Mater. Today Bio*, 2024, **25**, 100949, DOI: 10.1016/j.mtbio.2024.100949.
232 L. Li, S. Qin, J. Peng, A. Chen, Y. Nie, T. Liu and K. Song, *Int. J. Biol. Macromol.*, 2020, **145**, 262–271, DOI: 10.1016/j.ijbiomac.2019.12.174.
233 Y. J. Shin, R. T. Shafranek, J. H. Tsui, J. Walcott, A. Nelson and D. H. Kim, *Acta Biomater.*, 2021, **119**, 75–88, DOI: 10.1016/j.actbio.2020.11.006.
234 D. Kim, M. Kim, J. Lee and J. Jang, *Front. Bioeng. Biotechnol.*, 2022, **10**, 764682, DOI: 10.3389/fbioe.2022.764682.
235 Y. Chen, L. Xu, W. Li, W. Chen, Q. He, X. Zhang, J. Tang, Y. Wang, B. Liu and J. Liu, *Biofabrication*, 2022, **14**(2), 025002, DOI: 10.1088/1758-5090/ac48e4.
236 S. Fleischer and T. Dvir, *Curr. Opin. Biotechnol.*, 2013, **24**(4), 664–671, DOI: 10.1016/j.copbio.2012.10.016.
237 N. Tripathi and M. K. Goshisht, *ACS Appl. Bio Mater.*, 2022, **5**, 1391–1463.
238 P. Khullar, M. K. Goshisht, L. Moudgil, G. Singh, D. Mandial, H. Kumar, G. K. Ahluwalia and M. S. Bakshi, *ACS Sustainable Chem. Eng.*, 2017, **5**, 1082–1093.
239 M. K. Goshisht, L. Moudgil, P. Khullar, G. Singh, A. Kaura, H. Kumar, G. Kaur and M. S. Bakshi, *ACS Sustainable Chem. Eng.*, 2015, **3**, 3175–3187.
240 A. Mahal, M. K. Goshisht, P. Khullar, H. Kumar, N. Singh, G. Kaur and M. S. Bakshi, *Phys. Chem. Chem. Phys.*, 2014, **16**, 14257–14270.
241 U. Song, K. S. Pyo, H. H. Song, S. Lee and J. Kim, *Emerg. Contam.*, 2024, **10**, 100293.
242 A. Sharmila, S. M. Roopan and C. I. Selvaraj, *J. Drug Delivery Sci. Technol.*, 2024, **96**, 105731.
243 N. Tripathi, N. Tripathi and M. K. Goshisht, *Mol. Divers.*, 2022, **26**, 629–645, DOI: 10.1007/s11030-020-10176-1.

244 N. Tripathi and M. K. Goshisht, *Aggregation of luminophores in supramolecular systems: From mechanism to applications*, CRC Press, 2020, pp. 201–220. DOI: 10.1201/9781003027706.
245 D.-D. Varsou, P. D. Kolokathis, M. Antoniou, N. K. Sidiropoulos, A. Tsoumanis, A. G. Papadiamantis, G. Melagraki, I. Lynch and A. Afantitis, *Comput. Struct. Biotechnol. J.*, 2024, **25**, 47–60.
246 J. M. Hillegass, A. Shukla, S. A. Lathrop, M. B. MacPherson, N. K. Fukagawa and B. T. Mossman, *Wiley Interdiscip. Rev.: Nanomed. Nanobiotechnol.*, 2010, **2**, 219–231.
247 . *In Vitro* Toxicology Testing Market Size, Share & Trends by Product & Service (Assays (ELISA & Western Blot), Equipment, Consumable, Software), Toxicity Endpoints (ADME, Genotoxicity, Cytotoxicity), Technology, Method, Industry (Pharma, Cosmetics) - Global Forecast to 2028. https://www.marketsandmarkets.com/Thanks/subscribepurchaseNew.asp?id=209577065&ld=1555905 (accessed June 03, 2024).
248 T. Wu and M. Tang, *J. Appl. Toxicol.*, 2018, **38**, 25–40.
249 B. Kong, J. H. Seog, L. M. Graham and S. B. Lee, *Nanomedicine*, 2011, **6**, 929–941.
250 C. Lo Giudice, J. Yang, M. A. Poncin, L. Adumeau, M. Delguste, M. Koehler, K. Evers, A. C. Dumitru, K. A. Dawson and D. Alsteens, *ACS Nano*, 2022, **16**, 306–316, DOI: 10.1021/acsnano.1c06301.
251 S. Hočevar, A. Milošević, L. Rodriguez-Lorenzo, L. Ackermann-Hirschi, I. Mottas, A. Petri-Fink, B. Rothen-Rutishauser, C. Bourquin and M. J. D. Clift, *ACS Nano*, 2019, **13**(6), 6790–6800, DOI: 10.1021/acsnano.9b01492.
252 J. Duan, V. K. Kodali, M. J. Gaffrey, J. Guo, R. K. Chu, D. G. Camp, R. D. Smith, B. D. Thrall and W. J. Qian, *ACS Nano*, 2016, **10**, 524–538, DOI: 10.1021/acsnano.5b05524.
253 S. Devasahayam, *Characterization and Biology of Nanomaterials for Drug Delivery: Nanoscience and Nanotechnology in Drug Delivery*, Elsevier, 2018, pp. 477–522.
254 S. Jesus, M. Schmutz, C. Som, G. Borchard, P. Wick and O. Borges, *Front. Bioeng. Biotechnol.*, 2019, **7**, 261.
255 M. G. Tirumala, P. Anchi, S. Raja, M. Rachamalla and C. Godugu, *Front. Pharmacol.*, 2021, **12**, 612659, DOI: 10.3389/fphar.2021.612659.
256 B. Halamoda-Kenzaoui, U. Holzwarth, G. Roebben, A. Bogni and S. Bremer-Hoffmann, *WIREs Nanomed. Nanobiotechnol.*, 2019, **11**, e1531.
257 B. Drasler, D. Vanhecke, L. Rodriguez-Lorenzo, A. Petri-Fink and B. Rothen-Rutishauser, *Nanomedicine*, 2017, **12**, 1095–1099.
258 M. Reifarth, S. Hoeppener and U. S. Schubert, *Adv. Mater.*, 2018, **30**, 1703704.
259 A. Salvati, I. Nelissen, A. Haase, C. Aberg, S. Moya, A. Jacobs, F. Alnasser, T. Bewersdorff, S. Deville, A. Luch and K. A. Dawson, *NanoImpact*, 2018, **9**, 42–50.
260 H. Garcia Romeu, S. Deville and A. Salvati, *Small*, 2021, **17**(34), 2100887.
261 E. Frohlich, *Artif. Cells, Nanomed Biotechnol.*, 2018, **46**, 1091–1107.
262 V. V. Chrishtop, A. Y. Prilepskii, V. G. Nikonorova and V. A. Mironov, *Toxicology*, 2021, **462**, 152952, DOI: 10.1016/j.tox.2021.152952.
263 Y. Kohl, M. Biehl, S. Spring, M. Hesler, V. Ogourtsov, M. Todorovic, J. Owen, E. Elje, K. Kopecka, O. H. Moriones, N. G. Bastús, P. Simon, T. Dubaj, E. Runden-Pran, V. Puntes, N. William, H. Briesen, S. Wagner, N. Kapur, E. Mariussen, A. Nelson, A. Gabelova, M. Dusinska, T. Velten and T. Knoll, *Small*, 2021, **17**, 2006012.
264 . Markets and Markets. In Vivo Toxicology Market - Global Forecast to 2025. https://www.marketsandmarkets.com/Market-Reports/in-vivo-toxicology-testing-market-105308811.html (accessed 2024-06-06).
265 Y. Yang, Z. Qin, W. Zeng, T. Yang, Y. Cao, C. Mei and Y. Kuang, *Nanotechnol. Rev.*, 2017, **6**, 279–289.
266 S.-K. Jung, X. Qu, B. Aleman-Meza, T. Wang, C. Riepe, Z. Liu, Q. Li and W. Zhong, *Environ. Sci. Technol.*, 2015, **49**, 2477–2485.
267 M. T. Jacques, J. L. Oliveira, E. V. R. Campos, L. F. Fraceto and D. S. Ávila, *Ecotoxicol. Environ. Saf.*, 2017, **139**, 245–253.
268 B. Liu, E. M. Campo and T. Bossing, *PLoS One*, 2014, **9**, e88681.
269 G. Peng, Y. He, X. Wang, Y. Cheng, H. Zhang, K. Savolainen, L. Madler, S. Pokhrel and S. Lin, *ACS Nano*, 2020, **14**, 4166–4177.
270 S. Rajabi, A. Ramazani, M. Hamidi and T. Naji, *Daru*, 2015, **23**, 20.
271 C. Hurel, C. Bignon, C. Said-Mohamed, S. Amigoni, T. Devers and F. Guittard, *Environ. Sci. Pollut. Res.*, 2018, **25**, 21216–21223.
272 B. H. Mao, Y. K. Luo, B. J. Wang, C. W. Chen, F. Y. Cheng, Y. H. Lee, S. J. Yan and Y. J. Wang, *Part. Fibre Toxicol.*, 2022, **19**, 6.
273 B. Cunningham, A. E. Engstrom, B. J. Harper, S. L. Harper and M. R. Mackiewicz, *Nanomaterials*, 2021, **11**, 1516.
274 J. Li, J. Tian, H. Yin, Y. Peng, S. Liu, S. Yao and L. Zhang, *Environ. Int.*, 2021, **152**, 106497.
275 A. K. Mittal and U. C. Banerjee, *Mater. Today Commun.*, 2021, **26**, 102001.
276 M. K. Uchiyama, C. B. Hebeda, S. Sandri, M. de Paula-Silva, M. Romano, R. M. Cardoso, S. H. Toma, K. Araki and S. H. P. Farsky, *Nanomedicine*, 2021, **16**, 741–758.
277 T. Sun, X. Liu, X. Zhan, L. Ou and R. Lai, *Process Saf. Environ. Prot.*, 2021, **147**, 134–145.
278 M. R. Wani, N. Maheshwari and G. Shadab, *Environ. Sci. Pollut. Res.*, 2021, **28**, 22664–22678.
279 P. E. Feuser, M. d. M.s Cardoso, N. C. Galvani, R. P. Zaccaron, L. M. Venturini, F. K. Rigo, R. A. Machado-de-ávila, P. C. L. Silveira, C. Sayer and P. H. Hermes de Araá»§jo, *J. Biomed. Mater. Res., Part B*, 2022, **110**, 702–711.
280 Z. Alvi, M. Akhtar, N. U. Rahman, K. M. Hosny, A. M. Sindi, B. A. Khan, I. Nazir and H. Sadaquat, *Polymers*, 2021, **13**, 4350.

281 P. Andreozzi, C. Simo, P. Moretti, J. M. Porcel, T. U. Lüdtke, M. d. l. A. Ramirez, L. Tamberi, M. Marradi, H. Amenitsch, J. Llop, M. G. Ortore and S. E. Moya, *Small*, 2021, **17**, 2102211.
282 T. Deptuch, A. Florczak, A. Lewandowska, E. Leporowska, K. Penderecka, A. Marszalek, A. Mackiewicz and H. Dams-Kozlowska, *Nanomedicine*, 2021, **16**, 1553–1565.
283 H. Sadaquat, M. Akhtar, M. Nazir, R. Ahmad, Z. Alvi and N. Akhtar, *Int. J. Pharm.*, 2021, **598**, 120363.
284 S. Rana, J. Singh, A. Wadhawan, A. Khanna, G. Singh and M. Chatterjee, *J. Pharm. Sci.*, 2021, **110**, 1727–1738.
285 J. S. Stine, B. J. Harper, C. G. Conner, O. D. Velev and S. L. Harper, *Nanomaterials*, 2021, **11**, 111.
286 K. V. Chandekar, M. Shkir, T. Alshahrani, E. H. Ibrahim, M. Kilany, Z. Ahmad, M. A. Manthrammel, S. AlFaify, B. Kateb and A. Kaushik, *Mater. Sci. Eng., C*, 2021, **122**, 111898.
287 K. Akhtar, N. A. Shad, M. M. Sajid, Y. Javed, F. Muhammad, B. Akhtar, M. Irfan Hussain, A. Sharif and W. A. Munawar, *Adv. Appl. Ceram.*, 2021, **120**(287–299), 111898.
288 M.-H. Tsai, H.-R. Chao, J.-J. Jiang, Y.-H. Su, M. P. Cortez, L. L. Tayo, I.-C. Lu, H. Hsieh, C.-C. Lin, S.-L. Lin, W. N. W. Mansor, C.-K. Su, S.-T. Huang and W.-L. Hsu, *Aerosol Air Qual. Res.*, 2021, **21**, 200559.
289 A. Bakhtiar, A. S. Neah, K. Y. Ng and E. H. Chowdhury, *J. Pharm. Investig.*, 2022, **52**, 95–107.
290 A. Shah, I. Tauseef, M. A. Yameen, S. K. Haleem, S. Haq and S. Shoukat, *Microsc. Res. Technol.*, 2022, **85**, 181–192.
291 M. A. Heinrich, B. Martina and J. Prakash, *Nano Today*, 2020, **35**, 100961.
292 A. Sarkar, T. S. Mahendran, A. Meenakshisundaram, R. V. Christopher, P. Dan, V. Sundararajan, N. Jana, D. Venkatasubbu and S. S. Mohideen, *Chemosphere*, 2021, **284**, 131363.
293 E. J. S. Pinto, J. T. C. d. Araujo, R. M. d. A. Ferreira, R. N. P. Souto, L. A. Lima, P. G. d. B. Silva, M. T. Garcia, A. de la Fuente and F. F. O. d. Sousa, *J. Drug Delivery Sci. Technol.*, 2021, **63**, 102513.
294 A. S. Barnard, B. Motevalli, A. J. Parker, J. M. Fischer, C. A. Feigl and G. Opletal, *Nanoscale*, 2019, **11**, 19190–19201, DOI: 10.1039/c9nr05912a.
295 M. Gonzalez-Durruthy, A. V. Werhli, V. Seus, K. S. Machado, A. Pazos, C. R. Munteanu, H. Gonzalez-Diaz and J. M. Monserrat, *Sci. Rep.*, 2017, **7**(1), 1–19.
296 I. Lynch, A. Afantitis, D. Greco, M. Dusinska, M. A. Banares and G. Melagraki, *Nanomaterials*, 2021, **11**, 121.
297 S. K. Verma, A. Nandi, F. Z. Simnani, D. Singh, A. Sinha, S. S. Naser, J. Sahoo, S. S. Lenka, P. K. Panda, A. Dutt, N. K. Kaushik, D. Singh and M. Suar, *Mater. Des.*, 2023, **235**, 112452, DOI: 10.1016/j.matdes.2023.112452.
298 H. I. Labouta, N. Asgarian, K. Rinker and D. T. Cramb, *ACS Nano*, 2019, **13**(2), 1583–1594.
299 Y. Jia, X. Hou, Z. Wang and X. Hu, *ACS Sustainable Chem. Eng.*, 2021, **9**, 6130–6147, DOI: 10.1021/acssuschemeng.1c00483.
300 M. K. Goshisht, *ACS Omega*, 2024, **9**(9), 9921–9945, DOI: 10.1021/acsomega.3c05913.
301 N. Tripathi, M. K. Goshisht, S. K. Sahu and C. Arora, *Mol. Divers.*, 2021, **25**(3), 1643–1664, DOI: 10.1007/s11030-021-10237-z.
302 N. A. Subramanian and A. Palaniappan, *ACS Omega*, 2021, **6**(17), 11729–11739, DOI: 10.1021/acsomega.1c01076.
303 A. V. Singh, R. S. Maharjan, A. Kanase, K. Siewert, D. Rosenkranz, R. Singh, P. Laux and A. Luch, *ACS Appl. Mater. Interfaces*, 2021, **13**(1), 1943–1955.
304 A. M. Nystrom and B. Fadeel, *J. Controlled Release*, 2012, **161**, 403–408.
305 A. B. Raies and V. B. Bajic, *Wiley Interdiscip. Rev.: Comput. Mol. Sci*, 2016, **6**, 147–172.
306 N. Basant, S. Gupta and K. P. Singh, *Toxicol. Res.*, 2016, **5**(4), 1029–1038.
307 M. Na, S. H. Nam, K. Moon and J. Kim, *Environ. Sci. Nano*, 2023, **10**, 325, DOI: 10.1039/d2en00672c.
308 D. Fourches, D. Pu, C. Tassa, R. Weissleder, S. Y. Shaw, R. J. Mumper and A. Tropsha, *ACS Nano*, 2010, **4**(10), 5703–5712.
309 R. Concu, V. V. Kleandrova, A. Speck-Planche and M. N. D. S. Cordeiro, *Nanotoxicology*, 2017, **11**(7), 891–906.
310 M. K. Goshisht, *Adv. Mater. Proc.*, 2017, **2**, 535–546, DOI: 10.5185/amp.2017/690.
311 X. Yan, A. Sedykh, W. Wang, X. Zhao, B. Yan and H. Zhu, *Nanoscale*, 2019, **11**(17), 8352–8362.
312 P. P. Fu, Q. Xia, H. M. Hwang, P. C. Ray and H. Yu, *J. Food Drug Anal.*, 2014, **22**, 64–75, DOI: 10.1016/j.jfda.2014.01.005.
313 R. Alshehri, A. M. Ilyas, A. Hasan, A. Arnaout, F. Ahmed and A. Memic, *J. Med. Chem.*, 2016, **59**, 8149–8167, DOI: 10.1021/acs.jmedchem.5b01770.
314 M. Gonzalez-Durruthy, A. V. Werhli, L. Cornetet, K. S. Machado, H. Gonzalez-Diaz, W. Wasiliesky, C. P. Ruas, M. A. Gelesky and J. M. Monserrat, *RSC Adv.*, 2016, **6**(63), 58680–58693.
315 M. González-Durruthy, A. K. Giri, I. Moreira, R. Concu, A. Melo, J. M. Ruso and M. N. D. S. Cordeiro, *Nano Today*, 2020, **34**, 100913, DOI: 10.1016/j.nantod.2020.100913.
316 Z. Gu, L. D. Plant, X. Y. Meng, J. M. Perez-Aguilar, Z. Wang, M. Dong, D. E. Logothetis and R. Zhou, *ACS Nano*, 2018, **12**(1), 705–717.
317 A. Albanese, P. S. Tang and W. C. Chan, *Annu. Rev. Biomed. Eng.*, 2012, **14**, 1–16, DOI: 10.1146/annurev-bioeng-071811-150124.
318 A. Manke, L. Wang and Y. Rojanasakul, *Biomed. Res. Int.*, 2013, **2013**, 942916, DOI: 10.1155/2013/942916.
319 K. Pondman, S. L. Gac and U. Kishore, *Immunobiology*, 2023, **228**(2), 152317, DOI: 10.1016/j.imbio.2022.152317.
320 M. Encinas-Gimenez, P. Martin-Duque and A. Martín-Pardillos, *Int. J. Mol. Sci.*, 2024, **25**, 1983, DOI: 10.3390/ijms25041983.
321 Y. Sun, Y. Zhou, M. Rehman, Y.-F. Wang and S. Guo, *Chem. Biol. Eng.*, 2024, **1**(9), 757–772, DOI: 10.1021/cbe.4c00105.

322 Y. Feng, H. Fu, X. Zhang, S. Liu and X. Wei, *Ecotoxicol. Environ. Saf.*, 2024, **286**, 117215, DOI: 10.1016/j.ecoenv.2024.117215.
323 S. K. Misra, J. M. Rosenholm and K. Pathak, *Molecules*, 2023, **28**, 4701, DOI: 10.3390/molecules28124701.
324 V. Alcolea-Rodriguez, V. I. Dumit, R. Ledwith, R. Portela, M. A. Bañares and A. Haase, *Nano Lett.*, 2024, **24**(38), 11793–11799, DOI: 10.1021/acs.nanolett.4c01573.
325 M. Aloisi and A. M G. Poma, *Environments*, 2025, **12**, 234, DOI: 10.3390/environments12070234.
326 F. Farjadian, A. Ghasemi, O. Gohari, A. Roointan, M. Karim and M. R. Hamblin, *Nanomedicine*, 2019, **14**, 93–126.
327 L. Cattel, M. Ceruti and F. Dosio, *J. Chemother.*, 2004, **16**, 94–97.
328 M. L. Immordino, P. Brusa, S. Arpicco, B. Stella, F. Dosio and L. Cattel, *J. Controlled Release*, 2003, **91**, 417–429.
329 G. M. Jensen and D. F. Hodgson, *Adv. Drug Delivery Rev.*, 2020, **154**, 2–12.
330 DOXIL approved by FDA, *AIDS Patient Care*, 1995, **9**, 306. Available online: https://pubmed.ncbi.nlm.nih.gov/11361446/ (accessed on 11 November 2024).
331 Y. A. Tereshkina, T. I. Torkhovskaya, E. G. Tikhonova, L. V. Kostryukova, M. A. Sanzhakov, E. I. Korotkevich, Y. Y. Khudoklinova, N. A. Orlova and E. F. Kolesanova, *J. Drug Target.*, 2022, **30**, 313–325.
332 L. Kager, U. Pötschger and S. Bielack, *Ther. Clin. Risk Manag.*, 2010, **6**, 279–286.
333 S. S. Legha, *Med. Toxicol.*, 1986, **1**, 421–427.
334 . FDA Approves Liposomal Vincristine (Marqibo) for Rare Leukemia. Available online: https://www.cancernetwork.com/view/fda-approves-liposomal-vincristine-marqibo-rare-leukemia (accessed on 11 November 2024).
335 S. Hong, D. W. Choi, H. N. Kim, C. G. Park, W. Lee and H. H. Park, *Pharmaceutics*, 2020, **12**, 604.
336 J. T. Zhang, J. Ma, R. K. Kankala, Q. Yu, B. Wang and A. Z. Chen, *ACS Appl. Bio Mater.*, 2021, **4**, 4039–4048.
337 P. A. Dinndorf, J. Gootenberg, M. H. Cohen, P. Keegan and R. Pazdur, *Oncologist*, 2007, **12**, 991–998.
338 Y. A. Heo, Y. Y. Syed and S. J. Keam, *Drugs*, 2019, **79**, 767–777.
339 A. P. Singh, S. Sharma and D. K. Shah, *J. Pharmacokinet. Pharmacodyn.*, 2016, **43**, 567–582.
340 J. M. Lambert and R. V. J. Chari, *J. Med. Chem.*, 2014, **57**, 6949–6964.
341 A. I. Fraguas-Sánchez, I. Lozza and A. I. Torres-Suárez, *Cancers*, 2022, **14**, 1198.
342 S. J. Keam, *Drugs*, 2020, **80**, 501–508.
343 K. Mahmoudi, A. Bouras, D. Bozec, R. Ivkov and C. Hadjipanayis, *Int. J. Hyperth.*, 2018, **34**, 1316–1328.
344 P. Rivera Gil, D. Hühn, L. L. del Mercato, D. Sasse and W. J. Parak, *Pharmacol. Res.*, 2010, **62**, 115–125.
345 D. Bobo, K. J. Robinson, J. Islam, K. J. Thurecht and S. R. Corrie, *Pharm. Res.*, 2016, **33**, 2373–2387.
346 T. M. Allen and P. R. Cullis, *Adv. Drug Delivery Rev.*, 2013, **65**, 36–48.
347 K. L. Aillon, Y. Xie, N. El-Gendy, C. J. Berkland and M. L. Forrest, *Adv. Drug Delivery Rev.*, 2009, **61**, 457–466.
348 M. K. Goshisht, G. K. Patra, A. Mahal, A. K. Singh, Shobha and M. Parshad, *Inorg. Chim. Acta*, 2025, **574**, 122403, DOI: 10.1016/j.ica.2024.122403.
349 M. A. Dobrovolskaia and S. E. McNeil, *Nat. Nanotechnol.*, 2007, **2**, 469–478.
350 A. E. Nel, L. Mädler, D. Velegol, T. Xia, E. M. Hoek, P. Somasundaran, F. Klaessig, V. Castranova and M. Thompson, *Nat. Mater.*, 2009, **8**, 543–557.
351 C. Fornaguera and M. J. García-Celma, *J. Pers. Med.*, 2017, **7**, 12.
352 J. K. Vasir and V. Labhasetwar, *Adv. Drug Delivery Rev.*, 2007, **59**, 718–728.
353 D. C. Drummond, O. Meyer, K. Hong, D. B. Kirpotin and D. Papahadjopoulos, *Pharmacol. Rev.*, 1999, **51**, 691–743.
354 N. Desai, *AAPS J.*, 2012, **14**, 282–295.
355 R. van der Meel, E. Sulheim, Y. Shi, F. Kiessling, W. J. M. Mulder and T. Lammers, *Nat. Nanotechnol.*, 2019, **14**, 1007–1017.
356 M. Samadzadeh, A. Khosravi, A. Zarepour, G. J. Soufi, A. Hekmatnia, A. Zarrabi and S. Iravani, *RSC Adv.*, 2025, **15**, 24696–24725, DOI: 10.1039/D5RA03927D.
357 M. M. Mahmud, N. Pandey, J. A. Winkles, G. F. Woodworth and A. J. Kim, *Nano Today*, 2024, **56**, 102314, DOI: 10.1016/j.nantod.2024.102314.
358 S. Gujjar, S. Kukal, P. Jayabal, N. Balaji, S. Sainger, S. Roy, S. Rallapalli, R. Mahadevappa, S. Minocha, S. Kumar and S. Mathapati, *Nano Trends*, 2025, **11**, 100127, DOI: 10.1016/j.nwnano.2025.100127.
359 X. Ma, Y. Tian, R. Yang, H. Wang, L. W. Allahou, J. Chang, G. Williams, J. C. Knowles and A. Poma, *J. Nanobiotechnol.*, 2024, **22**, 715, DOI: 10.1186/s12951-024-02901-x.
360 A. Bigham, M. Serrano-Ruiz, M. Caporali, I. Fasolino, M. Peruzzini, L. Ambrosio and M. G. Raucci, *Chem. Soc. Rev.*, 2025, **54**, 827–897, DOI: 10.1039/D4CS00007B.
361 H. Lin, T. Buerki-Thurnherr, J. Kaur, P. Wick, M. Pelin, *et al.*, *ACS Nano*, 2024, **18**(8), 6038–6094, DOI: 10.1021/acsnano.3c09699.
362 C. A. d. Assis, L. G. Greca, M. Ago, M. Y. Balakshin, H. Jameel, R. Gonzalez and O. J. Rojas, *ACS Sustainable Chem. Eng.*, 2018, **6**(9), 11853–11868, DOI: 10.1021/acssuschemeng.8b02151.
363 J. Kleynhans, M. Sathekge and T. Ebenhan, *Materials*, 2021, **14**, 4784, DOI: 10.3390/ma14174784.